

Vol. 25, no. 1, 2025

eISSN 2687-1653

PEER-REVIEWED SCIENTIFIC AND PRACTICAL JOURNAL

# Advanced Engineering Research (Rostov-on-Don)

Mechanics

Machine Building  
and Machine Science

Information Technology,  
Computer Science  
and Management



[www.vestnik-donstu.ru](http://www.vestnik-donstu.ru)  
DOI 10.23947/2687-1653



# Advanced Engineering Research (Rostov-on-Don)

Peer-reviewed scientific and practical journal

eISSN 2687–1653

Published since 2000

Periodicity – 4 issues per year

DOI: 10.23947/2687–1653

**Founder and Publisher — Don State Technical University (DSTU), Rostov-on-Don, Russian Federation**

The journal is aimed at informing the readership about the latest achievements and prospects in the field of mechanics, mechanical engineering, computer science and computer technology. The publication is a forum for cooperation between Russian and foreign scientists, it contributes to the convergence of the Russian and world scientific and information space.

**The journal is included in the List of the leading peer-reviewed scientific publications (Higher Attestation Commission under the Ministry of Science and Higher Education of the Russian Federation), where basic scientific results of dissertations for the degrees of Doctor and Candidate of Science in scientific specialties and their respective branches of science should be published.**

**The journal publishes articles in the following fields of science:**

- Theoretical Mechanics, Dynamics of Machines (Engineering Sciences)
- Deformable Solid Mechanics (Engineering, Physical and Mathematical Sciences)
- Mechanics of Liquid, Gas and Plasma (Engineering Sciences)
- Mathematical Simulation, Numerical Methods and Program Systems (Engineering Sciences)
- System Analysis, Information Management and Processing, Statistics (Engineering Sciences)
- Automation and Control of Technological Processes and Productions (Engineering Sciences)
- Software and Mathematical Support of Machines, Complexes and Computer Networks (Engineering Sciences)
- Computer Modeling and Design Automation (Engineering, Physical and Mathematical Sciences)
- Computer Science and Information Processes (Engineering Sciences)
- Machine Science (Engineering Sciences)
- Machine Friction and Wear (Engineering Sciences)
- Technology and Equipment of Mechanical and Physicotechnical Processing (Engineering Sciences)
- Engineering Technology (Engineering Sciences)
- Welding, Allied Processes and Technologies (Engineering Sciences)
- Methods and Devices for Monitoring and Diagnostics of Materials, Products, Substances and the Natural Environment (Engineering Sciences)
- Hydraulic Machines, Vacuum, Compressor Equipment, Hydraulic and Pneumatic Systems (Engineering Sciences)

---

<i>Registration</i>	Extract from the Register of Registered Mass Media ЭЛ № ФС 77 – 78854 dated August 07, 2020, issued by the Federal Service for Supervision of Communications, Information Technology and Mass Media
<i>Indexing and Archiving</i>	RISC, CyberLeninka, CrossRef, Dimensions, DOAJ, EBSCO, Index Copernicus, Internet Archive, Google Scholar
<i>Website</i>	<a href="http://vestnik-donstu.ru">http://vestnik-donstu.ru</a>
<i>Address of the Editorial Office</i>	1, Gagarin sq., Rostov-on-Don, 344003, Russian Federation
<i>E-mail</i>	<a href="mailto:vestnik@donstu.ru">vestnik@donstu.ru</a>
<i>Telephone</i>	+7 (863) 2–738–372
<i>Date of Publication No.1,2025</i>	30.03.2025





ДОНСКОЙ ГОСУДАРСТВЕННЫЙ  
ТЕХНИЧЕСКИЙ УНИВЕРСИТЕТ

## Advanced Engineering Research (Rostov-on-Don)

Рецензируемый научно-практический журнал

eISSN 2687–1653

Издается с 2000 года

Периодичность – 4 выпуска в год

DOI: 10.23947/2687–1653

Учредитель и издатель — Федеральное государственное бюджетное образовательное учреждение высшего образования «Донской государственный технический университет» (ДГТУ), г. Ростов-на-Дону

Создан в целях информирования читательской аудитории о новейших достижениях и перспективах в области механики, машиностроения, информатики и вычислительной техники. Издание является форумом для сотрудничества российских и иностранных ученых, способствует сближению российского и мирового научно-информационного пространства.

**Журнал включен в перечень рецензируемых научных изданий, в котором должны быть опубликованы основные научные результаты диссертаций на соискание ученой степени кандидата наук, на соискание ученой степени доктора наук (Перечень ВАК) по следующим научным специальностям:**

- 1.1.7 – Теоретическая механика, динамика машин (технические науки)
- 1.1.8 – Механика деформируемого твердого тела (технические, физико-математические науки)
- 1.1.9 – Механика жидкости, газа и плазмы (технические науки)
- 1.2.2 – Математическое моделирование, численные методы и комплексы программ (технические науки)
- 2.3.1 – Системный анализ, управление и обработка информации, статистика (технические науки)
- 2.3.3 – Автоматизация и управление технологическими процессами и производствами (технические науки)
- 2.3.5 – Математическое и программное обеспечение вычислительных систем, комплексов и компьютерных сетей (технические науки)
- 2.3.7 – Компьютерное моделирование и автоматизация проектирования (технические, физико-математические науки)
- 2.3.8 – Информатика и информационные процессы (технические науки)
- 2.5.2 – Машиноведение (технические науки)
- 2.5.3 – Трение и износ в машинах (технические науки)
- 2.5.5 – Технология и оборудование механической и физико-технической обработки (технические науки)
- 2.5.6 – Технология машиностроения (технические науки)
- 2.5.8 – Сварка, родственные процессы и технологии (технические науки)
- 2.5.9 – Методы и приборы контроля и диагностики материалов, изделий, веществ и природной среды (технические науки)
- 2.5.10 – Гидравлические машины, вакуумная, компрессорная техника, гидро- и пневмосистемы (технические науки)

---

<i>Регистрация</i>	Выписка из реестра зарегистрированных средств массовой информации ЭЛ № ФС 77 – 78854 от 07 августа 2020 г., выдано Федеральной службой по надзору в сфере связи, информационных технологий и массовых коммуникаций
<i>Индексация и архивация</i>	РИНЦ, CyberLeninka, CrossRef, Dimensions, DOAJ, EBSCO, Index Copernicus, Internet Archive, Google Scholar
<i>Сайт</i>	<a href="http://vestnik-donstu.ru">http://vestnik-donstu.ru</a>
<i>Адрес редакции</i>	344003, Российская Федерация, г. Ростов-на-Дону, пл. Гагарина, 1
<i>E-mail</i>	<a href="mailto:vestnik@donstu.ru">vestnik@donstu.ru</a>
<i>Телефон</i>	+7 (863) 2–738–372
<i>Дата выхода №1, 2025 в свет</i>	30.03.2025



## **Editorial Board**

### **Editor-in-Chief**

**Alexey N. Beskopylny**, Dr.Sci. (Eng.), Professor, Don State Technical University (Rostov-on-Don, Russian Federation)

### **Deputy Chief Editor**

**Alexandr I. Sukhinov**, Corresponding Member, Russian Academy of Sciences, Dr.Sci. (Phys.-Math.), Professor, Don State Technical University (Rostov-on-Don, Russian Federation)

### **Executive Editor**

**Manana G. Komakhidze**, Cand.Sci. (Chemistry), Don State Technical University (Rostov-on-Don, Russian Federation)

### **Executive Secretary**

**Nadezhda A. Shevchenko**, Don State Technical University (Rostov-on-Don, Russian Federation)

**Ahilan Appathurai**, National Junior Research Fellow, Anna University Chennai (India)

**Ahmet Uyumaz**, PhD (Eng.), Professor, Burdur Mehmet Akif Ersoy University (Turkey)

**Alexander T. Rybak**, Dr.Sci. (Eng.), Professor, Don State Technical University (Rostov-on-Don, Russian Federation)

**Ali M. Hasan**, PhD (Computer Engineering), Al Nahrain University (Baghdad, Iraq)

**Andrey V. Nasedkin**, Dr.Sci. (Phys.-Math.), Professor, Southern Federal University (Rostov-on-Don, Russian Federation)

**Arestak A. Sarukhanyan**, Dr.Sci. (Eng.), Professor, National University of Architecture and Construction of Armenia (Armenia)

**Arkady N. Solovyev**, Dr.Sci. (Phys.-Math.), Professor, Crimean Engineering and Pedagogical University the name of Fevzi Yakubov (Simferopol, Republic of Crimea)

**Batyr M. Yazyev**, Dr.Sci. (Eng.), Professor, Don State Technical University (Rostov-on-Don, Russian Federation)

**Bertram Torsten**, Dr.Sci. (Eng.), Professor, TU Dortmund University (Germany)

**Evgenii A. Demekhin**, Dr.Sci. (Phys.-Math.), Professor, Financial University under the RF Government, Krasnodar branch (Krasnodar, Russian Federation)

**Geny V. Kuznetsov**, Dr.Sci. (Phys.-Math.), Professor, Tomsk Polytechnic University (Tomsk, Russian Federation)

**Gultekin Basmaci**, PhD (Eng.), Professor, Burdur Mehmet Akif Ersoy University (Turkey)

**Hamid A. Jalab**, PhD (Computer Science & IT), University of Malaya (Malaysia)

**Hubert Anysz**, PhD (Eng.), Assistant Professor, Warsaw University of Technology (Republic of Poland)

**Huchang Liao**, Professor, IAAM Fellow, IEEE Business School Senior Fellow, Sichuan University (China)

**Igor M. Verner**, PhD (Eng.), Professor, Technion — Israel Institute of Technology (Israel)

**Ilya I. Kudish**, PhD (Phys.-Math.), Kettering University (USA)

**Imad R. Antipas**, Cand.Sci. (Eng.), Don State Technical University (Rostov-on-Don, Russian Federation)

**Janusz Witalis Kozubal**, Dr.Sci. (Eng.), Wrocław Polytechnic University (Republic of Poland)

**José Carlos Quadrado**, PhD (Electrical Engineering and Computers), DSc Habil, Polytechnic Institute of Porto (Portugal)

**Kamil S. Akhverdiev**, Dr.Sci. (Eng.), Professor, Rostov State Transport University (Rostov-on-Don, Russian Federation)

**Karen O. Egiazaryan**, Dr.Sci. (Eng.), Professor, Tampere University of Technology (Finland)

**Konstantin V. Podmaster'ev**, Dr.Sci. (Eng.), Professor, Orel State University named after I.S. Turgenev (Orel, Russian Federation)

**LaRoux K. Gillespie**, Dr.Sci. (Eng.), Professor, President-Elect of the Society of Manufacturing Engineers (USA)

**Mezhlum A. Sumbatyan**, Dr.Sci. (Phys.-Math.), Professor, Southern Federal University (Rostov-on-Don, Russian Federation)

**Mikhail A. Tamarkin**, Dr.Sci. (Eng.), Professor, Don State Technical University (Rostov-on-Don, Russian Federation)

**Murat Tezer**, Professor, Near East University (Turkey)

**Murman A. Mukutadze**, Dr.Sci. (Eng.), Professor, Rostov State Transport University (Rostov-on-Don, Russian Federation)

**Muzafer H. Saračević**, Full Professor, Novi Pazar International University (Serbia)

**Nguyen Dong Ahn**, Dr.Sci. (Phys.-Math.), Professor, Academy of Sciences and Technologies of Vietnam (Vietnam)

**Nguyen Xuan Chiem**, Dr.Sci. (Eng.), Le Quy Don Technical University (Vietnam)

**Nikolay E. Galushkin**, Dr.Sci. (Eng.), Professor, Institute of Service and Business, DSTU branch (Shakhty, Russian Federation)

**Nikolay N. Prokopenko**, Dr.Sci. (Eng.), Professor, Don State Technical University (Rostov-on-Don, Russian Federation)

**Oleg V. Dvornikov**, Dr.Sci. (Eng.), Professor, Belarusian State University (Belarus)

**Revaz Z. Kavtaradze**, Dr.Sci. (Eng.), Professor, Raphiel Dvali Institute of Machine Mechanics (Georgia)

**Roman N. Polyakov**, Dr.Sci. (Eng.), Associate Professor, Orel State University named after I.S. Turgenev (Orel, Russian Federation)

**Sergei A. Voronov**, Dr.Sci. (Eng.), Associate Professor, Russian Foundation of Fundamental Research (Moscow, Russian Federation)

**Sergey G. Parshin**, Dr.Sci. (Eng.), Associate Professor, St. Petersburg Polytechnic University (St. Petersburg, Russian Federation)

**Sergey M. Aizikovich**, Dr.Sci. (Phys.-Math.), Professor, Don State Technical University (Rostov-on-Don, Russian Federation)

**Tamaz M. Natriashvili**, Academician, Raphiel Dvali Institute of Machine Mechanics (Georgia)

**Umid M. Turdaliev**, Dr.Sci. (Eng.), Professor, Andijan Machine-Building Institute (Uzbekistan)

**Valentin L. Popov**, Dr.Sci. (Phys.-Math.), Professor, Berlin University of Technology (Germany)

**Valery N. Varavka**, Dr.Sci. (Eng.), Professor, Don State Technical University (Rostov-on-Don, Russian Federation)

**Victor A. Ereemeev**, Dr.Sci. (Phys.-Math.), Professor, Southern Scientific Center of RAS (Rostov-on-Don, Russian Federation)

**Victor M. Kureychik**, Dr.Sci. (Eng.), Professor, Southern Federal University (Rostov-on-Don, Russian Federation)

**Vilor L. Zakovorotny**, Dr.Sci. (Eng.), Professor, Don State Technical University (Rostov-on-Don, Russian Federation)

**Vladimir I. Lysak**, Dr.Sci. (Eng.), Professor, Volgograd State Technical University (Volgograd, Russian Federation)

**Vladimir I. Marchuk**, Dr.Sci. (Eng.), Professor, Institute of Service and Business, DSTU branch (Shakhty, Russian Federation)

**Vladimir M. Mladenovic**, Dr.Sci. (Eng.), Professor, University of Kragujevac (Serbia)

**Vladimir N. Sidorov**, Dr.Sci. (Eng.), Russian University of Transport (Moscow, Russian Federation)

**Vyacheslav G. Tsybulin**, Dr.Sci. (Phys.-Math.), Associate Professor, Southern Federal University (Rostov-on-Don, Russian Federation)

**Yuri O. Chernyshev**, Dr.Sci. (Eng.), Professor, Don State Technical University (Rostov-on-Don, Russian Federation)

## Редакционная коллегия

### Главный редактор

**Бескопыйный Алексей Николаевич**, доктор технических наук, профессор, Донской государственный технический университет (Ростов-на-Дону, Российская Федерация)

### Заместитель главного редактора

**Сухинов Александр Иванович**, член-корреспондент РАН, доктор физико-математических наук, профессор, Донской государственный технический университет (Ростов-на-Дону, Российская Федерация)

### Ответственный редактор

**Комахидзе Манана Гивневна**, кандидат химических наук, Донской государственный технический университет (Ростов-на-Дону, Российская Федерация)

### Ответственный секретарь

**Шевченко Надежда Анатольевна**, Донской государственный технический университет (Ростов-на-Дону, Российская Федерация)

**Айзикович Сергей Михайлович**, доктор физико-математических наук, профессор, Донской государственный технический университет (Ростов-на-Дону, Российская Федерация)

**Антибас Имад Ризакалла**, кандидат технических наук, Донской государственный технический университет (Ростов-на-Дону, Российская Федерация)

**Ахилан Аппатурай**, младший научный сотрудник, Инженерно-технологический колледж PSN, Университет Анны Ченнаи (Индия)

**Ахвердиев Камил Самед Оглы**, доктор технических наук, профессор, Ростовский государственный университет путей сообщения (Ростов-на-Дону, Российская Федерация)

**Варавка Валерий Николаевич**, доктор технических наук, профессор, Донской государственный технический университет (Ростов-на-Дону, Российская Федерация)

**Вернер Игорь Михайлович**, доктор технических наук, профессор, Технологический институт в Израиле (Израиль)

**Воронов Сергей Александрович**, доктор технических наук, доцент, Российский фонд фундаментальных исследований (Москва, Российская Федерация)

**Галушкин Николай Ефимович**, доктор технических наук, профессор, Институт сферы обслуживания и предпринимательства, филиал ДГТУ (Шахты, Российская Федерация)

**Лару Гиллеси**, доктор технических наук, профессор, Президент Общества машиностроителей (США)

**Аныш Губерт**, доктор наук, доцент, Варшавский технологический университет (Польша)

**Басмачи Гюльтекин**, доктор наук, профессор, Университет Бурдура Мехмета Акифа Эрсея (Турция)

**Дворников Олег Владимирович**, доктор технических наук, профессор, Белорусский государственный университет (Беларусь)

**Демехин Евгений Афанасьевич**, доктор физико-математических наук, профессор, Краснодарский филиал Финансового университета при Правительстве РФ (Краснодар, Российская Федерация)

**Хамид Абдулла Джалаб**, доктор наук (информатика и ИТ), университет Малайя (Малайзия)

**Егназарян Карен Оникович**, доктор технических наук, профессор, Технологический университет Тампере (Финляндия)

**Еремеев Виктор Анатольевич**, доктор физико-математических наук, профессор, Южный научный центр РАН (Ростов-на-Дону, Российская Федерация)

**Заковоротный Вилор Лаврентьевич**, доктор технических наук, профессор, Донской государственный технический университет (Ростов-на-Дону, Российская Федерация)

**Кавтарадзе Реваз Зурабович**, доктор технических наук, профессор, Институт механики машин им. Р. Двали (Грузия)

**Козубал Януш Виталис**, доктор технических наук, профессор, Вроцлавский технический университет (Польша)

**Хосе Карлос Куадрало**, доктор наук (электротехника и компьютеры), Политехнический институт Порту (Португалия)

**Кудиш Илья Исидорович**, доктор физико-математических наук, Университет Кеттеринга (США)

**Кузнецов Гений Владимирович**, доктор физико-математических наук, профессор, Томский политехнический университет (Томск, Российская Федерация)

**Курейчик Виктор Михайлович**, доктор технических наук, профессор, Южный федеральный университет (Ростов-на-Дону, Российская Федерация)

**Лысак Владимир Ильич**, доктор технических наук, профессор, Волгоградский государственный технический университет (Волгоград, Российская Федерация)

**Марчук Владимир Иванович**, доктор технических наук, профессор, Институт сферы обслуживания и предпринимательства, филиал ДГТУ (Шахты, Российская Федерация)

**Владимир Младенович**, доктор технических наук, профессор, Крагуевацкий университет (Сербия)

**Мукутадзе Мурман Александрович**, доктор технических наук, доцент, Ростовский государственный университет путей сообщения (Ростов-на-Дону, Российская Федерация)

**Наседкин Андрей Викторович**, доктор физико-математических наук, профессор, Южный федеральный университет (Ростов-на-Дону, Российская Федерация)

**Натришвили Тамаз Мамиевич**, академик, Институт механики машин им. Р. Двали (Грузия)

**Нгуен Донг Ань**, доктор физико-математических наук, профессор, Институт механики Академии наук и технологий Вьетнама (Вьетнам)

**Нгуен Суан Тьем**, доктор технических наук, Вьетнамский государственный технический университет им. Ле Куи Дона (Вьетнам)

**Паршин Сергей Георгиевич**, доктор технических наук, доцент, Санкт-Петербургский политехнический университет (Санкт-Петербург, Российская Федерация)

**Подмастерьев Константин Валентинович**, доктор технических наук, профессор, Орловский государственный университет им. И. С. Тургенева (Орел, Российская Федерация)

**Поляков Роман Николаевич**, доктор технических наук, доцент, Орловский государственный университет им. И. С. Тургенева (Орел, Российская Федерация)

**Попов Валентин Леонидович**, доктор физико-математических наук, профессор, Институт механики Берлинского технического университета (Германия)

**Прокопенко Николай Николаевич**, доктор технических наук, профессор, Донской государственный технический университет (Ростов-на-Дону, Российская Федерация)

**Рыбак Александр Тимофеевич**, доктор технических наук, профессор, Донской государственный технический университет (Ростов-на-Дону, Российская Федерация)

**Музафер Сарачевич**, доктор наук, профессор, Университет Нови-Пазара (Сербия)

**Саруханиян Арестак Арамаисович**, доктор технических наук, профессор, Национальный университет архитектуры и строительства Армении (Армения)

**Сидоров Владимир Николаевич**, доктор технических наук, Российский университет транспорта (Москва, Российская Федерация)

**Соловьёв Аркадий Николаевич**, доктор физико-математических наук, профессор, Крымский инженерно-педагогический университет имени Февзи Якубова (Симферополь, Республика Крым)

**Сумбатян Межлум Альбертович**, доктор физико-математических наук, профессор, Южный федеральный университет (Ростов-на-Дону, Российская Федерация)

**Тамаркин Михаил Аркадьевич**, доктор технических наук, профессор, Донской государственный технический университет (Ростов-на-Дону, Российская Федерация)

**Мурат Тезер**, профессор, Ближневосточный университет (Турция)

**Бертрам Торстен**, доктор технических наук, профессор, Технический университет Дортмунда (Германия)

**Турдалиев Умид Мухтаралиевич**, доктор технических наук, профессор, Андижанский машиностроительный институт (Узбекистан)

**Ахмет Уюмаз**, доктор технических наук, профессор, университет Бурдура Мехмета Акифа Эрсея (Турция)

**Али Маджид Хасан Алваэли**, доктор наук (компьютерная инженерия), доцент, Университет Аль-Нахрейн (Ирак)

**Цибулин Вячеслав Георгиевич**, доктор физико-математических наук, доцент, Южный федеральный университет (Ростов-на-Дону, Российская Федерация)

**Чернышев Юрий Олегович**, доктор технических наук, профессор, Донской государственный технический университет (Ростов-на-Дону, Российская Федерация)

**Хучан Ляо**, профессор, научный сотрудник ИААМ Старший член Школы бизнеса IEEE, Университет Сычуань (Китай)

**Языев Батыр Меретович**, доктор технических наук, профессор, Донской государственный технический университет (Ростов-на-Дону, Российская Федерация).

## Contents

### MECHANICS

- Dynamics of a Flat Rigid Body on a Horizontal Plane** ..... 7  
*Aleksander I. Munitsyn, Valeryan E. Tsoy*
- Analysis of a Four-Legged Robot Kinematics during Rotational Movements of Its Body** ..... 14  
*Marcelino J. Fernando, Gasan R. Saypulaev, Musa R. Saypulaev*
- Numerical Solution to the Problem of Thermal Conductivity in a Porous Plate with a Topology of Triply Periodic Minimal Surfaces** ..... 23  
*Kristina V. Gubareva, Anton V. Eremin*

### MACHINE BUILDING AND MACHINE SCIENCE

- Effect of Periodic Fluctuations of Cutting Mode Parameters on the Temperature of the Front Face of a Turning Tool** ..... 32  
*Evgeny V. Fominov, Valery E. Gvindjiliya, Andrey A. Marchenko, Constantine G. Shuchev*
- Investigation of the Optimal Vacuum Depth Created by an Ejector Depending on the Value of the Supply Pressure** ..... 43  
*Sergey I. Savchuk, Ervin D. Umerov, Aziz U. Abdulgazis*
- Using Surrogate Models in the Construction of a Pareto-Optimal Positioning Electropneumatic Actuator with Discrete Pneumatic Valves** ..... 52  
*Maxim O. Sheykin, Sergey N. Cherkasskikh, Denis V. Shilin, Vladimir V. Fedenkov*

### INFORMATION TECHNOLOGY, COMPUTER SCIENCE AND MANAGEMENT

- Controllability Analysis and Optimization of Hydrocannon Nozzle Shape Based on Direct Extreme Approach** ..... 65  
*Victor K. Tolstykh, Yuliia V. Dmitruk*

## Содержание

### МЕХАНИКА

- Динамика плоского твердого тела на горизонтальной плоскости** ..... 7  
*А.И. Муницын, В.Э. Цой*
- Анализ кинематики четвероногого робота при поворотных движениях его корпуса** ..... 14  
*М.Ж. Фернандо, Г.Р. Сайпулаев, М.Р. Сайпулаев*
- Численное решение задачи теплопроводности в пористой пластине с топологией трижды периодических минимальных поверхностей** ..... 23  
*К.В. Губарева, А.В. Еремин*

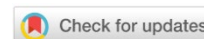
### МАШИНОСТРОЕНИЕ И МАШИНОВЕДЕНИЕ

- Влияние периодических флуктуаций параметров режимов резания на температуру передней поверхности токарного резца** ..... 32  
*Е.В. Фоминов, В.Е. Гвинджилия, А.А. Марченко, К.Г. Шучев*
- Исследование оптимальной глубины вакуума, создаваемой эжектором в зависимости от величины питающего давления** ..... 43  
*С.И. Савчук, Э.Д. Умеров, А.У. Абдулгазис*
- Использование суррогатных моделей при построении множества Парето позиционного электропневматического привода с дискретными пневмораспределителями** ..... 52  
*М.О. Шейкин, С.Н. Черкасских, Д.В. Шилин, В.В. Феденков*

### ИНФОРМАТИКА, ВЫЧИСЛИТЕЛЬНАЯ ТЕХНИКА И УПРАВЛЕНИЕ

- Анализ управляемости и оптимизация формы сопла гидропушки на основе прямого экстремального подхода** ..... 65  
*В.К. Толстых, Ю.В. Дмитрук*

# MECHANICS МЕХАНИКА



UDC 531.46

Original Empirical Research

<https://doi.org/10.23947/2687-1653-2025-25-1-7-13>

## Dynamics of a Flat Rigid Body on a Horizontal Plane

**Aleksander I. Munitsyn** , **Valeryan E. Tsoy**  

National Research University MPEI, Moscow, Russian Federation

✉ [tsoyve@mpei.ru](mailto:tsoyve@mpei.ru)

EDN: ATOYXO

### Abstract

**Introduction.** The study of the motion of a rigid body carrying moving masses greatly simplifies the design of capsule robots that can move inside aggressive environments and perform the required operations. The following cases have been studied quite well: movement during interaction of a solid body with a reference plane and in aggressive environments; vibratory displacement of bulk media and solids on a vibrating base; optimization of rigid body motion; variation of average speed and acceleration at different intervals of motion; dependence of average speed on task parameters; control of the motion speed of the internal mass for the fastest possible rotation of a rigid body. However, at present, insufficient attention has been paid in the literature to the problems of studying the motion of a heavy flat body along a horizontal plane under the action of a harmonic force directed at an angle to the horizon, specifically, in terms of taking into account all possible driving modes and their features. This does not allow determining the optimal parameters of the problem. Therefore, the objective of this research was to identify the features of all possible modes of motion of a heavy solid body along a horizontal plane under the action of a harmonic force directed at an angle to the horizon.

**Materials and Methods.** The equations of motion of the mechanical system were used. Both analytical approaches and numerical methods were used to solve the steady-state equations of motion of the system. The dry friction model was adopted as a friction model, which made it possible to obtain accurate solutions for positive and negative values of the slip velocity up to constants. Values of these constants were determined from the docking conditions and the periodicity of the solution.

**Results.** An analytical solution to the problem for periodic solutions was obtained. Three possible motion modes were identified. Using numerical analysis, the dependences of the average speed of a body motion over the period on the angle of inclination of the force to the horizon were constructed. The optimal direction of force was established.

**Discussion and Conclusion.** The results of the conducted research allowed us to determine the optimal values of the problem parameters in order to reach the required value of the average velocity of a solid body. In particular, optimal values of the amplitude of the force and its direction can be found to reach the maximum value of the average velocity of motion of a solid.

**Keywords:** reference plane, dry friction, nonlinear vibrations, motion mode, flat rigid body, horizontal plane

**Acknowledgements.** The authors would like to thank the Editorial board and the reviewers for their attentive attitude to the article and for the specified comments that improved the quality of the article.

**For Citation.** Munitsyn AI, Tsoy VE. Dynamics of a Flat Rigid Body on a Horizontal Plane. *Advanced Engineering Research (Rostov-on-Don)*. 2025;25(1):7–13. <https://doi.org/10.23947/2687-1653-2025-25-1-7-13>

## Динамика плоского твердого тела на горизонтальной плоскости

А.И. Муницын , В.Э. Цой  

Национальный исследовательский университет «МЭИ», г. Москва, Российская Федерация

 [tsoyve@mpei.ru](mailto:tsoyve@mpei.ru)

### Аннотация

**Введение.** Исследование движения твердого тела, несущего подвижные массы, значительно упрощает проектирование капсульных роботов, которые могут перемещаться внутри агрессивных сред и выполнять необходимые операции. Достаточно хорошо изучены случаи: движения при взаимодействии твердого тела с опорной плоскостью и в агрессивных средах; вибрационного перемещения сыпучих сред и твердых тел на вибрирующем основании; оптимизации движения твердых тел; варьирования средней скорости и ускорения на различных интервалах движения; зависимости средней скорости от параметров задачи; управления скоростью перемещения внутренней массы для наискорейшего поворота твердого тела. Однако в настоящее время в литературе уделено недостаточно внимания задачам исследования движения тяжелого плоского тела по горизонтальной плоскости под действием гармонической силы, направленной под углом к горизонту, особенно в плане учета всех возможных режимов движения и их особенностей. Это не позволяет определять оптимальные параметры задачи. Поэтому целью данной работы стало выявление особенностей всех возможных режимов движения тяжелого твердого тела по горизонтальной плоскости под действием гармонической силы, направленной под углом к горизонту.

**Материалы и методы.** В работе использовали уравнения движения механической системы. Для решения стационарных уравнений движения системы применялись как аналитические подходы, так и численные методы. В качестве модели трения была принята модель сухого трения, что позволило получить точные решения для положительного и отрицательного значения скорости проскальзывания с точностью до констант. Значения этих констант определялись из условий стыковки и периодичности решения.

**Результаты исследования.** Получено аналитическое решение задачи для периодических решений. Выявлены три возможных режима движения. С помощью численного анализа построены зависимости средней за период скорости движения тела от угла наклона силы к горизонту. Установлено оптимальное направление силы.

**Обсуждение и заключение.** Результаты проведенных исследований позволяют определить оптимальные значения параметров задачи для достижения необходимого значения средней скорости движения твердого тела. В частности, могут быть найдены оптимальные значения амплитуды силы и ее направления для достижения максимального значения средней скорости движения твердого тела.

**Ключевые слова:** опорная плоскость, сухое трение, нелинейные колебания, режим движения, плоское твердое тело, горизонтальная плоскость

**Благодарности.** Авторы выражают благодарность редакции и рецензентам за внимательное отношение к статье и указанные замечания, которые позволили повысить ее качество.

**Для цитирования.** Муницын А.И., Цой В.Э. Динамика плоского твердого тела на горизонтальной плоскости. *Advanced Engineering Research (Rostov-on-Don)*. 2025;25(1):7–13. <https://doi.org/10.23947/2687-1653-2025-25-1-7-13>

**Introduction.** Recently, the tasks of designing the movement of robots carrying the required objects, including those moving in aggressive environments [1] and capable of performing the requested operations [2], have become increasingly urgent. As a rule, the model that takes into account the interaction of a solid body with a reference plane is the dry friction model [3]. This task has a lot in common with the task of vibratory movement of bulk media and solids on a vibrating base [4]. Optimization of the capsule robot motion with varying average speed was considered in [5]. In [6], acceleration was varied at different motion intervals. A capsule robot, the control of which was based on these two principles, was studied in [7]. In [8], optimization of average speed was presented. In [9], a mathematical model of the electromagnetic force of core retraction was constructed. The dependence of average speed on excitation parameters was studied in [10]. In [11], the law of control of the speed of the internal mass for the fastest turn of the robot was investigated. The motion of a capsule robot with two masses moving along parallel guides was considered in [12], and along two mutually perpendicular guides — in [13]. Robots with linearly moving masses and a rotor were described in [14]. In all the listed papers, the motion of a rigid body along a horizontal plane under the action of a harmonic force directed at an angle to the horizon was not studied, and various motion modes and their features were not

established. Therefore, this research was aimed at identifying the features of all possible modes of motion of a rigid body along a horizontal plane under the action of a harmonic force directed at an angle to the horizon. Achieving this objective allows us to determine the optimal parameters of the research problem, such as: the optimal angle of action of the force to build up maximum speed, the necessary and optimal values of the parameters of the research problem to build up the required speed of motion of a rigid body.

**Materials and Methods.** To solve the problem, we compose an equation of motion for a mechanical system. The solution to the equation for each mode of motion can be obtained separately.

*Equations of Motion.* A body has mass  $m$  and moves along the horizontal plane along the  $x$ -axis. The body is subjected to harmonic force  $F = A_0 \cos(\theta t)$ , directed at angle  $\beta$  to the horizontal plane, where  $A_0$  — amplitude of the acting external force;  $\theta$  — frequency of the acting external force. Let  $V_x$  be the speed of the body in the horizontal direction;  $V_y$  — speed of the body in the vertical direction.

The motion of a rigid body is described by a system of two equations:

$$\begin{aligned} m \frac{dV_x}{dt} &= \eta N s + A_0 \cos \beta \cos(\theta t), \\ m \frac{dV_y}{dt} &= A_0 \sin \beta \cos(\theta t) + N - mg, \end{aligned}$$

where  $g$  — gravitational acceleration;  $N$  — reaction force of the base. In the equations given, the friction force is taken into account using the Coulomb model. For this purpose, the coefficient of dry friction  $\eta$  and dimensionless parameter  $s$  are introduced, which at rest can take any value in the range from  $-1$  to  $1$ . In the case of slippage, when  $V_x$  is not equal to zero, the friction force is constant and directed opposite to the slip velocity. The dimensionless parameter is given by expression  $s = -\text{sign}(V_x)$ .

Next, we assume that the reaction forces of the base are distributed uniformly over the reference surface, and the body moves without separation from the base, i.e., the body speed in the vertical direction is zero. Of the two equations for describing the motion of a rigid body, one remains — for movement in the horizontal direction:

$$\frac{dV}{dt} = \eta s (1 - A \sin \beta \cos T) + A \cos \beta \cos T, \quad (1)$$

where  $T = \theta t$  — nondimensional time;  $V = V_x \theta / g$  — dimensionless speed and dimensionless amplitude of vibration excitation  $A = A_0 / (mg)$ .

A similar problem of the motion of a rigid body carrying an unbalanced rotor along an inclined plane was considered in [15]. Equation (1) has a trivial solution at  $V(t)=0$ . This means that the body is at rest during the time interval under consideration. Then, the friction force parameter changes according to the following law:

$$s = \frac{A \cos \beta \cos T}{\eta (1 - A \sin \beta \cos T)}. \quad (2)$$

At this, the amplitude value of the projection of the external force onto the horizontal axis is not enough to start the body movement.

*Motion with two instantaneous stops.* The solution to equation (1) in the case of slippage between the body and the base:

$$V_k(T) = \eta s_k [T - A \sin \beta \cos T] + A \cos \beta \sin T + C_k, \quad k = 1, 2. \quad (3)$$

Here, the following notations are introduced:  $V_1$  — for the positive velocity of the body, to which  $s_1 = -1$  corresponds;  $V_2$  — for the negative velocity;  $s_2 = 1$ . From here on, we will consider stationary solutions to the equation of motion of the body. We introduce the following notations for the motion of the body with a positive velocity:  $\varphi_{11}$  denotes the start time of the motion, and  $\varphi_{12}$  — the end time of the motion of the body, through  $\varphi_{21}$  and  $\varphi_{22}$  — the same values for motion with negative velocity. For six unknowns, we obtain four equations:

$$V_k(\varphi_{k_1}) = -\eta s_k A \sin \beta \sin(\varphi_{k_1}) + A \cos \beta \sin(\varphi_{k_1}) + \eta s_k \varphi_{k_1} + C_k = 0; \quad (4)$$

$$V_k(\varphi_{k_2}) = -\eta s_k A \sin \beta \sin(\varphi_{k_2}) + A \cos \beta \sin(\varphi_{k_2}) + \eta s_k \varphi_{k_2} + C_k = 0. \quad (5)$$

$$k = 1, 2.$$

From the condition of absence of a long stop of the body, we obtain two more conditions:

$$\varphi_{12} = \varphi_{21}, \quad (6)$$

$$\varphi_{22} = \varphi_{11} + 2p. \quad (7)$$

The integration constants  $C_1$  and  $C_2$  can be eliminated from equations (4) and (5). From the obtained equations, phases  $\varphi_{11}$ ,  $\varphi_{12}$ ,  $\varphi_{21}$  and  $\varphi_{22}$  are found numerically. The resulting transcendental equations have two solutions each. To select the correct solution, we determine the second derivative of the velocity:

$$\frac{d^2V_k}{dT^2}(\varphi_{k_1}) = A(-\cos\beta\cos(\varphi_{k_1}) + \eta s_k \sin\beta\sin(\varphi_{k_1})), \quad (8)$$

which should be positive at  $k = 1$  and negative at  $k = 2$ .

*Motion with two long stops.* In this case, conditions (6) and (7) are not valid. When moving from rest to motion, the acceleration of the body must be zero:

$$\frac{dV_k}{dT}(\varphi_{k_1}) = \eta s_k (1 - A \sin\beta \cos(\varphi_{k_1})) + A \cos\beta \cos(\varphi_{k_1}) = 0; k = 1, 2. \quad (9)$$

From equation (9), we obtain an exact solution for the phases of motion:

$$\varphi_{k_1} = \arccos\left(-\frac{\eta s_k}{A \cos\beta - \eta s_k \sin\beta}\right). \quad (10)$$

The required root is determined similarly to the previous case. Constant  $C_k$  and phase  $\varphi_{k2}$  are found from (4) and (5). If the condition  $A > \eta / (\cos\beta + \eta \sin\beta)$  is true, the body can move with a speed greater than zero; and provided that the amplitude of the excitation of oscillations is  $A > \eta / (\cos\beta + \eta \sin\beta)$ , the body moves with a speed less than zero.

If the end time of the body motion with positive velocity  $\varphi_{12}$  is less than the start time of the body motion with negative velocity  $\varphi_{21}$ , and  $\varphi_{21}$  is less than  $\varphi_{11} + 2p$ , then the motion of the rigid body can have two long stops.

*Let us consider the motion of a body with instantaneous and prolonged stops.* The reaction of the horizontal base, as well as the force acting on the body, changes according to a harmonic law, periodic solutions are possible here.

In the case of a rigid body moving with a positive velocity and an instantaneous transition to negative, and from negative to positive, after a long stop, we obtain a system of equations (4), (5) for  $k = 1, 2$  (9), for  $k = 1$  and condition  $\varphi_{12} = \varphi_{21}$ . Phase  $\varphi_{11}$  is determined by expression (10). For the remaining unknowns, an exact solution is also determined. The obtained solution is valid when the condition  $\varphi_{22} < \varphi_{11} + 2p$  is met.

In the instantaneous transition from negative to positive velocity of a rigid body, and from positive to negative, after a long stop, the system of equations (4–5) for  $k = 1, 2$  remains unchanged. We compose equation (9) for  $k = 2$ , and replace the instantaneous stop condition with  $\varphi_{22} = \varphi_{11} + 2p$ .

Thus, for all possible modes of stationary motion of a rigid body, four phases and two integration constants are determined. On one period of motion, using formulas (3), it is possible to construct the dependence of the average velocity of motion of rigid body  $v_m$  on the angle of inclination of the line of action of the external force  $\beta$ . On the interval  $\varphi_{11} < t < \varphi_{12}$ , the rigid body moves with a velocity greater than zero, and when  $\varphi_{21} < t < \varphi_{22}$ , the rigid body moves with a velocity less than zero. On the interval  $\varphi_{12} < t < \varphi_{21}$  and  $\varphi_{22} < t < \varphi_{11} + 2p$ , the rigid body does not move. When  $\varphi_{12}$  and  $\varphi_{21}$  or  $\varphi_{22}$  and  $\varphi_{11} + 2p$  coincide, the velocity of the body at these points changes instantly.

The constructed solution for three types of motion and a state of rest (2) for one period of oscillations allows us to determine the average speed of motion of a rigid body:

$$V_m = \frac{1}{2\pi} \int_{\varphi_{11}}^{\varphi_{22}} V(T) dT.$$

**Research Results.** The results of the study were obtained with dry friction coefficient  $\eta = 0.1$  and excitation amplitude  $A = 0.6$ . The dependences of the four phases  $\varphi_{kj}(\beta)$ , ( $ji k = 1, 2$ ) on the angle of inclination of the external force to the horizon are shown in Figure 1. The dotted curves indicate the points of instantaneous change in the speed of the body, and the solid curves indicate the points of change in speed with a long stop.

At small angles of inclination of force  $\varphi_{12} = \varphi_{21}$ ,  $\varphi_{22} = \varphi_{11} + 2p$ , the motion of the rigid body occurs with two instantaneous stops. The motion pattern changes when angle  $\beta$  increases. At point  $B_1$ , the curve branches  $\varphi_{22}(\beta) = \varphi_{11}(\beta) + 2p$ . As a result, we have two curves:  $\varphi_{22}(\beta)$  and  $\varphi_{11}(\beta)$ , and at point  $B_2$ , the curve  $\varphi_{12}(\beta) = \varphi_{21}(\beta)$  branches into  $\varphi_{12}(\beta)$  and  $\varphi_{21}(\beta)$ . Between points  $B_1$  and  $B_2$ , the rigid body may have a long and instantaneous stop. Between points  $B_2$  and  $B_3$ , the motion may have two long stops. At point  $B_3$ , curves  $\varphi_{22}(\beta)$  and  $\varphi_{21}(\beta)$  merge. Between points  $B_3$  and  $B_4$ , during the motion of the rigid body within one period at a speed greater than zero, there may be one long stop. At large values of the angle of inclination, the body is at rest.

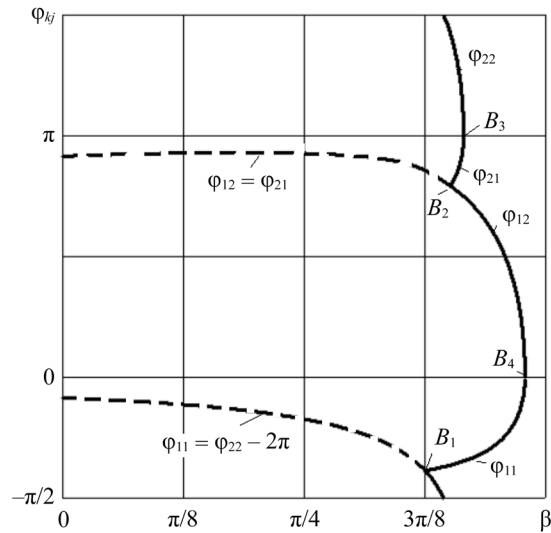


Fig. 1. Dependences of phases of stationary motion on the angle of inclination of the applied force

Figure 2 shows the dependences of the average velocity of solid body  $v_m$  on the angle of inclination of the line of action of the external force  $\beta$  for friction coefficient 0.1 and several excitation amplitudes. For any values of the excitation amplitude and horizontal action of the force ( $\beta = 0$ ), the average velocity of the solid body is zero. With an increase in  $\beta$ , the average velocity grows up. The points of change of the motion modes are indicated only on the curve  $A = 0.6$ . For each value of the force amplitude, there is an optimal angle at which the average velocity of motion is maximum.

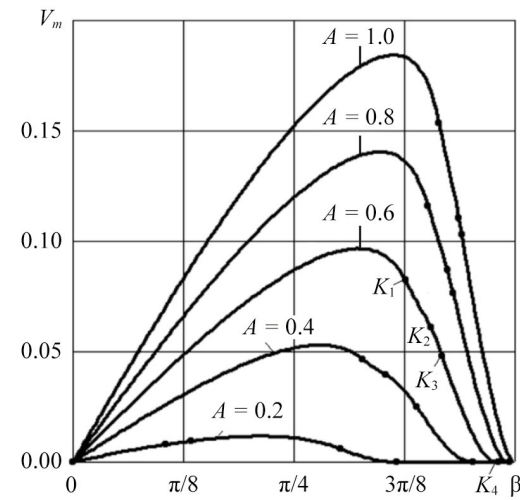


Fig. 2. Dependence of average speed  $V_m$  on angle  $\beta$

**Discussion and Conclusion.** The motion of a rigid body along a horizontal plane under the action of a harmonic force directed at an angle to the horizon is studied. The analytical and numerical results show that for all possible modes of stationary motion of a rigid body, four phases are determined. The obtained dependences of the phases of stationary motion and the average speed of motion of a rigid body on the angle of inclination of the line of action of an external force allow us to determine the necessary and optimal values of the parameters of the problem to achieve the required speed of motion of a rigid body. It is shown that for each value of the amplitude of the force, there is an optimal angle at which the average speed of motion is maximum.

The results obtained can be used in the development of algorithms and design of the movement of robotic devices when moving along a horizontal plane, taking into account the action of harmonic loads.

### References

1. Chernousko FL. Plane Motions by Rigid Body Controlled by means of Movable Mass. *Doklady RAN: Physics*. 2020;494(1):69–74.
2. Chernousko FL. Optimal Motion Control of a Two–Mass System. *Doklady AN*. 2018;480(5):528–532. (In Russ.)
3. Andronov VV, Zhuravlev VF. *Dry Friction in Problems of Mechanics*. Monograph. Moscow–Izhevsk: Publ. House “IKI”; 2010. 184 p. (In Russ.)

4. Blekhman II. *Vibrational Mechanics and Vibrational Rheology (Theory and Applications)*. Moscow: Fizmatlit; 2018. 751 p. (In Russ.)
5. Chernousko FL. On the Motion of a Body Containing a Movable Internal Mass. *Doklady AN*. 2005;405(1):56–60. (In Russ.)
6. Chernous'ko FL. Analysis and Optimization of the Motion of a Body Controlled by means of a Movable Internal Mass. *Journal of Applied Mathematics and Mechanics*. 2006;70(6):819–842. <https://doi.org/10.1016/j.jappmathmech.2007.01.003>
7. Hongyi Li, Katsuhisa Furuta, Felix L Chernousko. Motion Generation of the Capsbot Using Internal Force and Static Friction. In: *Proc. 45th IEEE Conference on Decision and Control*. New York City: IEEE; 2006. P. 6575–6580. <https://doi.org/10.1109/CDC.2006.377472>
8. Nunuparov AM, Sukhanov AN, Syrykh NV. Optimization of the Average Speed of a Capsule Robot by Nonlinear Model-Proactive Control. In: *Proc. XXXIII International Innovative Conference of Young Scientists and Students on Problems of Machine Science*. Moscow: IMASH RAN; 2021. P. 436–441. (In Russ.)
9. Syrykh NV, Nunuparov AM, Sukhanov AN. On Building a Mathematical Model of the Electromagnetic Force of a Solenoid for a Capsule Robot. In: *Proc. XXXIII International Innovative Conference of Young Scientists and Students on Problems of Machine Science*. Moscow: IMASH RAN; 2021. P. 484–490. (In Russ.)
10. Bolotnik NN, Nunuparov AM, Chashchukhin VG. Capsule-Type Vibration-Driven Robot with an Electromagnetic Actuator and an Opposing Spring: Dynamics and Control of Motion. *Journal of Computer and Systems Sciences International*. 2016;(6):146–160.
11. Shmatkov AM. Periodic Solutions to the Optimal Control Problem of Rotation of a Rigid Body Using Internal Mass. *Moscow University Bulletin. Mathematics. Mechanics*. 2020;(3):63–67. URL: <https://www.mathnet.ru/links/3f7d22880247a4d39922b11f27ea3c8c/vmumm4333.pdf> (accessed: 18.11.2024).
12. Sakharov AV. Rotation of a Body with Two Movable Internal Masses on a Rough Plane. *Journal of Applied Mathematics and Mechanics*. 2015;79(2):132–141. URL: <https://pmm.ipmnet.ru/ru/Issues.php?y=2015&n=2&p=196> (accessed: 18.11.2024).
13. Xiong Zhang, Jian Xu, Hongbin Fang. A Vibration-Driven Planar Locomotion Robot – *Shell*. *Robotica*. 2018;36(9):1402–1420. <http://doi.org/10.1017/S0263574718000383>
14. Chernousko FL. Movement of a Body along a Plane under the Influence of Moving Internal Masses. *Doklady AN*. 2016;470(4):406–410. (In Russ.)
15. Munitsyn AI, Krainova LN. Vibratory Motion of a Rigid Body along an Inclined Plane. *Engineering and Automation Problems*. 2023;(1):31–35.

#### **About the Authors:**

**Alexander I. Munitsyn**, Dr.Sci. (Eng.), Professor of the Robotics, Mechatronics, Dynamics and Strength of Machines Department, National Research University MPEI (14, Krasnokazarmennaia Str., Moscow, 111250, Russian Federation), [SPIN-code](#), [ORCID](#)

**Valeryan E. Tsoy**, Cand.Sci. (Phys.-Math.), Associate Professor of the Robotics, Mechatronics, Dynamics and Strength of Machines Department, National Research University MPEI (14, Krasnokazarmennaia Str., Moscow, 111250, Russian Federation), [SPIN-code](#), [ORCID](#), [tsoyve@mpei.ru](mailto:tsoyve@mpei.ru)

#### **Claimed Contributorship:**

**AI Munitsyn**: description of the theoretical part of the study of the movement of a heavy flat body along a horizontal plane under the action of a harmonic force directed at an angle to the horizon; preparation of the scientific paper.

**VE Tsoy**: conducting numerical simulations, preparation of the scientific paper.

**Conflict of Interest Statement: the authors declare no conflict of interest.**

**All the authors have read and approved the final manuscript.**

#### **Об авторах:**

**Александр Иванович Муницын**, доктор технических наук, профессор кафедры робототехники, мехатроники, динамики и прочности машин Национального исследовательского университета «МЭИ» (111250, Российская Федерация, г. Москва, ул. Красноказарменная, д. 14, стр. 1), [SPIN-код](#), [ORCID](#)

**Валерьян Эдуардович Цой**, кандидат физико-математических наук, доцент кафедры робототехники, мехатроники, динамики и прочности машин Национального исследовательского университета «МЭИ» (111250, Российская Федерация, г. Москва, ул. Красноказарменная, д. 14, стр. 1), [SPIN-код](#), [ORCID](#), [tsoyve@mpei.ru](mailto:tsoyve@mpei.ru)

***Заявленный вклад авторов:***

**А.И. Муницын:** описание теоретической части исследования движения тяжелого плоского тела по горизонтальной плоскости под действием гармонической силы, направленной под углом к горизонту; оформление научной статьи.

**В.Э. Цой:** проведение численного моделирования, оформление научной статьи.

***Конфликт интересов:*** авторы заявляют об отсутствии конфликта интересов.

***Все авторы прочитали и одобрили окончательный вариант рукописи.***

**Received / Поступила в редакцию 16.12.2024**

**Reviewed / Поступила после рецензирования 14.01.2025**

**Accepted / Принята к публикации 20.01.2025**

# MECHANICS МЕХАНИКА



UDC 531.133.1

Original Theoretical Research

<https://doi.org/10.23947/2687-1653-2025-25-1-14-22>

## Analysis of a Four-Legged Robot Kinematics during Rotational Movements of Its Body

Marcelino J. Fernando , Gasan R. Saypulaev ✉, Musa R. Saypulaev 

National Research University MPEI, Moscow, Russian Federation

✉ [saypulaevgr@mail.ru](mailto:saypulaevgr@mail.ru)



EDN: YINENP

### Abstract

**Introduction.** Walking robots are widely used in industry due to their unique capabilities for moving on uneven and complex surfaces. To provide high precision in controlling their movement, it is required to develop mathematical models and algorithms for planning the robot movement along various trajectories. A key aspect of the motion control system of walking robots is the planning of their leg movements. Despite significant advances in the field of modeling the kinematics of quadruped robots, existing scientific publications do not provide a complete kinematic model for robots similar to the Mini Cheetah. This research was aimed at the development of a kinematic model of a quadruped robot based on Mini Cheetah, as well as the formulation of recommendations for optimizing its gait to provide rotation around various axes. The creation of such a model will improve the smoothness and accuracy of the robot movements, which, in turn, will increase its efficiency under real production conditions.

**Materials and Methods.** The process of constructing a kinematic model of the robot was based on the use of formulas for the geometry of spatial motion of solids. To test the efficiency of the proposed algorithms for moving the robot legs when performing rotational movements of its body, numerical modeling of the robot kinematics was used. Numerical calculations were performed using the *Wolfram Mathematica* package.

**Results.** The laws of changing the endpoints of the robot legs during its rotation around the vertical axis were proposed. The conducted numerical modeling of the robot kinematics covered the rotation of the body at the course, roll and pitch angles. Based on the simulation results, it was established that the dependences of the rotation angles of the leg links were periodic functions. The considered rotational movements of the robot platform could take place without the occurrence of singular configurations.

**Discussion and Conclusion.** The results of numerical modeling of the robot platform rotation movements confirmed the operability of the proposed leg transfer plan, which allowed for smooth movement of the robot body and avoidance of singular configurations. The resulting kinematic model can be used to control the robot motion at the kinematic level when moving along curvilinear trajectories. As a prospect for further research, it is worth highlighting the development of a mathematical model of the dynamics of a four-legged robot, as well as the creation of laws for controlling its movement at a dynamic level. This will significantly expand the functionality of the robot and increase its efficiency under various operating conditions.

**Keywords:** four-legged robot, inverse kinematics, mobile robot, kinematic model, motion planning

**Acknowledgements.** The authors would like to thank their colleagues for valuable comments made during the work on the publication

**For Citation.** Fernando MJ, Saypulaev GR, Saypulaev MR. Analysis of a Four-Legged Robot Kinematics during Rotational Movements of Its Body. *Advanced Engineering Research (Rostov-on-Don)*. 2025;25(1):14–22. <https://doi.org/10.23947/2687-1653-2025-25-1-14-22>

## Анализ кинематики четвероногого робота при поворотных движениях его корпуса

М.Ж. Фернандо , Г.Р. Сайпулаев ✉, М.Р. Сайпулаев 

Национальный исследовательский университет «МЭИ», г. Москва, Российская Федерация

✉ [saypulaevgr@mail.ru](mailto:saypulaevgr@mail.ru)

### Аннотация

**Введение.** Шагающие роботы находят широкое применение в промышленности благодаря своим уникальным возможностям передвижения по неровным и сложным поверхностям. Для обеспечения высокой точности управления их движением необходимо разработать математические модели и алгоритмы планирования перемещения робота по различным траекториям. Ключевым аспектом системы управления движением шагающих роботов является планирование перемещений их ног. Несмотря на значительные достижения в области моделирования кинематики четвероногих роботов, в существующих научных публикациях не представлено полноценной кинематической модели для роботов, аналогичных Mini Cheetah. Цель данной работы заключается в разработке кинематической модели четвероногого робота на основе Mini Cheetah, а также в формулировании рекомендаций по оптимизации его походки для обеспечения вращения вокруг различных осей. Создание такой модели позволит улучшить плавность и точность движений робота, что, в свою очередь, повысит его эффективность в реальных производственных условиях.

**Материалы и методы.** Процесс построения кинематической модели робота основан на использовании формул геометрии пространственного движения твердых тел. Для проверки эффективности предложенных алгоритмов перемещения ног робота при осуществлении поворотных движений его корпуса было применено численное моделирование кинематики робота. Численные расчеты выполнены с использованием математического пакета *Wolfram Mathematica*.

**Результаты исследования.** Предложены законы изменения конечных точек ног робота при его вращении вокруг вертикальной оси. Проведенное численное моделирование кинематики робота охватывало повороты корпуса по углам курса, крена и тангажа. По результатам моделирования установлено, что зависимости углов поворота звеньев ног являются периодическими функциями.

Рассмотренные поворотные движения платформы робота могут происходить без возникновения сингулярных конфигураций.

**Обсуждение и заключение.** Результаты численного моделирования поворотных движений платформы робота подтвердили работоспособность предложенного плана переноса ног, который позволяет осуществлять плавное движение корпуса робота и избегать сингулярных конфигураций. Полученная кинематическая модель может быть использована для управления движением робота на кинематическом уровне при перемещениях по криволинейным траекториям. В качестве перспективы для дальнейших исследований стоит выделить разработку математической модели динамики четвероногого робота, а также создание законов управления его движением на динамическом уровне. Это позволит значительно расширить функциональные возможности робота и повысить эффективность его работы в различных условиях эксплуатации.

**Ключевые слова:** четвероногий робот, обратная кинематика, мобильный робот, кинематическая модель, планирование движения

**Благодарности.** Авторы выражают признательность коллегам с кафедры РМДиПМ «НИУ «МЭИ» за ценные замечания, высказанные в ходе работы над публикацией.

**Для цитирования.** Фернандо М.Ж., Сайпулаев Г.Р., Сайпулаев М.Р. Анализ кинематики четвероногого робота при поворотных движениях его корпуса. *Advanced Engineering Research (Rostov-on-Don)*. 2025;25(1):14–22. <https://doi.org/10.23947/2687-1653-2025-25-1-14-22>

**Introduction.** Currently, walking mobile robots are widely used to solve problems of observation and exploration of territories [1]. An example of one of the common designs of such robots is the four-legged robot *Mini Cheetah* (Fig. 1), developed at *MIT Biomimetic Robotics Lab* (<https://biomimetics.mit.edu>). These four-legged robots can move on various types of terrain, unlike wheeled or tracked robots.



Fig. 1. Four-legged robot *Mini Cheetah* <sup>1</sup>

The design of the walking robots under consideration includes a platform to which four legs are attached. Each of the legs is a three-link manipulator. One of the key aspects of a walking robot is the topology of its leg structure [2, 3]. The topology of the legs refers to the composition and arrangement of the links, as well as the hinges of the limbs of a four-legged robot, which play an important role in providing its movement and stability. The development of an optimal topology for the leg structure of quadruped robots is one of the challenges in engineering. The solution to this problem not only helps to provide stable and efficient gait (locomotion) of the robot on various surfaces, but also makes its mechanical design more reliable and energy efficient.

Another aspect that needs to be considered is the drive system applied in quadruped robots [4]. Different types of drives are widely used in such robots, including pneumatic [5], hydraulic [6, 7], and electric [2, 6], each of which has its own advantages and disadvantages.

Four-legged robots have complex kinematics due to a large number of degrees of freedom. The robot considered in this paper has 18 degrees of freedom. To provide successful locomotion of four-legged robots, it is necessary to solve both direct and inverse problems of kinematics, which allows organizing dynamic control of the position of the legs of these robots. This control should provide the robot balancing, the ability to overcome various surfaces, and adaptation to various types of locomotion, including walking, running and jumping. The direct problem of walking robot kinematics is to determine the position and orientation of the robot platform based on the known rotation angles of the leg links. The inverse problem is to find the rotation angles of the leg links that provide a given position and orientation of the robot platform.

Paper [8] described in detail the application of the Denavit-Hartenberg method for modeling the forward and inverse kinematics of a walking robot. The study on the kinematic model of the robot was conducted with the aim of creating a gait algorithm.

The authors of [9] developed advanced kinematic and dynamic modeling methodologies based on the screw theory for quadruped robots. The proposed methods accounted for different gaits and leg mechanism topologies using simplified models of foot contact (e.g., a ball-and-socket model). Models were described for three separate phases of robot motion: standing, walking, and unsupported (flying) phase. The developed control strategies used the presented models for gait planning and jogging.

In recent years, scientists have been working on control and trajectory planning systems. The motion control method is the basis of a four-legged robot, directly affecting flexibility, stability and the ability to adapt to various support surfaces [3].

The authors of [10] specified the design of a regulator for the force control of a four-legged robot. The main purpose of the regulator was to equalize the forces acting on the robot during symmetrical gait, as well as to reduce disturbances and absorb impacts.

In [11], a new motion control strategy for a quadruped robot that enabled it to navigate efficiently on uneven terrains regardless of visual perception conditions was proposed. Paper [12] discussed the design of a motion controller for a quadruped robot that used torque optimization and performance control to account for the impact of unpredictable external forces such as surface irregularities.

Experimental studies devoted to the application of hierarchical controllers for motion control of quadruped robots were presented in [13], illustrated by the ANYmal robot, and in [14], exemplified by the StarLETH robot.

In [15], the authors discussed the development of a quadruped robot designed for construction and emergency response tasks. Their paper examined the statics, kinematics, and control system for the specific design of this robot.

Finally, in [16], a new central pattern generator model controller and gait switching tactic based on the Wilson-Cowan model were presented. This development aimed to create a smooth robot gait and reduce the adjustment time in the oscillating mechanical system.

Despite the development of the problem of modeling the kinematics of quadruped robots, in existing publications there was no complete kinematic model of the motion of robots whose leg design was similar to the *Mini Cheetah* robot (Fig. 1). Therefore, the objective of this work was to develop a kinematic model of a quadruped robot using the example of the *Mini Cheetah* and to develop proposals for planning the movements of the robot links that could provide the rotation of the robot around various axes.

<sup>1</sup> Massachusetts Institute of Technology. URL: <https://news.mit.edu/2019/mit-mini-cheetah-first-four-legged-robot-to-backflip-0304> (accessed: 07.11.2024).

To achieve the stated goal, we needed to formulate the laws of change of coordinates of the endpoints of the robot legs and angular coordinates of its body. It was also necessary to solve the inverse problem of robot kinematics to check the operability of the proposed motion plan. The results obtained can be used to develop robot control at the kinematic level.

**Materials and Methods. System Definition.** The object of the study is a robotic system consisting of a rigid body (robot platform) and four legs with three degrees of freedom for each of the legs. The links of the legs are connected to the robot platform by several hinges, which are driven by electric drives. Angle  $\beta_i$  is the angle of rotation of link  $O_iA_i$  around the longitudinal axis of the robot body and characterizes the rotation of the plane of the leg (containing points  $A_i, B_i, K_i$ ) relative to the vertical plane of symmetry  $CXZ$ . And angles  $\alpha_i, \beta_i$  characterize the rotation of links  $A_iB_i$  and  $B_iK_i$  in the plane of the leg. The hinges of the leg links at points  $O_i, A_i, B_i$  are controlled, i.e., the rotation of the leg links at angles  $\varphi_i, \alpha_i, \beta_i$  is provided independently by the corresponding drives.

Fixed coordinate system  $XYZ$  and moving coordinates  $Cxyz$  are introduced, where point  $C$  is the geometric center of the robot platform (Fig. 2 a). The orientation of the robot platform is described by course angles  $\psi$  (rotation around axis  $z$ ), roll  $\theta$  (rotation around axis  $x$ ) and pitch  $\gamma$  (rotation around axis  $y$ ), and the position of the robot platform is determined by the coordinates of the geometric center  $x_C, y_C$  and  $z_C$  in the fixed coordinate system.

The distances along the longitudinal and transverse axes of the robot platform from the center of mass  $C$  and the attachment points of the legs to the robot platform  $O_i$  in the moving axes  $x_iy_iz_i$  are specified by  $\rho_{xi}$  and  $\rho_{yi}$ . The lengths of the links are designated as  $l_0 = |O_iA_i|, l_1 = |A_iB_i|, l_2 = |B_iK_i|$  ( $i = \overline{1,4}$ ) (Fig. 2 b).

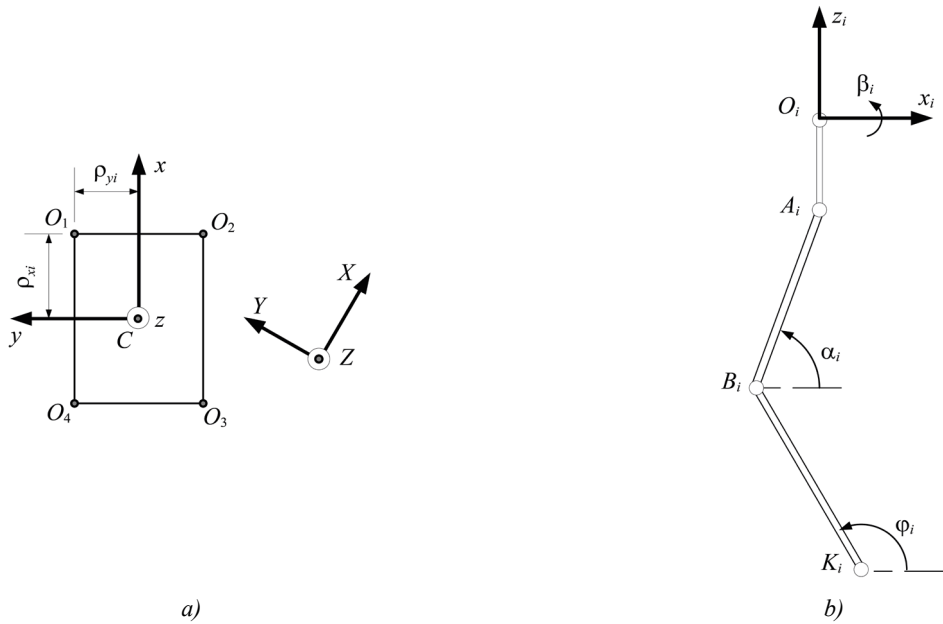


Fig. 2. Kinematic diagram of the robot:  
a — top view of the robot body; b — side view of the robot leg

In projections onto the axes of the fixed coordinate system  $XYZ$ , the position vector of the endpoint of the leg  $K_i$  (or the point in contact with the surface) is determined from the formula:

$$\vec{r}_{Ki} = \vec{r}_C + \Gamma_{\psi\theta\gamma} (\vec{r}_{CO_i} + \vec{r}_{O_iA_i} + \Gamma_{\beta_i} (\vec{r}_{A_iB_i} + \vec{r}_{B_iK_i})), \quad (1)$$

where  $\vec{r}_C = (x_C \ y_C \ z_C)^T$  — position vector of the geometric center of the robot platform  $C$ ;  $\Gamma_{\psi\theta\gamma} = \Gamma_{\psi}\Gamma_{\theta}\Gamma_{\gamma}$  — rotation matrix, which is calculated as the product of the elementary rotation matrices by the course, roll, and pitch angles. The rotation matrices included in equation (1), have the form:

$$\Gamma_{\psi} = \begin{pmatrix} \cos \psi & -\sin \psi & 0 \\ \sin \psi & \cos \psi & 0 \\ 0 & 0 & 1 \end{pmatrix}, \quad \Gamma_{\theta} = \begin{pmatrix} 1 & 0 & 0 \\ 0 & \cos \theta & -\sin \theta \\ 0 & \sin \theta & \cos \theta \end{pmatrix}, \quad (2)$$

$$\Gamma_{\gamma} = \begin{pmatrix} \cos \gamma & 0 & \sin \gamma \\ 0 & 1 & 0 \\ -\sin \gamma & 0 & \cos \gamma \end{pmatrix}, \quad \Gamma_{\beta_i} = \begin{pmatrix} 1 & 0 & 0 \\ 0 & \cos \beta_i & -\sin \beta_i \\ 0 & \sin \beta_i & \cos \beta_i \end{pmatrix}.$$

Other radius vectors included in equation (1) are determined from the expressions:

$$\begin{aligned} \vec{r}_{COi} &= (\rho_{xi} \ \rho_{yi} \ 0)^T, & \vec{r}_{O_iA_i} &= (0 \ -l_0 \sin \beta_i \ -l_0 \cos \beta_i)^T, \\ \vec{r}_{A_iB_i} &= (-l_1 \cos \alpha_i \ 0 \ -l_1 \sin \alpha_i)^T, & \vec{r}_{B_iK_i} &= (-l_2 \cos \varphi_i \ 0 \ -l_2 \sin \varphi_i)^T, \end{aligned} \quad (3)$$

here, the superscript “T” means the vector transpose operation.

After performing intermediate calculations on the right side of equation (1), taking into account expressions (2) and (3), we obtain projections of the position vector  $r_{Ki}$  for each leg.

Differentiating equation (1) with respect to time, we obtain a kinematic model in the form:

$$v_{Ki} = v_C + J_0(q_{\psi\theta\gamma}, q_{\alpha\varphi\beta i}) \dot{q}_{\psi\theta\gamma} + J_i(q_{\psi\theta\gamma}, q_{\alpha\varphi\beta i}) \dot{q}_{\alpha\varphi\beta i}, \quad (4)$$

where  $q_{\psi\theta\gamma} = (\psi \ \theta \ \gamma)^T$  — vector of angular generalized coordinates of the robot platform;  $q_{\alpha\varphi\beta i} = (\beta_i \ \alpha_i \ \varphi_i)^T$  — vector of angular generalized coordinates of the robot leg links;  $v_{Ki} = (\dot{x}_{Ki} \ \dot{y}_{Ki} \ \dot{z}_{Ki})^T$  — vector of linear velocity of the endpoint of the  $i$ -th leg;  $v_C = (\dot{x}_C \ \dot{y}_C \ \dot{z}_C)^T$  — vector of linear velocity of the geometric center of the robot platform;  $J_0(q_{\psi\theta\gamma}, q_{\alpha\varphi\beta i}), J_i(q_{\psi\theta\gamma}, q_{\alpha\varphi\beta i})$  — matrices of coefficients for the corresponding vectors of generalized velocities.

**Research Results.** To analyze the rotational motions of the robot by solving the equations of motion geometry (1) (or integrating the kinematic equations (4)), we set the initial conditions for the rotation angles of the leg links and the laws of change in the velocities of the endpoints of the legs  $v_{Ki}$ , the geometric center of the robot platform  $v_C$  and the vector of angular generalized coordinates  $q_{\psi\theta\gamma}$ . Considering the rotational movements of the robot platform, we assume that the geometric center is stationary during the movement  $v_C = 0$ .

As the initial position of the leg links, we take the following angle values  $\varphi_i, \alpha_i, \beta_i$  ( $i = \overline{1,4}$ ) for each of the legs:

$$\varphi_i(0) = 120^\circ, \alpha_i(0) = 60^\circ, \beta_i(0) = 0^\circ. \quad (i = \overline{1,4}). \quad (5)$$

The given combination of angle values  $\varphi_i, \alpha_i, \beta_i$  ( $i = \overline{1,4}$ ) corresponds to the robot standing on semi-bent legs, which is presented in a simplified visualization (Fig. 3) made in *Wolfram Mathematica*. The following values of the robot geometric parameters were used in the visualization:  $l_0 = 0.15$  m,  $l_1 = 0.45$  m,  $l_2 = 0.45$  m,  $\rho_{x1} = \rho_{x2} = -\rho_{x3} = -\rho_{x4} = 0.5$  m,  $\rho_{y1} = -\rho_{y2} = -\rho_{y3} = \rho_{y4} = 0.25$  m.

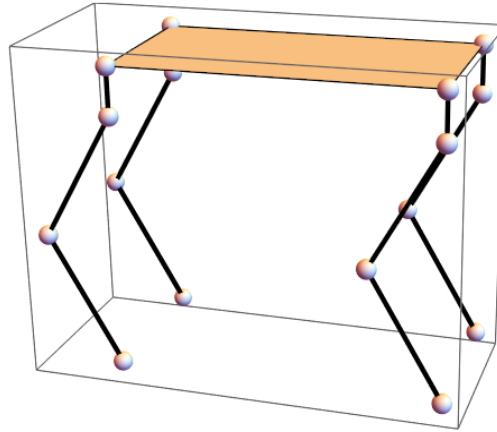


Fig. 3. Simplified visualization of the robot initial position

To perform periodic rotary movements of the robot platform, limited only by the roll angle, we set the laws for changing the orientation angles of the platform in the form:

$$\theta(t) = \theta_0 + A \sin\left(2\pi \frac{t}{T}\right), \quad \gamma(t) = \gamma_0, \quad \psi(t) = \psi_0, \quad (6)$$

where  $\psi_0 = 0^\circ, \theta_0 = 0^\circ, \gamma_0 = 0^\circ$  — initial values of orientation angles;  $A = 0.2$  rad and  $T = 20$  s — constants characterizing the amplitude and period of oscillations by angle. Since it is optional to move the legs when the robot platform is rotated along the roll angle, the coordinates of the contact points of the legs with the support surface remain unchanged ( $v_{Ki} = 0$ ):

$$x_{Ki}(t) = x_{Ki}(0), \quad y_{Ki}(t) = y_{Ki}(0), \quad z_{Ki}(t) = 0. \quad (i = \overline{1, \dots, 4}), \quad (7)$$

where  $x_{Ki}(0)$  and  $y_{Ki}(0)$  — initial coordinates of the contact points of the robot legs with the support surface.

Solving equations (1) with respect to (2) and (3), when substituting the program motion (6) and (7), we obtain the dependences of the rotation angles  $\varphi_i, \alpha_i, \beta_i$  of the leg links (Fig. 4).

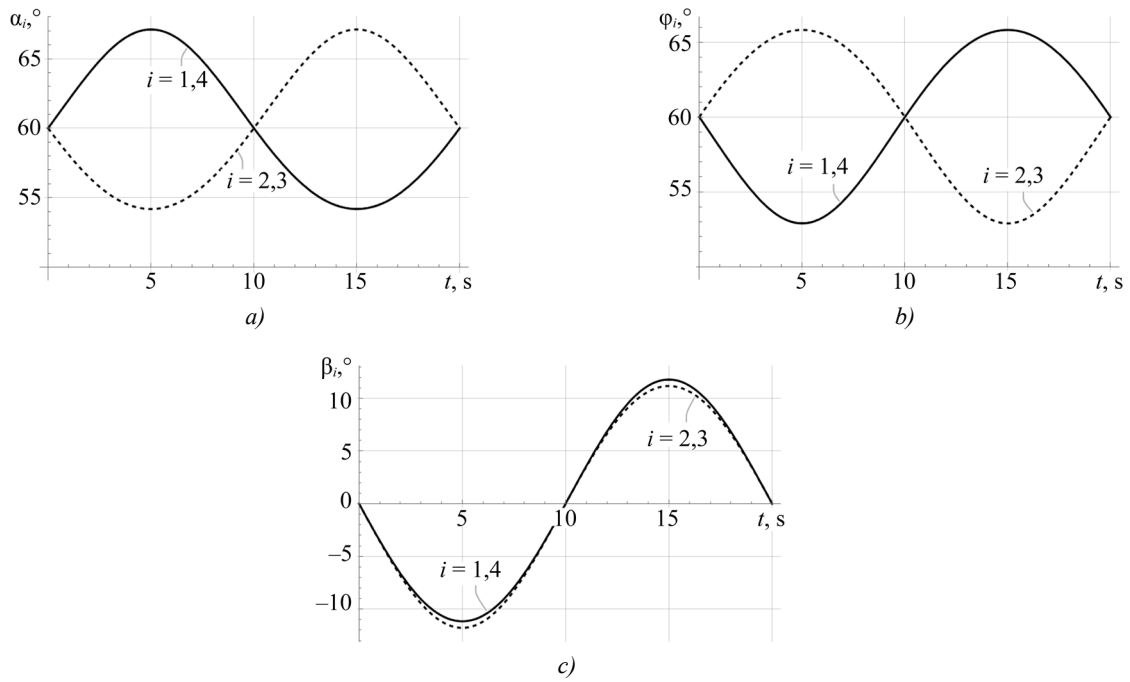


Fig. 4. Roll angle turn simulation results: *a* — angles  $\alpha_i(t)$ ; *b* — angles  $\varphi_i(t)$ ; *c* — angles  $\beta_i(t)$

According to the results of the simulation presented in Figure 4, it can be noted that the rotation angles of the leg links are harmonic functions. As a consequence, it can be mentioned that the rotations of the robot platform around the longitudinal axis of symmetry of the robot (6) can be performed without tearing the contact points of the legs from the surface.

To perform periodic rotary movements of the robot platform, only in pitch angle, we set the laws for changing the orientation angles of the platform in the form:

$$\theta(t) = \theta_0, \quad \gamma(t) = \gamma_0 + A \sin\left(2\pi \frac{t}{T}\right), \quad \psi(t) = \psi_0. \quad (8)$$

When the robot platform rotates along the pitch angle, the transfer of the legs is optional, and the coordinates of the points of contact of the legs with the supporting surface remain unchanged.

Solving equations (1) taking into account (2) and (3), and substituting program movements (7) and (8), we obtain the dependences of the rotation angles  $\varphi_i$ ,  $\alpha_i$ ,  $\beta_i$  of the leg links (Fig. 5).

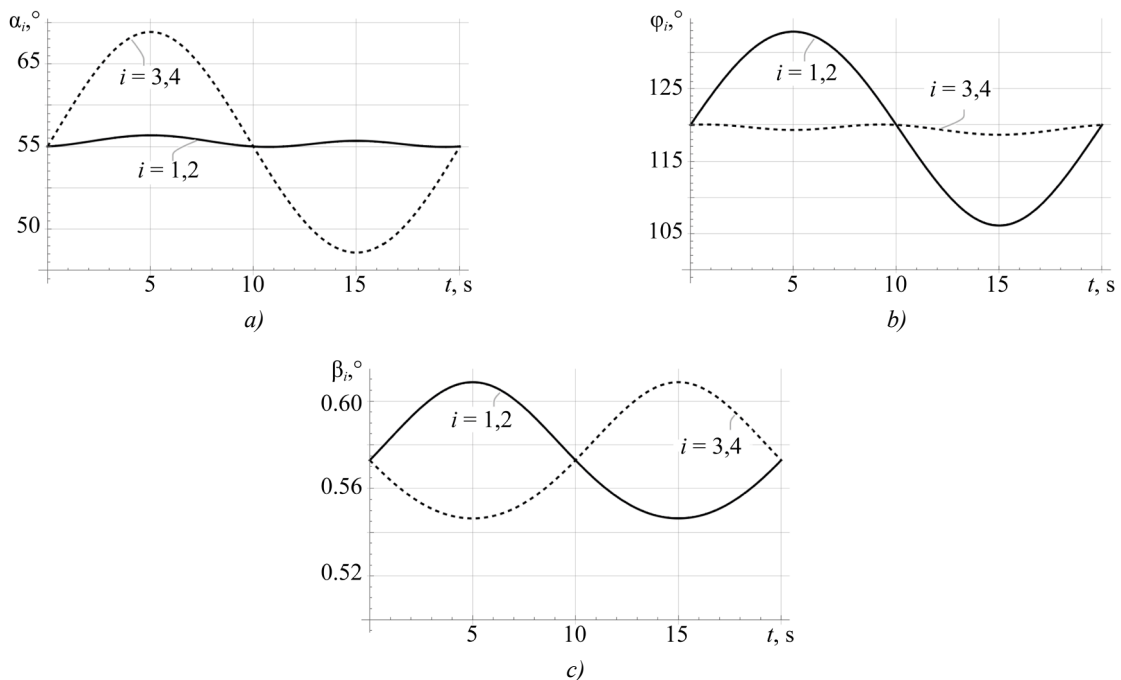


Fig. 5. Pitch angle turn simulation results: *a* — angles  $\alpha_i(t)$ ; *b* — angles  $\varphi_i(t)$ ; *c* — angles  $\beta_i(t)$

According to the simulation results presented in Figure 5, it can be noted that the rotation angles of the leg links are harmonic functions. As a consequence, it can be mentioned that the rotations of the robot platform around the transverse axis of symmetry of the robot (8) can be performed without tearing the contact points of the legs from the surface.

To perform rotation around axis  $Z$ , we consider the laws of changing the orientation angles of the robot platform in the form:

$$\theta(t) = \theta_0, \quad \gamma(t) = \gamma_0, \quad \psi(t) = \psi_0 - \omega_z t, \quad (9)$$

where  $\omega_z = 0.085$  rad/s angular velocity of rotation of the robot platform.

To provide the rotation of the robot around the vertical axis, it is required to plan the movement of the legs. Let us consider the case when the trajectories of the contact points of the legs in projections onto the horizontal plane  $XY$  belong to a circle of radius  $\rho$ . In this case, we will assume that the axis, around which the rotation of the robot platform occurs, passes through the geometric center of the platform. Then, the expressions for the coordinates of the endpoints of the legs can be determined from the relations:

$$\begin{aligned} x_{K1} &= \rho \sin(\omega_z \Delta_{13} + \alpha_1), & y_{K1} &= -\rho \cos(\omega_z \Delta_{13} + \alpha_1), \\ x_{K2} &= \rho \sin(\omega_z \Delta_{24} + \alpha_2), & y_{K2} &= -\rho \cos(\omega_z \Delta_{24} + \alpha_2), \\ x_{K3} &= \rho \sin(\omega_z \Delta_{13} + \alpha_3), & y_{K3} &= -\rho \cos(\omega_z \Delta_{13} + \alpha_3), \\ x_{K4} &= \rho \sin(\omega_z \Delta_{24} + \alpha_4), & y_{K4} &= -\rho \cos(\omega_z \Delta_{24} + \alpha_4), \\ z_{K1} = z_{K3} &= \frac{1}{2} \left[ \operatorname{sgn} \left( \sin \left( \frac{2\pi t}{T_1} \right) \right) + 1 \right] \cdot h_K \sin \left( \frac{2\pi t}{T_1} \right), \\ z_{K2} = z_{K4} &= \frac{1}{2} \left[ \operatorname{sgn} \left( \sin \left( \frac{2\pi t}{T_1} - \pi \right) \right) + 1 \right] \cdot h_K \sin \left( \frac{2\pi t}{T_1} - \pi \right), \end{aligned} \quad (10)$$

where  $\rho = \sqrt{\rho_{Xi}^2 + \rho_{Yi}^2}$ ;  $\alpha_i = \arctan(\rho_{Yi}/\rho_{Xi})$  — angle characterizing the position of the endpoint of the  $i$ -th leg at the initial moment of time;  $h_K = 0.3$  m — maximum height to which the endpoints of the robot legs rise;  $T_1 = 6$  s — time of one step;  $\Delta_{13}, \Delta_{24}$  — auxiliary functions used to provide a piecewise assignment of the change in the coordinates of the endpoints of the legs:

$$\begin{aligned} \Delta_{13} &= \left[ \operatorname{sgn} \left( \sin \left( \frac{2\pi t}{T_1} \right) \right) + 1 \right] \cdot (t \bmod T_1) + \left( t + \frac{T_1}{2} - \left( t - \frac{T_1}{2} \right) \bmod T_1 \right), \\ \Delta_{24} &= \left[ \operatorname{sgn} \left( \sin \left( \frac{2\pi t}{T_1} - \pi \right) \right) + 1 \right] \cdot \left( t + \frac{T_1}{2} \right) \bmod T_1 + (t - (t - T_1) \bmod T_1). \end{aligned} \quad (11)$$

Here, function  $(t) \bmod T_1$  returns the remainder of the integer division  $t$  by  $T_1$ . The piecewise character of the coordinate change assignment is associated with the consideration of gaits (elementary leg movements), in which a sequential transfer of the crossed legs is performed.

Solving equation (1) with respect to (2) and (3), when substituting the program movement (9)–(11), we obtain the dependences of the rotation angles  $\varphi_i, \alpha_i, \beta_i$  of the leg links (Fig. 6).

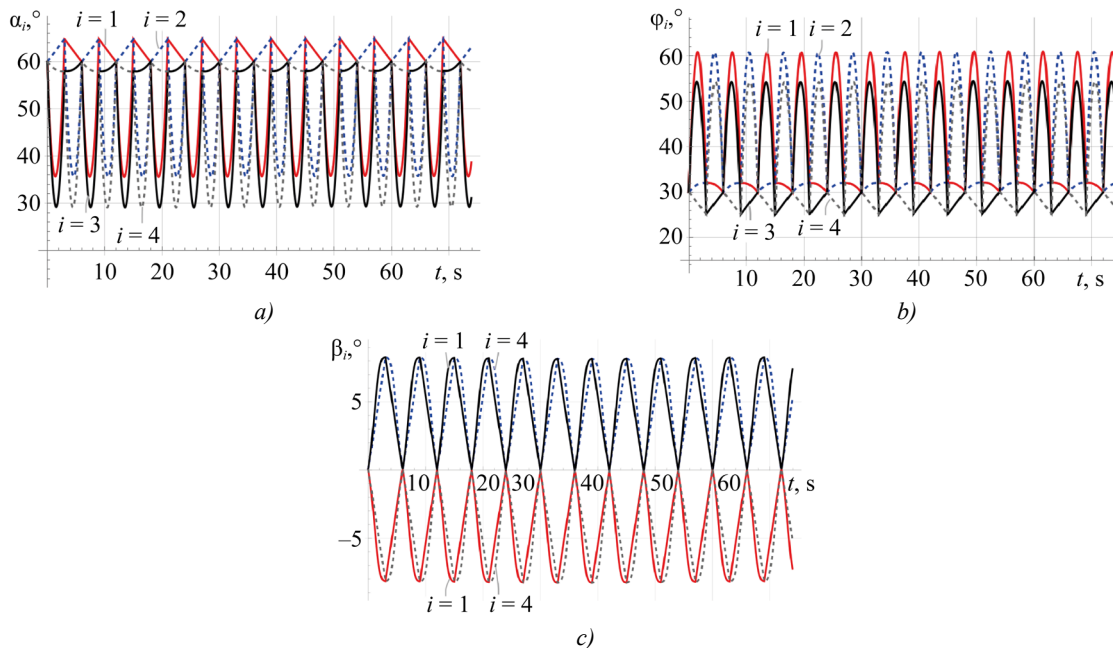


Fig. 6. Course angle turn simulation results:  $a$  — angles  $\alpha_i(t)$ ;  $b$  — angles  $\varphi_i(t)$ ;  $c$  — angles  $\beta_i(t)$

The simulation results show that the dependences of the rotation angles of the leg links are periodic functions and, as a consequence, the considered rotational movements of the robot platform can take place without the occurrence of singular configurations. Thus, the proposed plan for transferring the legs (10), (11) during rotation around vertical axis  $Z$  is suitable for implementing the rotation of the robot at an arbitrary angle  $\psi$ .

**Discussion and Conclusion.** The constructed mathematical model of kinematics allows for the determination of the angles in the joints of the robot leg links, which must be provided to implement the desired movement of the robot platform. The obtained results of numerical modeling of the rotary movements of the robot body confirmed the operability of the developed kinematic model for assessing the implementation of the specified robot movements, taking into account the limitations and dimensions of the structure.

In cases where the robot platform performs a flat motion (at zero pitch and roll angles), the constructed mathematical model of kinematics coincides with the published results of other authors. The results obtained in this paper are a generalization and refinement of the equations that couple the rotation angles of the robot leg links with the position and orientation of the robot platform.

The application of the developed kinematic model (1), (4), as well as the proposed plan for transferring legs (10), (11) during rotation around the vertical axis, will allow constructing control at the kinematic level for the robot movement along curvilinear trajectories. This approach will significantly expand the robot functionality and increase its performance efficiency under various operating conditions.

## References

1. Pavlovsky VE. For Elaboration of Walking Machines. *Keldysh Institute Preprints*. 2013;(101):1–32. URL: [https://keldysh.ru/papers/2013/prep2013\\_101.pdf](https://keldysh.ru/papers/2013/prep2013_101.pdf) (accessed: 20.11.2024).
2. Taheri H, Mozayani N. A Study on Quadruped Mobile Robot. *Mechanism and Machine Theory*. 2023;190:105448. <https://doi.org/10.1016/j.mechmachtheory.2023.105448>
3. Hui Chai, Yibin Li, Rui Song, Guoteng Zhang, Qin Zhang, Song Liu, et al. A Survey of the Development of Quadruped Robots: Joint Configuration, Dynamic Locomotion Control Method and Mobile Manipulation Approach. *Biomimetic Intelligence and Robotics*. 2022;2(1):100029. <https://doi.org/10.1016/j.birob.2021.100029>
4. Liang ZJ, Jiang L, Zhao JX, Xing BY, Xu P, Su B. Design and Analysis of High Dynamic Actuator and Implementation on Quadruped Robot. *Journal of Physics: Conferences Series*. 2023;2478:102002. <https://doi.org/10.1088/1742-6596/2478/10/102002>
5. Jiupeng Chen, Hongjun San, Xing Wu. Gait Regulation of a Bionic Quadruped Robot with Antiparallelogram Leg Based on CPG Oscillator. *Complexity*. 2019;2019(5):5491298. <https://doi.org/10.1155/2019/5491298>
6. Khan H, Kitano S, Frigerio M, Camurri M, Barasuol V, Featherstone R, et al. Development of the Lightweight Hydraulic Quadruped Robot — MiniHyQ. In: *Proceedings of the 2015 IEEE International Conference on Technologies for Practical Robot Applications (TePRA)*. New York City: IEEE; 2015. P. 1–6. <https://doi.org/10.1109/TePRA.2015.7219671>
7. Lizhou Fang, Junhui Zhang, Huaizhi Zong, Ximeng Wang, Kun Zhang, Jun Shen, et al. Open-Source Lower Controller for Twelve Degrees of Freedom Hydraulic Quadruped Robot with Distributed Control Scheme. *HardwareX*. 2023;13:e00393. <https://doi.org/10.1016/j.ohx.2022.e00393>
8. Yunde Shi, Shilin Li, Mingqiu Guo, Yuan Yang, Dan Xia, Xiang Luo. Structural Design, Simulation and Experiment of Quadruped Robot. *Applied Sciences*. 2021;11(22):10705. <https://doi.org/10.3390/app112210705>
9. Wei Yan, Yang Pan, Junjie Che, Jiexian Yu, Zhuchen Han. Whole-Body Kinematic and Dynamic Modeling for Quadruped Robot under Different Gaits and Mechanism Topologies. *PeerJ Computer Science*. 2021;7(1):e821. <https://doi.org/10.7717/peerj-cs.821>
10. Havoutis I, Semini C, Buchli J, Caldwell DG. Quadrupedal Trotting with Active Compliance. In: *Proceedings of the 2013 IEEE International Conference on Mechatronics (ICM)*. New York City: IEEE; 2013. P. 610–616. <https://doi.org/10.1109/ICMECH.2013.6519112>
11. Jiawei Chen, Kun Xu, Xilun Ding. Adaptive Gait Planning for Quadruped Robot Based on Center of Inertia over Rough Terrain. *Biomimetic Intelligence and Robotics*. 2021;2(1):100031. <https://doi.org/10.1016/j.birob.2021.100031>
12. Guiyang Xin, Wolfslag W, Hsiu-Chin Lin, Tiseo C, Mistry M. An Optimization-Based Locomotion Controller for Quadruped Robots Leveraging Cartesian Impedance Control. *Frontiers in Robotics and AI*. 2020;7:48. <https://doi.org/10.3389/frobt.2020.00048>
13. Bellicoso CD, Gehring C, Hwangbo J, Fankhauser P, Hutter M. Perception-less Terrain Adaptation through Whole Body Control and Hierarchical Optimization. In: *Proceedings of the 2016 IEEE-RAS 16th International Conference on Humanoid Robots (Humanoids)*. New York City: IEEE; 2017. P. 558–564. <https://doi.org/10.1109/HUMANOIDS.2016.7803330>

14. Hutter M, Sommer H, Gehring C, Hoepflinger M, Bloesch M, Siegwart R. Quadrupedal Locomotion Using Hierarchical Operational Space Control. *The International Journal of Robotics Research*. 2014;33(8):1047–1062. <https://doi.org/10.1177/0278364913519834>

15. Zhao Z, Noritsugu T, Takaiwa M, Sasaki D. Development of Quadruped Robot with Pneumatic Actuator. In: *Proceedings of the 8th International Symposium on Fluid Power*. New York City: IEEE; 2010. P. 325–330. <https://doi.org/10.1299/jsmeicam.2010.5.325>

16. Junmin Li, Jinge Wang, Simon X Yang, Kedong Zhou, Huijuan Tang. Gait Planning and Stability Control of a Quadruped Robot. *Computational Intelligence and Neuroscience*. 2016:2016;9853070. <https://doi.org/10.1155/2016/9853070>

#### **About the Authors:**

**Marcelino J. Fernando**, student of the Department of Robotics, Mechatronics, Dynamics and Strength of Machines, National Research University MPEI (14, Krasnokazarmennaya Str., Moscow, 111250, Russian Federation), [ORCID](#), [ScopusID](#), [themarcfernando98@outlook.com](mailto:themarcfernando98@outlook.com)

**Gasán R. Saypulaev**, Cand.Sci. (Eng.), Senior Lecturer of the Department of Robotics, Mechatronics, Dynamics and Strength of Machines, National Research University MPEI (14, Krasnokazarmennaya Str., Moscow, 111250, Russian Federation), [SPIN-code](#), [ORCID](#), [ScopusID](#), [saypulaevgr@mail.ru](mailto:saypulaevgr@mail.ru)

**Musa R. Saypulaev**, Cand.Sci. (Eng.), Senior Lecturer of the Department of Robotics, Mechatronics, Dynamics and Strength of Machines, National Research University MPEI (14, Krasnokazarmennaya Str., Moscow, 111250, Russian Federation), [SPIN-code](#), [ORCID](#), [ScopusID](#), [saypulaevmr@mail.ru](mailto:saypulaevmr@mail.ru)

#### **Claimed Contributorship:**

**MJ Fernando:** concept development, conducting research, manuscript drafting, formal analysis.

**GR Saypulaev:** academic advising, validation of the results, administrative management of the research project, data curation.

**MR Saypulaev:** methodology development, software development, visualization, manuscript writing and editing.

**Conflict of Interest Statement:** the authors declare no conflict of interest.

*All the authors have read and approved the final manuscript.*

#### **Об авторах:**

**Марселино Жулио Фернандо**, студент кафедры робототехники, мехатроники, динамики и прочности машин Национального исследовательского университета «МЭИ» (111250, Российская Федерация, г. Москва, ул. Красноказарменная, д. 14), [ORCID](#), [ScopusID](#), [themarcfernando98@outlook.com](mailto:themarcfernando98@outlook.com)

**Гасан Русланович Сайпулаев**, кандидат технических наук, старший преподаватель кафедры робототехники, мехатроники, динамики и прочности машин Национального исследовательского университета «МЭИ» (111250, Российская Федерация, г. Москва, ул. Красноказарменная, д. 14), [SPIN-код](#), [ORCID](#), [ScopusID](#), [saypulaevgr@mail.ru](mailto:saypulaevgr@mail.ru)

**Муса Русланович Сайпулаев**, кандидат технических наук, старший преподаватель кафедры робототехники, мехатроники, динамики и прочности машин Национального исследовательского университета «МЭИ» (111250, Российская Федерация, г. Москва, ул. Красноказарменная, д. 14), [SPIN-код](#), [ORCID](#), [ScopusID](#), [saypulaevmr@mail.ru](mailto:saypulaevmr@mail.ru)

#### **Заявленный вклад авторов:**

**М.Ж. Фернандо:** разработка концепции, проведение исследования, написание черновика рукописи, формальный анализ.

**Г.Р. Сайпулаев:** научное руководство, валидация результатов, административное руководство исследовательским проектом, курирование данных.

**М.Р. Сайпулаев:** разработка методологии, разработка программного обеспечения, визуализация, написание рукописи и редактирование.

**Конфликт интересов:** авторы заявляют об отсутствии конфликта интересов.

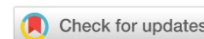
*Все авторы прочитали и одобрили окончательный вариант рукописи.*

Received / Поступила в редакцию 20.12.2024

Reviewed / Поступила после рецензирования 15.01.2025

Accepted / Принята к публикации 24.01.2025

# MECHANICS МЕХАНИКА



УДК 536.21

Original Theoretical Research

<https://doi.org/10.23947/2687-1653-2025-25-1-23-31>

## Numerical Solution to the Problem of Thermal Conductivity in a Porous Plate with a Topology of Triply Periodic Minimal Surfaces



EDN: YYGRFP

 Kristina V. Gubareva , Anton V. Eremin 

Samara State Technical University, Samara, Russian Federation

✉ [r.kristina2017@mail.ru](mailto:r.kristina2017@mail.ru)

### Abstract

**Introduction.** Thermal performance of materials based on triply periodic minimal surfaces (TPMS) is becoming increasingly important in view of the growing interest in materials with special thermophysical properties and their applications in engineering, energy, and other fields. Since these materials have unique structural and functional characteristics, understanding the relationship between their geometry and thermal parameters plays a key role in optimizing their use. Despite the considerable attention paid to the problem, the study of the relationship between the geometry of porous structures and their thermal characteristics remains incomplete. Existing scientific papers cover only individual options, and a complete understanding of the effect of complex micro- and macrostructure on thermal conductivity requires further study. The current gap in scientific knowledge is the lack of systematization and generalization of existing data, which complicates the development of universal approaches to calculating thermal conductivity in such materials. The objective of this study was to develop simplified formulas for calculating the effective thermal conductivity of porous structures based on S-type TPMC cells proposed by Fisher and Koch. The authors also set the task of analyzing the heat-conducting process in a plate with given porosity parameters. This will improve the understanding of the thermodynamic processes occurring in such systems.

**Materials and Methods.** To achieve the stated objectives, mathematical modeling was performed, including the solution to the boundary value problem taking into account the identified correlations. A cellular structure made of PETG plastic and having pores consisting of identical repeating elements was considered. These elements formed a three-dimensional minimal surface that corresponded to the Fisher-Koch model. The analysis was performed using two methods: calculations in MathCAD based on the finite difference method, and modeling in ANSYS using the finite element method. In this case, the effect of the geometric parameters of the porous structure on its thermal characteristics was taken into account.

**Results.** The research results represented a numerical solution to the thermal conductivity problem for a porous plate, taking into account the symmetrical boundary conditions of the first kind, and the presence of internal heat sources that remained constant in time and considered the topological features of the material. In the course of the study, temperature distributions were obtained, both in the spatial coordinate and in time. The change in heat flow depending on variations in the plate porosity coefficient was estimated. The graphs of isotherm distribution and their speed of movement were constructed and analyzed, which allowed for a deeper understanding of the heat transfer dynamics in the system under consideration.

**Discussion and Conclusion.** The obtained mathematical dependences demonstrate the degree and nature of the effect of porosity on the distribution of heat flux density. It has been found that changes in the porosity of the plate can both increase and decrease the intensity of heat transfer, which provides reaching the required values of thermal resistance of the material. The obtained results are consistent with the findings presented in other studies on similar topics, which opens up opportunities for their application in further research. These results can be useful in designing thermal protection systems for heat-generating equipment, as well as for heat and mass transfer paths of heat-mechanical equipment and other applications. The solutions are presented in an accessible and understandable form, which makes them easy to use for a wide range of researchers and engineers, and does not require expensive software or specialized computing equipment.

**Keywords:** triply periodic minimal surfaces, Fischer-Koch S, porosity, internal heat sources, numerical solution, thermal conductivity, finite element method, finite difference method, speed of heat propagation

**Acknowledgements.** The authors would like to thank the Editorial board of the Journal and the reviewers for their attentive attitude to the article.

**Funding Information.** The research is done with the financial support from the Russian Science Foundation (project No. 23–79–10044, <https://rscf.ru/project/23-79-10044/>).

**For Citation.** Gubareva KV, Eremin AV. Numerical Solution to the Problem of Thermal Conductivity in a Porous Plate with a Topology of Triply Periodic Minimal Surfaces. *Advanced Engineering Research (Rostov-on-Don)*. 2025;25(1):23–31. <https://doi.org/10.23947/2687-1653-2025-25-1-23-31>

*Оригинальное теоретическое исследование*

## Численное решение задачи теплопроводности в пористой пластине с топологией трижды периодических минимальных поверхностей

К.В. Губарева  , А.В. Еремин 

Самарский государственный технический университет, г. Самара, Российская Федерация

 [r.kristina2017@mail.ru](mailto:r.kristina2017@mail.ru)

### Аннотация

**Введение.** Термические характеристики материалов, созданных на базе трижды периодических минимальных поверхностей (ТПМП), становятся все более важными в свете роста интереса к материалам с особыми теплофизическими свойствами и их применениям в инженерии, энергетике и других областях. Поскольку эти материалы обладают уникальными структурными и функциональными характеристиками, понимание взаимосвязи между их геометрией и теплофизическими параметрами играет ключевую роль в оптимизации их использования. Несмотря на значительное внимание, уделенное проблеме, исследование взаимосвязи между геометрией пористых структур и их термическими характеристиками остается неполным. Существующие научные работы охватывают лишь отдельные варианты, а полное понимание влияния сложной микро- и макроструктуры на теплопроводность требует дальнейшего изучения. Существующий пробел в научном знании заключается в недостаточной систематизации и обобщении существующих данных, что затрудняет разработку универсальных подходов к расчету теплопроводности в таких материалах. Целью данного исследования являлась разработка упрощенных формул для расчета показателя эффективной теплопроводности пористых структур, основанных на ТПМП-ячейках типа S, предложенных Фишером и Кохом. Авторы также ставили задачу анализа теплопроводного процесса в пластине с заданными параметрами пористости. Это позволит улучшить понимание термодинамических процессов, происходящих в таких системах.

**Материалы и методы.** Для достижения поставленных целей проведено математическое моделирование, включающее решение граничной задачи с учетом выявленных корреляций. Рассматривается ячеистая конструкция, изготовленная из PETG-пластика и имеющая поры, состоящие из одинаковых повторяющихся элементов. Эти элементы формируют трехмерную минимальную поверхность, которая соответствует модели Фишера-Коча. Анализ проводился с использованием двух методов: расчеты в MathCAD, основанные на методе конечных разностей, и моделирование в ANSYS методом конечных элементов. При этом учитывалось влияние геометрических параметров пористой структуры на ее теплофизические характеристики.

**Результаты исследования.** Результаты исследования представляют собой численное решение задачи теплопроводности для пористой пластины, принимая во внимание симметричные граничные условия первого рода и наличие внутренних источников тепла, которые остаются постоянными во времени и учитывают топологические особенности материала. В ходе работы были получены распределения температуры как по пространственной координате, так и во времени. Оценено изменение теплового потока в зависимости от вариаций коэффициента пористости пластины. Построены и проанализированы графики распределения изотерм и скорости их перемещения, что позволяет более глубоко понять динамику теплопередачи в рассматриваемой системе.

**Обсуждение и заключение.** Полученные математические зависимости демонстрируют степень и характер влияния пористости на распределение плотности теплового потока. Было установлено, что изменения в пористости пластины могут как увеличить, так и уменьшить интенсивность теплопереноса, что позволяет достигать необходимых значений термического сопротивления материала. Полученные результаты согласуются с выводами, изложенными в других исследованиях аналогичной тематики, что открывает возможности для их применения в дальнейших исследованиях. Эти результаты могут быть полезны при проектировании систем тепловой защиты

для тепловыделяющего оборудования, а также для теплообменных трактов тепломеханического оборудования и других приложений. Решения представлены в доступной и понятной форме, что облегчает их использование как для широкого круга исследователей, так и инженеров, и не требует привлечения дорогостоящего программного обеспечения или специализированной вычислительной техники.

**Ключевые слова:** трижды периодические минимальные поверхности, топология Фишера-Коха S, пористость, внутренние источники теплоты, численное решение, теплопроводность, метод конечных элементов, метод конечных разностей, скорость распространения теплоты

**Благодарности.** Авторы выражают благодарность редакции журнала и рецензентам за внимательное отношение к статье.

**Финансирование.** Исследование выполнено за счет средств гранта Российского научного фонда (проект № 23–79–10044, <https://rscf.ru/project/23-79-10044/>).

**Для цитирования.** Губарева К.В., Еремин А.В. Численное решение задачи теплопроводности в пористой пластине с топологией трижды периодических минимальных поверхностей. *Advanced Engineering Research (Rostov-on-Don)*. 2025;25(1):23–31. <https://doi.org/10.23947/2687-1653-2025-25-1-23-31>

**Introduction.** Porous materials are widely used in various industries, such as metallurgy [1], microelectronics [2], and construction [3]. Their unique properties, due to the presence of cavities and voids filled with gases that conduct heat poorly, make them ideal for use in the production of thermal insulation [4]. The urgency of this problem is related to the need to improve energy efficiency in various areas, which is an important aspect in the context of sustainable development. In light of this, in [4], the authors developed an energy- and resource-saving technology for producing an effective porous heat and sound insulation structural material, which emphasizes the importance of research in this area.

A comparative analysis of the literature shows that the problem raised by the authors has been sufficiently studied, but there are still a number of aspects that require more in-depth study. Paper [5] presents modern porous thermal insulation materials, including the use of silicate raw materials in their production. In [6], various types of porous material matrices are studied, and it is emphasized that the geometric size of the sample (specifically, its thickness, optimal for sound absorption — about 20 mm) significantly affects their characteristics. In addition, it should be noted that porous materials have a lower mass compared to homogeneous media, which makes them mostly attractive for use under conditions of mass and size restrictions, such as the aviation [7] and space industries [8]. In the context of the petrochemical industry, studies conducted by Mazitov A.A. [9] demonstrated the capabilities of a new web application for mathematical modeling of non-stationary oil flow in a porous medium, which emphasizes the importance of porous materials in this area as well. Paper [10] clearly demonstrated the relevance of the analysis of the mechanical properties of porous plastics, since an applied methodology for calculating the vibrations of piezoceramic porous plates was developed using the finite element method.

Despite their advantages, such as low weight, high strength characteristics and predictable thermal properties, porous materials have disadvantages related to the stochastic distribution of pores and the anisotropy of their properties, which complicates the mathematical and physical analysis of transport processes. In this regard, the analysis of a material with a porous structure created on the basis of triply periodic minimal surfaces (TPMS) is of considerable interest, since it demonstrates predictable properties depending on the geometric characteristics of the elementary cells.

Thermal properties of materials based on TPMP are actively studied in scientific circles [11]. To model the processes occurring in porous media, both numerical [12] and analytical methods are used. However, one of the main problems remains the search for a qualitative connection between the thermophysical characteristics [13] and the geometry of porous media [14]. In this context, the study of the temperature field in porous bodies, taking into account their geometric characteristics and cell porosity, as well as the application of modern numerical methods and algorithms, is an area with high potential and considerable topicality. The development of numerical algorithms capable of describing the behavior of temperature by coordinate and time, as well as heat flow depending on changes in the porosity coefficient, allows for a more accurate and effective approach to the design of heat exchangers and the development of thermal protection of equipment.

Thus, the objectives of this research were to study the process of thermal conductivity in a porous plate with a given porosity made of PETG plastic, and to search for dependences to determine the coefficient of effective thermal conductivity of such materials based on Fischer-Koch S cells. To achieve this goal, a problem of thermal conductivity in a porous plate was formulated and solved, and an analysis of the obtained solutions was performed. The results of this study can be useful for practitioners in the design of heat exchangers and in other areas of application.

**Materials and Methods.** The object of the study is a porous plate made of PETG material with a wall thickness of 0.0001 m. Its heat capacity is 1,050 J/(kg·K), density is 1300 kg/m<sup>3</sup>, and thermal conductivity is 0.2 W/(m·K). Figure 1 shows a sketch of this plate created using the ANSYS software package. The plate is formed from elementary Fisher-Koch cells in the S topology. The initial conditions are set as follows: the temperature at the initial moment of time  $T_0 = 20^\circ\text{C}$ , the temperature on the plate surface is  $T_{CT} = 100^\circ\text{C}$ , and the power of the heat source is 500 W/m<sup>3</sup>.

**Mathematical Formulation of the Problem.** The mathematical formulation of the problem under consideration is as follows: (1) – (4) [15]:

$$A \cdot (1 - \varphi) \cdot \frac{\partial \Theta(\xi, Fo)}{\partial Fo} = \frac{\partial^2 \Theta(\xi, Fo)}{\partial \xi^2} + Po \cdot A; \quad (1)$$

$$Fo > 0; \quad 0 < \xi < 1;$$

$$\Theta(\xi, 0) = 0; \quad (2)$$

$$\Theta(1, Fo) = 1; \quad (3)$$

$$\frac{\partial \Theta(\xi, Fo)}{\partial \xi} = 0, \quad (4)$$

$$\xi = \frac{x}{l}; \quad \Theta = \frac{T - T_0}{T_{CT} - T_0}; \quad Fo = \frac{a_s \tau}{l^2}; \quad Po = \frac{g_V L^2}{\lambda_{eff} A \cdot (T_{CT} - T)_0}; \quad A = \frac{\lambda_s}{\lambda_{eff}},$$

where  $\Theta$  — relative excess temperature;  $\xi$  — dimensionless coordinate;  $Fo$  — Fourier criterion (dimensionless time);  $Po$  — Pomerantsev criterion;  $T$  — temperature, °C;  $x$  — coordinate, m;  $\tau$  — time, s;  $T_{CT}$  — wall temperature, °C;  $T_0$  — initial temperature, °C;  $l$  — cell size, m;  $A$  — coefficient;  $g_V$  — power of internal heat source, W/m<sup>3</sup>;  $a_s = \lambda_s / c p_s$  — thermal diffusivity coefficient.

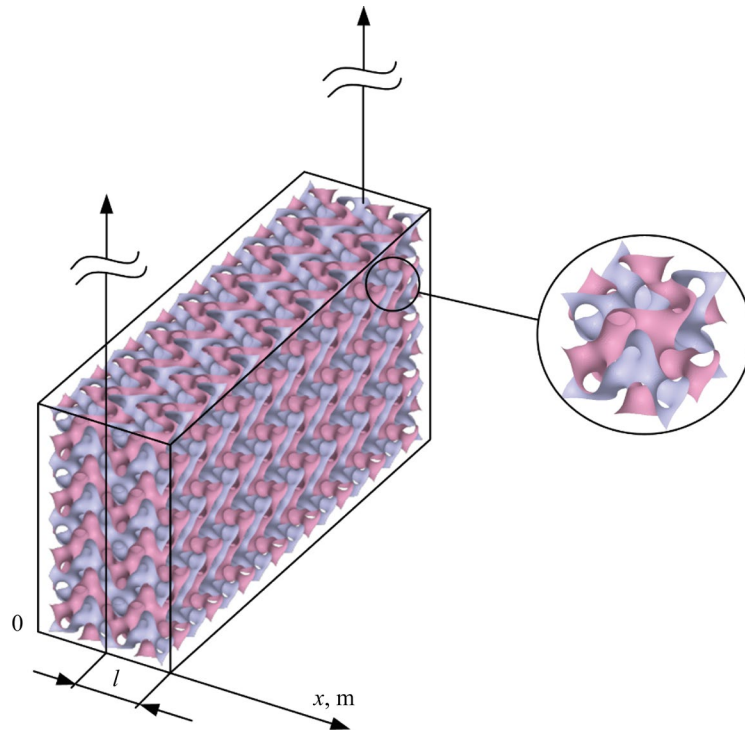


Fig. 1. Plate illustration

**Research Methods.** In the study of thermal conductivity in porous materials, a combination of two approaches was used: representative volume elementary (RVE) and computational homogenization. This methodology was implemented on Fisher-Koch S TPMP cells to calculate the effective thermal conductivity [15]. The effective thermal conductivity coefficient of the material was determined from formula [16]:

$$\lambda_{eff} = \lambda_s \cdot 0,73 \cdot (1 - \varphi),$$

where  $\lambda_s$  — thermal conductivity coefficient of the frame material;  $\varphi$  — porosity [17].

The density of the porous material was determined from formula [18]:

$$\rho_{eff} = \rho_s \cdot (1 - \varphi),$$

where  $\rho_s$  — density value of the material from which the cell is made.

The geometric characteristics of the cellular structure are the determining factors on which the degree of porosity of the material depends. They were calculated using the mathematical expression:

$$\varphi = 1 - V_{\text{ТИММ}} / V,$$

where  $V_{\text{ТИММ}}$  — cell volume;  $V$  — cube volume.

**Numerical Solution.** The solution to problem (1) – (4) was obtained by the finite difference method [19]. According to this method, a space-time grid with coordinate steps  $\Delta\xi$  and time steps  $\Delta Fo$  is introduced. In this case:

$$\xi_i = i\Delta\xi; \quad i = \overline{0, I}; \quad Fo_k = k\Delta Fo; \quad k = \overline{0, K}, \quad (5)$$

where  $I, K$  — number of steps along coordinate  $\xi$  and time  $Fo$ , respectively.

On grid (5), the grid functions  $\Theta_i^k = \Theta(\xi_i, Fo_k)$  are introduced [20]. Using the explicit approximation scheme of differential operators, problem (1) – (4) takes the following form [21]:

$$A \cdot (1 - \varphi) \cdot \frac{\Theta_i^{k+1} - \Theta_i^k}{\Delta Fo} = \frac{\Theta_{i-1}^k - 2\Theta_i^k + \Theta_{i+1}^k}{\Delta \xi^2} + Po \cdot A;$$

$$\Theta_i^0 = 0;$$

$$\Theta_i^k = 1;$$

$$\frac{\Theta_0^{k+1} - \Theta_0^k}{\Delta \xi} = 0.$$

2.5 million grid cells were used in the calculations.

Two key limitations were established during the calculations. First of all, the PETG material was characterized by constant and predetermined thermal parameters. It was also assumed that heat exchange occurred exclusively on surfaces with specified boundary conditions, while the remaining cell faces were thermally insulated.

In the course of the study, it was found that using a grid containing 2.5 to 3.0 million cells leads to an optimal solution to the problem. Increasing the number of grid elements does not significantly affect the accuracy of the solution, but drastically increases the time costs and complexity of the process.

To confirm the correctness of the results obtained in the MathCAD environment, the authors conducted additional modeling in the ANSYS system. The dynamics of temperature changes is graphically presented in Figure 2.

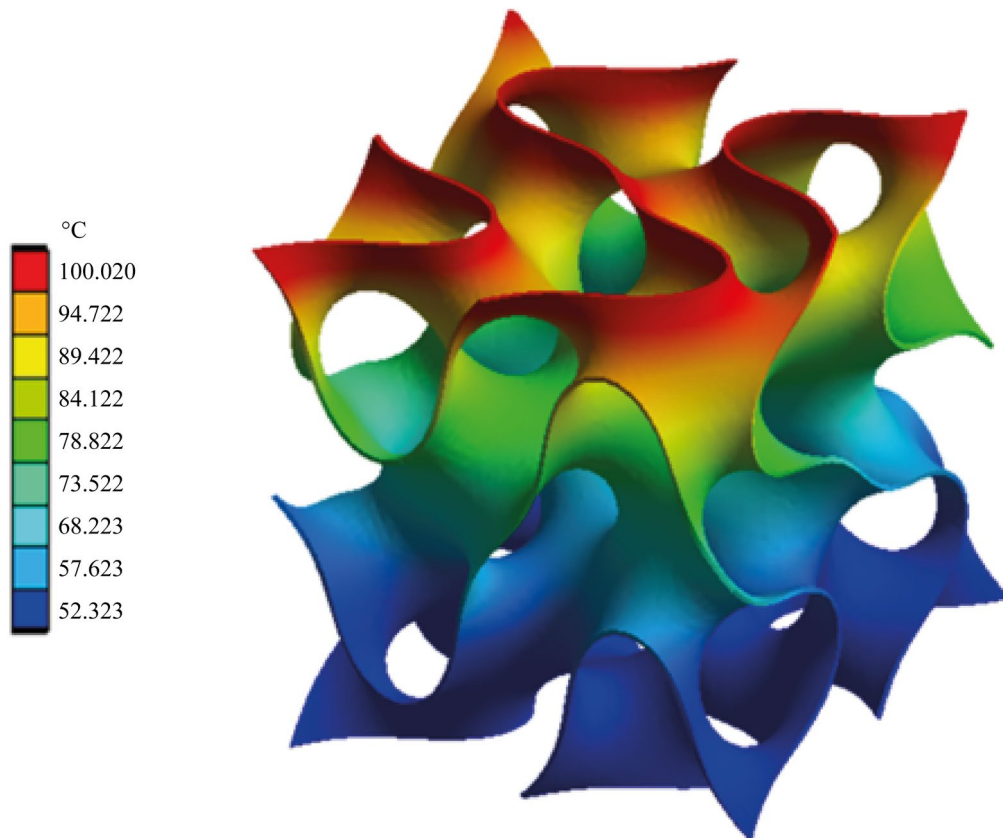


Fig. 2. Change in temperature in the cell

**Research Results.** Figure 3 shows the calculation results obtained by the finite element method (FEM) and the finite difference method (FDM). The analysis of the results allows us to conclude that the dimensionless temperatures obtained by the two methods are in satisfactory agreement. By analyzing the computational experiments, it is established that the Fisher-Koch S-type TPMP cell retains its structure (there are no internal intersections, complete filling of pores, etc.) in the wall thickness range  $0 < \delta < 0.002$  m. The time evolution of isotherms and the dynamics of their speed mode are shown in Figures 4, 5. A notable feature is that in the process of time development, each isothermal line is formed on the surface with a characteristic initial speed inherent in it. It is noteworthy that an increase in the porosity of the material causes an increase in the heat flow over the entire time interval of the research, which is clearly demonstrated in Figure 5. The dependence of the heat flow density on time with varying porosity is shown in Figure 6.

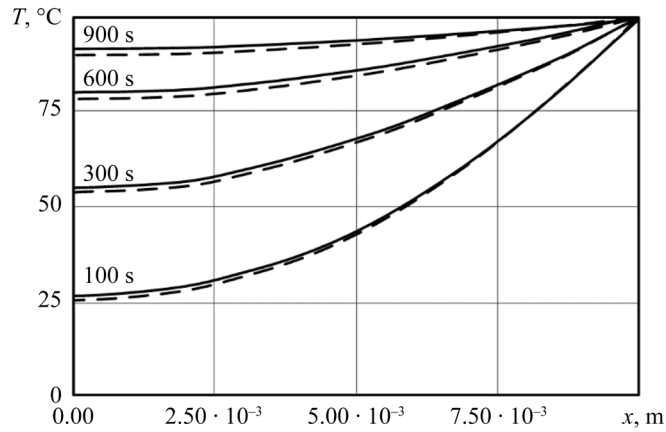


Fig. 3. Temperature distribution by coordinate:

— — solution according to FDM; - - - - solution according to FEM

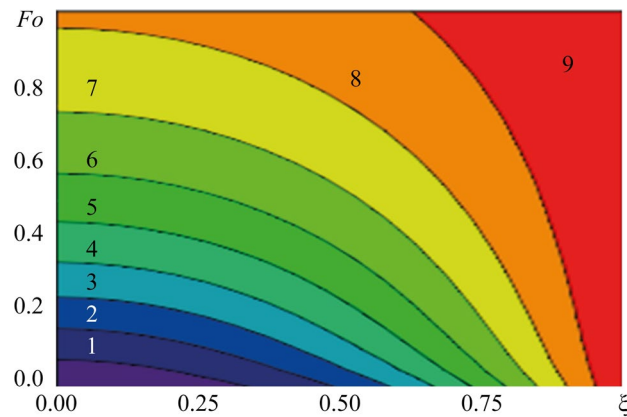


Fig. 4. Graphs of isotherm motion at coordinates depending on time at:  $\Theta = 0.1$  (1);  $0.2$  (2);  $0.3$  (3);  $0.4$  (4);  $0.5$  (5);  $0.6$  (6);  $0.7$  (7);  $0.8$  (8);  $0.9$  (9)

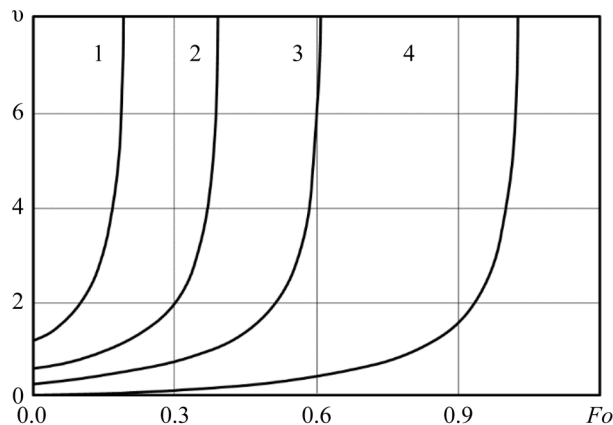


Fig. 5. Distribution of isotherm velocities in a porous plate at:  $\Theta = 0.2$  (1);  $0.5$  (2);  $0.7$  (3);  $0.9$  (4)

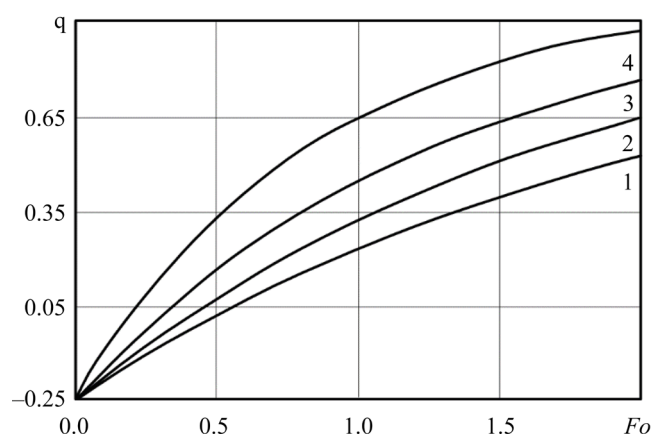


Fig. 6. Heat-flux density distribution at:  
 $\varphi = 0.75$  (1);  $0.80$  (2);  $0.85$  (3);  $0.90$  (4);

**Discussion and Conclusion.** In the course of the study, a mathematical model of heat transfer for a flat porous plate based on the Fisher-Koch prefractal S type TPMP was developed. The accuracy of the solution was confirmed by comparison with alternative calculation methods, such as finite-difference and finite-element analysis. The maximum deviation of the results according to the Chebyshev norm did not exceed 3%.

One of the significant advantages of the proposed approach is the ability to calculate the temperature distribution and heat losses in porous media without using complex computer programs and expensive computing equipment. The expressions obtained for the temperature function significantly simplify the process of engineering calculations of heat transfer in such materials.

The numerical modeling results, consistent with fundamental studies on thermal conductivity [20], methods for specifying boundary and initial conditions [15], as well as with various approaches to numerical calculations [11], open up new prospects for further scientific research. In particular, the developed approach can be applied to the analysis of one-dimensional heat transfer in porous media, including the calculation of temperature distribution, heat fluxes, and effective thermal conductivity coefficients of materials based on TPMP.

## References

1. Kem AYu. Surface Magnetic Properties and Fractality of Fe-P Powder Material – Iron Analogue Received by Porous Workpiece Forging. *Vestnik of Don State Technical University*. 2011;11(2):174–180. URL: <https://www.vestnik-donstu.ru/jour/article/view/707> (accessed: 25.10.2024).
2. Yi-Lung Cheng, Chih-Yen Lee. Porous Low-Dielectric-Constant Material for Semiconductor Microelectronics. In book: *Nanofluid Flow in Porous Media*. MSh Kandelousi, S Ameen, M Shaheer Akhtar, Hyung-Shik Shin (eds). London: InTech; 2020. 244 p. <https://doi.org/10.5772/intechopen.81577>
3. Su-Gwang Jeong, Jeonghun Lee, Seong Jin Chang, Sumin Kim. Thermal and Structural Behavior of Thermal Inertia-Reinforced Mortars for Building Envelope Applications. *Construction and Building Materials*. 2023;384:131452. <https://doi.org/10.1016/j.conbuildmat.2023.131452>
4. Maslov AA, Mironov SG, Poplavskaya TV, Kirilovskiy SV, Tsyryulnikov IS. Effect of Porous Inserts on Aerodynamics of Flying Vehicles. *Journal of Physics: Conference Series*. 2019;1382:012023. <https://doi.org/10.1088/1742-6596/1382/1/012023>
5. Goltzman BM, Yatsenko EA, Gerashchenko VS, Komunzhieva NYu, Yatsenko LA, Smoliy VA, et al. Porous Heat-Insulating Materials Based on Various Types of Silicate Raw Materials. *Bulletin of Higher Educational Institutions. North Caucasus Region. Technical Sciences*. 2020;(1):55–60. <https://doi.org/10.17213/1560-3644-2020-1-55-60>
6. Shashkeev KA, Shuldeshov EM, Popkov OV, Kraev ID, Yurkov GYu. Porous Sound-Absorbing Materials (Review). *Proceedings of VIAM*. 2016;42(6):46–56. <https://doi.org/10.18577/2307-6046-2016-0-6-6-6>
7. Gasanov SK. Polymeric Composite Materials for Aircraft and Space Equipment. *International Research Journal*. 2014;28(9):29–30. <https://research-journal.org/en/archive/9-28-2014-september> (accessed: 25.10.2024).
8. Péter Ádám, Levente Dudás, Ottó Temesi, András Nagy, Katalin Sinkó. Porous Aluminum Oxide Insulation Materials Tested in Space Mission. *CEAS Space Journal*. 2023;15:671–680. <https://doi.org/10.1007/s12567-022-00473-w>

9. Mazitov AA. Web Application for Mathematical Modeling of Unsteady Oil Flow in Porous Medium. *Advanced Engineering Research (Rostov-on-Don)*. 2023;23(4):422–432. <https://doi.org/10.23947/2687-1653-2023-23-4-422-432>
10. Soloviev AN, Chebanenko VA, Oganesyanyan PA, Fomenko EI. On a Method for Calculating Bending and Shear Vibrations of a Porous Piezoelement in the Low-Frequency Region. *Advanced Engineering Research (Rostov-on-Don)*. 2024;24(2):148–158. <https://doi.org/10.23947/2687-1653-2024-24-2-148-158>
11. Prosviryakov EYu, Ledyankina OA, Goruleva LS. Exact Solutions to the Navier–Stokes Equations for Describing the Flow of Multicomponent Fluids with Internal Heat Generation. *Russian Aeronautics*. 2024;67(1):60–69. <https://doi.org/10.3103/S1068799824010070>
12. Ershkov S, Leshchenko D, Prosviryakov E. Correction: A Novel Type of ER3BP Introducing Milankovitch Cycles or Seasonal Irradiation Processes Influencing onto Orbit of Planet. *Archive of Applied Mechanics*. 2023;93:823–824. <https://doi.org/10.1007/s00419-022-02328-6>
13. Pavlenko A, Koshlak H. Production of Porous Material with Projected Thermophysical Characteristics. *Metallurgical and Mining Industry*. 2015;(7):123–127.
14. Chaniot J, Moreaud M, Sorbier L, Fournel T, Becker J-M. Tortuosimetric Operator for Complex Porous Media Characterization. *Image Analysis and Stereology*. 2019;38(1):25–41. [https://doi.org/10.5566/ias.2039\\_15](https://doi.org/10.5566/ias.2039_15)
15. Bragin DM, Popov AI, Eremin AV, Olatuyi OJ, Zinina SA, Shulga AS. Thermal Conductivity of a Porous Material with an Ordered Structure. In: *Proc. 4th International Conference on Control Systems, Mathematical Modeling, Automation and Energy Efficiency*. New York City: IEEE; 2022. P. 858–861. <https://doi.org/10.1109/SUMMA57301.2022.9973913>
16. Mingwei Tian, Sukang Zhu, Ning Pan. Measuring the Thermophysical Properties of Porous Fibrous Materials with a New Unsteady-State Method. *Journal of Thermal Analysis and Calorimetry*. 2011;107:395–405. <https://doi.org/10.1007/s10973-011-1581-y>
17. Bicer Ayse, Kar Filiz. A Model for Determining the Effective Thermal Conductivity of Porous Heterogeneous Materials. *International Journal of Thermophysics*. 2019;40:9. <https://doi.org/10.1007/s10765-018-2468-y>
18. Dong Niu, Hongtao Gao. Thermal Conductivity of Ordered Porous Structures Coupling Gas and Solid Phases: A Molecular Dynamics Study. *Materials*. 2021;14(9):2221. <https://doi.org/10.3390/ma14092221>
19. Chau KV, Gaffney JJ. A Finite-Difference Model for Heat and Mass Transfer in Products with Internal Heat Generation and Transpiration. *Journal of Food Science*. 2006;55(2):484–487. <https://doi.org/10.1111/j.1365-2621.1990.tb06792.x>
20. Formalev VF, Reviznikov DL. *Numerical Methods*. Moscow: Fizmatlit; 2004. 400 p. (In Russ.)
21. Verzhbitsky VM. *Fundamentals of Numerical Methods*. Moscow: Vysshaya shkola; 2002. 840 p. (In Russ.)

#### **About the Authors:**

**Kristina V. Gubareva**, Cand.Sci. (Eng.), Associate Professor of the Department of Industrial Thermal Power Engineering, Samara Polytech (244, Molodogvardeyskaya Str., Samara, 443100, Russian Federation), [SPIN-code](#), [ORCID](#), [ScopusID](#), [r.kristina2017@mail.ru](mailto:r.kristina2017@mail.ru)

**Anton V. Eremin**, Dr.Sci. (Eng.), Associate Professor, Vice-rector for Integration Projects, Head of the Department of Industrial Thermal Power Engineering, Samara Polytech (244, Molodogvardeyskaya Str., Samara, 443100, Russian Federation), [SPIN-code](#), [ORCID](#), [ScopusID](#), [a.v.eremin@list.ru](mailto:a.v.eremin@list.ru)

#### **Claimed Contributorship:**

**KV Gubareva:** investigation, methodology, writing — review & editing, visualization.

**AV Eremin:** supervision, conceptualization, funding acquisition.

**Conflict of Interest Statement:** the authors claimed no conflict of interest.

**All the authors have read and approved the final version of manuscript.**

#### **Об авторах:**

**Кристина Владимировна Губарева**, кандидат технических наук, доцент кафедры промышленной теплоэнергетики Самарского государственного технического университета (443100, Российская Федерация, г. Самара, ул. Молодогвардейская, д. 244), [SPIN-код](#), [ORCID](#), [ScopusID](#), [r.kristina2017@mail.ru](mailto:r.kristina2017@mail.ru)

**Антон Владимирович Еремин**, доктор технических наук, доцент, проректор по интеграционным проектам, заведующий кафедрой промышленной теплоэнергетики Самарского государственного технического университета (443100, Российская Федерация, г. Самара, ул. Молодогвардейская, д. 244), [SPIN-код](#), [ORCID](#), [ScopusID](#), [a.v.eremin@list.ru](mailto:a.v.eremin@list.ru)

***Заявленный вклад авторов:***

**К.В. Губарева:** проведение исследования, разработка методологии, написание рукописи, редактирование, визуализация.

**А.В. Еремин:** научное руководство, разработка концепции, получение финансирования.

***Конфликт интересов:*** авторы заявляют об отсутствии конфликта интересов.

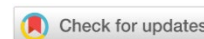
***Все авторы прочитали и одобрили окончательный вариант рукописи.***

**Received / Поступила в редакцию** 17.01.2025

**Reviewed / Поступила после рецензирования** 14.02.2025

**Accepted / Принята к публикации** 28.02.2025

# MACHINE BUILDING AND MACHINE SCIENCE МАШИНОСТРОЕНИЕ И МАШИНОВЕДЕНИЕ



UDC 621.9 + 539.62

Original Empirical Research

<https://doi.org/10.23947/2687-1653-2025-25-1-32-42>

## Effect of Periodic Fluctuations of Cutting Mode Parameters on the Temperature of the Front Face of a Turning Tool

Evgeny V. Fominov  , Valery E. Gvindjiliya , Andrey A. Marchenko ,  
Constantine G. Shuchev 

Don State Technical University, Rostov-on-Don, Russian Federation

✉ [fominoff83@mail.ru](mailto:fominoff83@mail.ru)

EDN: LQYCND

### Abstract

**Introduction.** Modern research aimed at improving the efficiency of the workpart procedures emphasizes the importance of taking into account the effect of periodic disturbances on the cutting dynamics. However, few works consider uncontrolled periodic disturbances, whose sources are spindle units and the supporting system of the machine. These disturbances also have a significant impact on the final quality indicators of the cutting process. Therefore, an urgent task in the mechanical engineering technology is to establish patterns of the effect of uncontrolled disturbances on the dynamics of the cutting process, which is particularly important for the development of systems for the automated selection of operating conditions or vibration diagnostics systems. This research is aimed at determining the mechanism of influence of periodic fluctuations of processing parameters caused by vibration disturbances on the temperature of the front face of the turning cutter, which is the key indicator of the development of diffusion wear of the carbide tool.

**Materials and Methods.** The study of the effect of periodic disturbances on the temperature of the front face of the tool was performed in two stages. At the first stage, based on a full-scale experiment on finishing longitudinal turning of blanks made of 10GN2MFA steel with cutters with T15K6 hard alloy plates, the parameters of the disturbance model in the system were identified, namely, the oscillatory accelerations of the tool under its wear. The vibration characteristics of the 16K20 universal lathe were measured using a vibration stand assembled on the basis of AP2089–100–3.3–02B vibration transducers, with a signal sampling frequency of 10 kHz. At the second stage, a digital study of the simulated disturbances and their effect on the dynamics of the cutting process was carried out. The results of the experiments were analyzed to compare the calculated maximum temperature of the front face of the tool at the moments when one of the specified output parameters of processing, obtained as a result of digital modeling, reaches an extreme value under the impact of periodic disturbances.

**Results.** It has been established that fluctuations in the parameters of operating cutting modes caused by periodic disturbances lead to temperature fluctuations in the contact zone of the tool and the blank. The greatest impact on the temperature in the cutting system under study was exerted by the combination of processing parameters at the moments of reaching extreme feed values. However, when fluctuations in cutting depth and speed reached extreme values, no significant changes in contact temperature were observed.

**Discussion and Conclusion.** The results of the conducted research emphasize the importance of analyzing the effect of periodic disturbances on pulse changes in contact temperature in the processing zone. The presented model of the relationship between tool vibrations and temperature in the cutting zone can be used to optimize turning modes. The criterion of optimality is the minimization of tool wear, which is determined on the basis of an analysis of temperature fluctuations and vibration activity signals of the tool.

**Keywords:** fluctuations of cutting modes, longitudinal turning, feed drive vibrations, front face temperature, plastic deformations

**Acknowledgments.** The authors would like to thank the Editorial board and the reviewers for their attentive attitude to the article and for the specified comments that improved the quality of the article.

**Funding Information.** The research is done under terms of economic agreement No. 16031262214 with JSC AEM-Technologies.

**For Citation.** Fominov EV, Gvindjiliya VE, Marchenko AA, Shuchev CG. Effect of Periodic Fluctuations of Cutting Mode Parameters on the Temperature of the Front Face of a Turning Tool. *Advanced Engineering Research (Rostov-on-Don)*. 2025;25(1):32–42. <https://doi.org/10.23947/2687-1653-2025-25-1-32-42>

Оригинальное эмпирическое исследование

## Влияние периодических флуктуаций параметров режимов резания на температуру передней поверхности токарного резца

Е.В. Фоминов , В.Е. Гвинджилия , А.А. Марченко , К.Г. Шучев 

Донской государственной технической университет, г. Ростов-на-Дону, Российская Федерация

✉ [fominoff83@mail.ru](mailto:fominoff83@mail.ru)

### Аннотация

**Введение.** Современные исследования, направленные на повышение эффективности процессов обработки деталей, подчеркивают важность учета влияния периодических возмущений на динамику резания. Однако немногие работы рассматривают неуправляемые периодические возмущения, источниками которых являются шпиндельные узлы и несущая система станка. Эти возмущения также оказывают значительное влияние на конечные показатели качества процесса резания. Поэтому актуальной задачей в области технологии машиностроения становится раскрытие закономерностей влияния неуправляемых возмущений на динамику процесса резания, что особенно важно для разработки систем автоматизированного выбора технологических режимов или систем вибродиагностики. Цель этой работы заключается в определении механизма влияния периодических флуктуаций параметров обработки, вызванных вибрационными возмущениями, на температуру передней поверхности токарного резца, что является основным показателем развития диффузионного износа твердосплавного инструмента.

**Материалы и методы.** Исследование влияния периодических возмущений на температуру передней поверхности инструмента проводилось в два этапа. В первом этапе на базе натурального эксперимента по чистовому продольному точению заготовок из стали 10ГН2МФА резцами с пластинами твёрдого сплава Т15К6 были идентифицированы параметры модели возмущений в системе, а именно колебательные ускорения инструмента в процессе его износа. Вибрационные характеристики используемого универсального токарного станка 16К20 измерялись с помощью вибростенда, собранного на основе вибропреобразователей AP2089–100–3.3–02Б, с частотой дискретизации сигнала 10 кГц. На втором этапе проводилось цифровое исследование моделируемых возмущений и их влияния на динамику процесса резания. Результаты опытов анализировались с целью сравнения расчетной максимальной температуры передней поверхности инструмента в моменты, когда один из заданных выходных параметров обработки, полученный в результате цифрового моделирования, достигает экстремального значения под воздействием периодических возмущений.

**Результаты исследования.** Установлено, что флуктуации параметров технологических режимов резания, вызванные периодическими возмущениями, приводят к колебаниям температуры в зоне контакта инструмента с заготовкой. Наибольшее влияние на температуру в исследуемой системе резания оказало сочетание параметров обработки в моменты достижения экстремальных значений подачи. При этом, когда флуктуации глубины и скорости резания достигали экстремальных величин, значительных изменений температуры контакта не наблюдалось.

**Обсуждение и заключение.** Результаты проведённого исследования подчеркивают важность анализа влияния периодических возмущений на импульсные изменения контактной температуры в зоне обработки. Приведённая модель взаимосвязи между вибрациями инструмента и температурой в зоне резания может быть использована для оптимизации режимов точения. Критерием оптимальности выступает минимизация износа инструмента, что определяется на основе анализа температурных колебаний и сигналов вибрационной активности инструмента.

**Ключевые слова:** флуктуации режимов резания, продольное точение, вибрации привода подач, температура передней поверхности, пластические деформации

**Благодарности.** Авторы выражают благодарность редакции и рецензентам за внимательное отношение к статье и указанные замечания, которые позволили повысить ее качество.

**Финансирование.** Работа выполнена в рамках хозяйственного договора № 16031262214 с АО «АЭМ-технологии».

**Для цитирования.** Фоминов Е.В., Гвинджилия В.Е., Марченко А.А., Шучев К.Г. Влияние периодических флуктуаций параметров режимов резания на температуру передней поверхности токарного резца. *Advanced Engineering Research (Rostov-on-Don)*. 2025;25(1):32–42. <https://doi.org/10.23947/2687-1653-2025-25-1-32-42>

**Introduction.** Metal cutting is a complex nonlinear process characterized by irreversible transformations of mechanical energy into thermal energy. Plastic deformations and friction processes between the material and the front and back faces of the tool form the main set of factors that directly affect the intensity of heat generation in the contact zone. In turn, this determines the level of wear and cyclic resistance of the cutting tool (CT). In the traditional consideration of the effect of temperature on the wear resistance of cutting tools, it is common to speak about the average value of this parameter in the cutting zone. However, it should be emphasized that the pattern of the temperature distribution on the contact areas [1] and in the volume of the tool material [2] also significantly affects the tool life period.

Cutting temperature is an important indicator of the thermal dissipative properties of wear-resistant coatings [3], the efficiency of using lubricating and cooling processing aids (LCPA) [4], and the selection of conditions for supplying LCPA to the cutting zone [5]. Temperature control is particularly important when cutting without using LCPA [6] or with their minimal use [7]. Evaluation of the thermal state of the cutting zone is of primary importance when processing blanks made of materials with low thermal conductivity [8], as well as when selecting optimal cutting conditions that provide a given surface quality of the part [9] and minimal wear of the cutting tool [10].

In this paper, the contact zone of the chip with the front face of the tool in the area of secondary plastic deformations (SPD) is considered as a heavily loaded tribosystem. The contact area and its speed depend significantly on the cutting modes [11, 12]. In accordance with the scientific approach of A.V. Chichinadze and K.G. Shuchev, the temperature distribution along the length of a heavily loaded tribocontact is described on the basis of the analysis of the surface plastically deformable microvolume in the blank (chip), which is considered as a zone of quasi-viscous flow of the material. This process is related to the heat release due to viscous dissipation of friction energy [13]. The key factors, that determine the contact temperature in a real cutting system and are considered as input parameters in the resulting mathematical model, may evolve, e.g., through changing the length of contact along the front surface of the tool with increasing wear, and also manifest themselves in the form of periodic fluctuations in the cutting operating practice.

Periodic fluctuations are deviations of the control system parameters, which are primarily affected by spindle group runouts and kinematic disturbances. As a result of spindle runouts, periodic variations in the area of the cut layer occur, which, in turn, causes a change in the parameters of the dynamic cutting system. These data are confirmed by the results of studies conducted by A.V. Push [14]. Fluctuations in the parameters relative to their nominal values can cause periodic or pulsed changes in the temperature distribution on the surface of the tribocontact “front face-chip”, along with such factors as adhesion and diffusion processes, as well as tribochemical reactions. Thus, a set of values of the parameters of cutting operating practice at each moment in time determines the change in temperature in the cutting system. The study of this relationship is based on both physical and mechanical experiments and a digital model of the dynamics of the cutting process [15, 16]. Unlike previously conducted studies, the experimental and analytical models presented in the article allow for a virtual assessment of temperature variation caused by fluctuations in cutting mode parameters. Pulse energy loads on the tool, determined using a digital model and caused by thermodynamic processes in the contact zone, can serve as a basis for predicting tool life and determining cutting modes by the criterion of minimizing resource costs for processing the blank. At the same time, the digital model of the system takes into account experimentally obtained data on the dynamics of the cutting process, received during full-scale tests using a vibration stand and a dynamometer, which allows reaching the most reliable results.

The objective of this research was to increase the efficiency of the cutting process by determining the mechanism of the effect of periodic fluctuations in the parameters of the processing modes on the temperature of the front face of the turning cutter, which is the main indicator of the development of diffusion and oxidation types of wear of the carbide tool. In the future, the presented mathematical models and methods will allow determining such cutting modes in which temperature variation in the contact zone “front surface – chips” will be minimal.

**Materials and Methods.** The experiments were conducted under natural conditions during external longitudinal turning without cooling the blanks with a diameter of  $d = 120$  mm, made of 10GN2MFA stainless steel using T15K6 carbide plates with a special coating. The cutting speed was  $V = 130$  m/min, feed —  $s = 0.15$  mm/rev, and the cutting depth —  $t = 0.5$  mm. The cutting geometry was as follows: rake angle  $\gamma = 10^\circ$ , clearance angle  $\alpha = 10^\circ$ , plan approach angle  $\varphi = 95^\circ$ , and the plate vertex radius  $r = 0.5$  mm. The average temperature in the cutting zone was measured by the relative thermal emf method, using a laboratory measuring stand for turning model STD 201.1 and digital converters from National Instruments, while preliminary calibration of the thermocouple was performed.

The vibration characteristics of the universal lathe 16K20 used in the experiments were recorded by the vibration stand, which was assembled on the basis of vibration transducers A603C01. For data processing, an external ADC/DAC module E14-440 was used, which provided signal conversion from vibration sensors, as well as a signal amplifier. The sampling frequency was 10 kHz per data acquisition channel. The sensors were installed on the cutter in three orthogonal directions relative to the blank — longitudinal, transverse, and tangential. Digital data processing was performed using Signal Processing Toolbox in the MATLAB software environment.

The model of the dynamic cutting system is represented by a set of three interconnected subsystems. The first subsystem provides the movement of the cutting tool relative to the blank, setting the operating cutting modes, as well as the inertial-dissipative properties of the system. The second subsystem is responsible for elastic deformations and cutting forces acting on the cutting tool. The third subsystem implements a block for generating uncontrolled disturbances, whose source are kinematic disturbances from the machine drive system and spindle unit runouts [15].

Uncontrolled disturbances affect the resulting velocity vector of the tool tip relative to the blank, as well as the cutting force of the tool. When modeling the dynamics of the treatment process, it is necessary to disclose the formation of the values of the parameters of the cutting speed  $V$  (mm/s), feed rate  $s$  (mm/rev), and cutting depth  $t$  (mm). For each parameter, they are represented by the sum of the value specified by the control system ( $V_0, s_0, t_0$ ), deformation displacements  $\delta$  (mm), and the rates of deformation displacements  $\eta = dH/d = \{\eta_x, \eta_y, \eta_z\}$  (mm/s), as well as vibration disturbances  $\Delta = \{\Delta_x, \Delta_y, \Delta_z\}$  (mm). Vibration disturbances are periodic functions of time in their structure, they can be represented as:

$$\Delta_i(t) = \sum_{n=1}^k A_n \sin(\omega_n t),$$

$$v_i^\Delta(t) = d\Delta_i / dt = \sum_{n=1}^k A_n \omega_n \cos(\omega_n t),$$

where  $A_n, \omega_n$  — respectively, the amplitudes and frequencies of the oscillators disturbing the tool movement in the directions  $i = \{X, Y, Z\}$ , determined experimentally. The final representation of the operating cutting modes is modeled in the following form:

$$V = V_0 - \eta_z + v_z^\Delta;$$

$$s = \int_{\tau-\tau_0}^{\tau} (V_2 - \eta_x + v_x^\Delta) d\tau;$$

$$t = t_0 - H_y + \Delta_y,$$

where  $\tau_0 = 1/\Omega$  — time of one revolution of the part, s;  $\Omega$  — frequency of rotation of the part, Hz;  $V_2 = s_0 \cdot \Omega$ , mm/s.

The evolutionary change in the contact length  $l_k$  along the front bevel and wear along the rear surface of the plate  $h$ , was determined using a metallographic inverted microscope LaboMet-14, which was equipped with a digital visualization system. In this case, the geometry of the plate was taken into account. The shrinkage coefficient of the chips was estimated by the weight method using laboratory scales of the Massa-K-150-1 type.

To construct a theoretical temperature distribution along the contact length, the dependence proposed by Chichinadze-Shuchev was used:

$$T(x, h) = \left( \frac{\omega_{01}}{k_1 + m_1} + \frac{\omega_{02}}{V_c} \cdot \frac{x}{k_2^3 \cdot a_2} \cdot \left( \frac{x}{V_c} \cdot k_2^3 \cdot a_2 + 1 - 2 \cdot k_2 \cdot \sqrt{a_2 \cdot \frac{x}{V_c}} \cdot \frac{1}{\pi} - \exp\left(\frac{x}{V_c} \cdot k_2^2 \cdot a_2\right) \cdot \operatorname{erfc}\left(k_2 \cdot \sqrt{a_2 \cdot \frac{x}{V_c}}\right) \right) \right) \cdot \left( \lambda_1 \cdot m_1 + \frac{2 \cdot \lambda_2}{\pi \cdot a_2 \cdot \frac{x}{V_c}} \right)^{-1}, \quad (1)$$

where  $x = 0 \dots l_k/2$ ;  $\omega_{02}$  — initial density of the heat source in the blank:

$$\omega_{02} = \frac{q_0 \cdot k \cdot t_H}{t_{ni} \cdot h \cdot \left( 1 - \exp\left(-k \cdot \frac{t_H}{t_{ni}}\right) \right)}, \quad (2)$$

where  $h$  — thickness of plastically deformed layer in chips;  $\omega_{01}$  — maximum volume density of heat source from friction forces in the tool body,  $W/m^3$ ;  $q_0$  — specific friction power for the front face,  $W/m^2$ ;  $k_{1,2}$  — localization coefficients of heat absorption source for the tool and blank, respectively,  $m^{-1}$ ;  $a_2$  — thermal diffusivity coefficient of the blank,  $m^2/s$ ;  $\lambda_{1,2}$  — thermal conductivity coefficient of the hard alloy and the blank material, respectively,  $W/m \cdot ^\circ C$ ;  $V_c$  — speed of the chip movement along the front face,  $m/s$ ;  $\tau_k$  — average shear stress on the front face, Pa;  $t_{ni}$  — melting temperature of the blank material,  $^\circ C$ ;  $k$  — temperature coefficient,  $^\circ C$ ,  $k = 7.143 \cdot 10^{-4} t_{ni}$ ;  $t_H$  — temperature difference inside the plastically deformed layer,  $^\circ C$ ;  $h$  — thickness of the secondary plastic deformation zone in the chip, m.

$$m_1 = \sqrt{\frac{\alpha_1}{\lambda_1 \cdot \left(\frac{A_k}{P_k}\right)}}$$

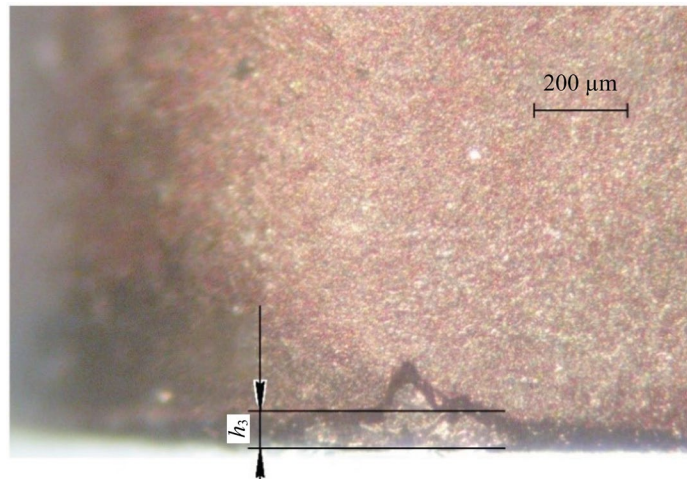
where  $A_k$  — contact area,  $m^2$ ;  $P_k$  — contact perimeter,  $m$ ;  $\alpha_1$  — heat transfer coefficient of the tool material,  $m^2/^\circ C$ .

The calculation of the temperature distribution according to dependence (1) was performed taking into account the change in the thickness of the plastically deformed layer along the length of the contact. The type of dependence  $h = f(x)$  was determined separately for each of the combinations of parameters  $V$ ,  $s$  and  $t$  at the moment of fluctuation through modeling the deformation processes in the chips using the finite element method according to the technique [17].

**Research Results.** An increase in the contact length on the front face of the cutter due to wear processes contributes to a growth of temperature, which reaches its maximum values as the cutting system approaches critical wear. According to the results of a full-scale experiment, the cutting system reaches the critical wear value on the rear face of the tool  $h_3 = 0.12$  mm (Fig. 1 *a*) in 24 minutes, the contact length on the front face by this time is  $l_k = 0.445$  mm (Fig. 1 *b*), the length of the SPD section is  $l_l = l_k/2 = 0.2225$  mm.



*a)*



*b)*

Fig. 1. Evaluation of wear of the plate working faces:  
*a* — contact area on the front face; *b* — contact area on the back face

Figure 2 *a* shows the real-time temperature change for the last pass of the life tests. The processing time for each pass was 5.97 minutes, and the length of the linear section of the machined surface of the blank was 300 mm. An increase in temperature was recorded over time during each experiment (Fig. 2 *b*), as well as a growth of the average temperature in the experiment with an increase in the number of passes performed by the cutting plate. The average actual temperature in the cutting zone for the last pass was  $T_{cp} = 921^\circ C$  with an average amplitude  $27.6^\circ C$  (Fig. 2 *b*).

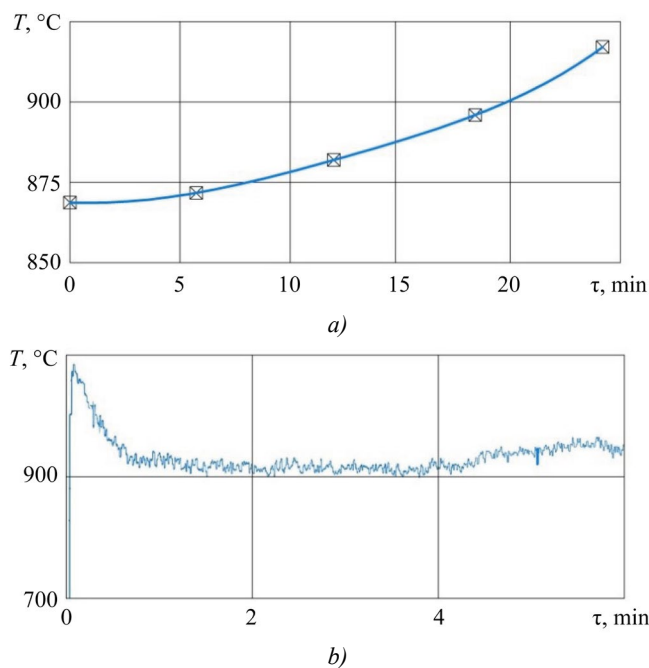


Fig. 2. Evaluation of the thermodynamic state of the cutting zone during life tests:  
 a — average temperatures for each completed pass;  
 b — temperature in the cutting zone for the last pass.

The values of the chip shrinkage coefficient based on the results of the full-scale experiment were 2.61–2.85, which confirmed the adequacy of the calculated values used for modeling (Table 1). Based on the analysis and processing of vibration acceleration data (Fig. 3 a), their power spectrum was determined. It is presented in relative units to the dispersion in Figure 3 b.

The spectral characteristic clearly shows three main peaks, which actually determine the fundamental resonant frequencies of the system based on the data of the measuring complex installed on the machine support system.

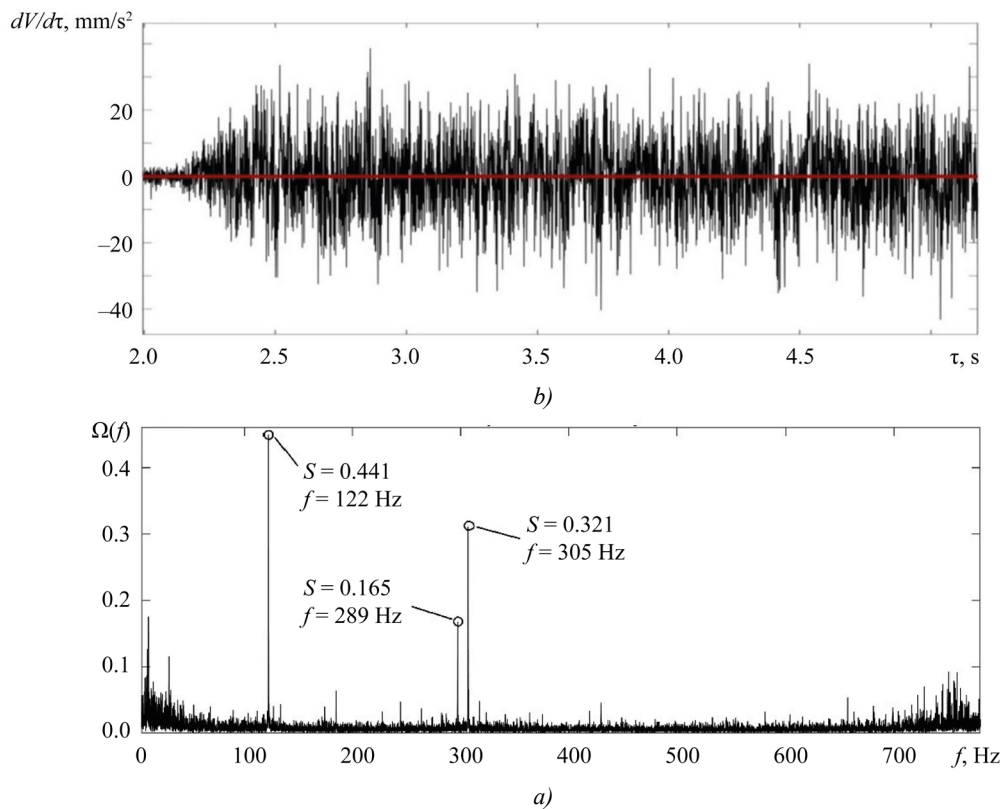


Fig. 3. Experimentally measured characteristics of the cutting process:  
 a — oscillatory accelerations of the tool tip in the tangential direction;  
 b — vibration signal spectrum  $dV/d\tau$

After identifying the parameters of vibration disturbances, we consider their effect on the trajectories of operating cutting modes in a digital simulation model of the cutting process using the example of changing the trajectories of the cutting speed (Fig. 4).

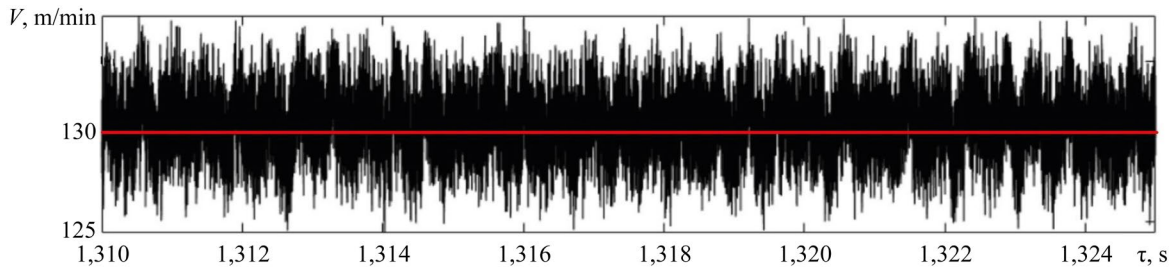


Fig. 4. Example of cutting speed trajectories  $V$  taking into account vibrations in the digital model

The analysis of the system dynamics at the stage of stabilization of the tool wear intensity ( $\tau = 20\text{--}25$  min), at the moments of extreme fluctuations in cutting modes, showed that the maximum calculated temperature of the front face  $T_{III}^{max}$ , reached according to dependence (1) at  $x = l_1$  for nominal values of the parameters  $V, s$  and  $t$ , was  $1,097.25^\circ\text{C}$  (Table 1).

Table 1

Calculated Values of Cutting Process Parameters at Fluctuation Moments

State of the parameter at the moment of fluctuation	$V, \text{ m/min}$	$s, \text{ mm/rev}$	$t, \text{ mm}$	$K_a$	$V_c, \text{ m/min}$	$T_{III}^{max}, ^\circ\text{C}$	$A_T, ^\circ\text{C}$
nominal	130.0	0.150	0.500	2.797	46.47	1,097.25	–
$V \rightarrow \text{max}$	135.1	0.151	0.541	2.861	47.08	1,100.31	18.130
$V \rightarrow \text{min}$	124.4	0.189	0.524	2.641	49.23	1,115.38	
$s \rightarrow \text{max}$	130.5	0.225	0.548	2.524	51.47	1,141.75	61.919
$s \rightarrow \text{min}$	132.1	0.101	0.463	3.101	42.03	1,079.83	
$t \rightarrow \text{max}$	133.8	0.177	0.552	2.658	48.90	1,112.37	15.120
$t \rightarrow \text{min}$	132.7	0.146	0.446	2.861	45.43	1,098.56	

Let us consider the maximum cutting speed  $V_{max} = 135.1$  m/min, which, according to the digital modeling results, is periodically repeated in the studied time interval. At this moment, the feed and cutting depth take values  $s = 0.151$  mm/rev and  $t = 0.541$  mm (Fig. 5 a, b, c).

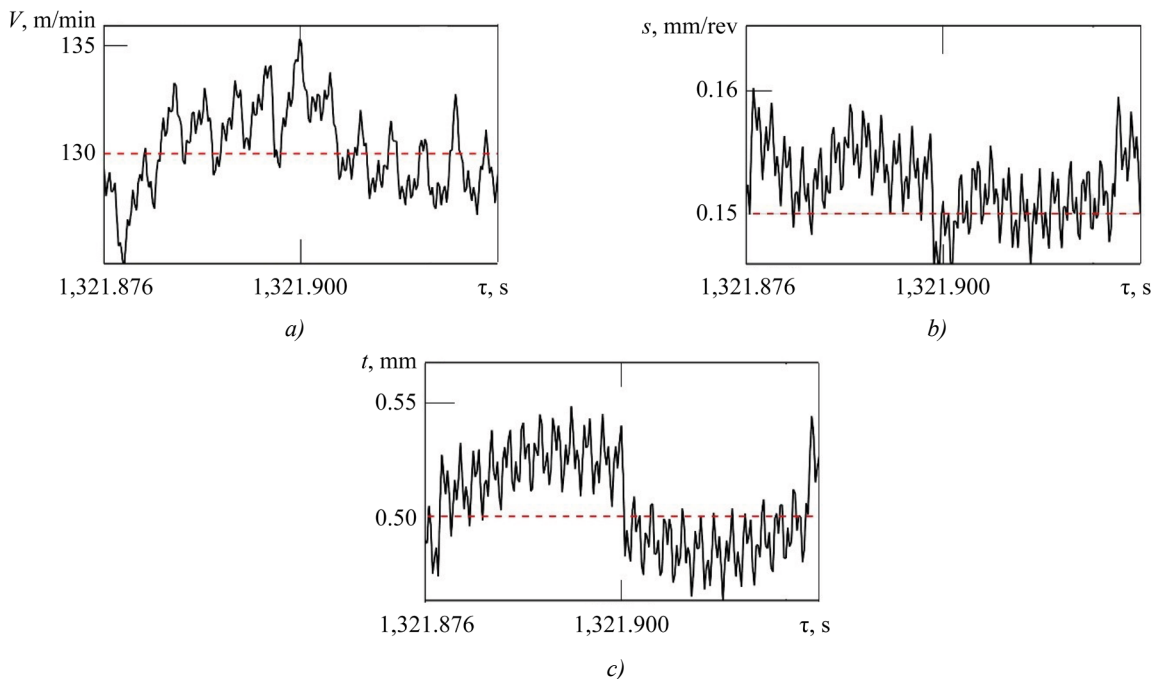


Fig. 5. Cutting mode values at maximum cutting speed: a — cutting speed; b — feed rate; c — cutting depth

As a result of this combination of cutting conditions, the maximum contact temperature at the moment of fluctuation increases slightly (Table 1). When the cutting speed reaches the lowest value (124.4 m/min), the accompanying change in the parameters  $s$  and  $t$  causes an increase in the maximum temperature to 1,115.38 °C, as shown in Table 1. In this case, temperature fluctuations reach  $A_T = 18.13^\circ\text{C}$ . At extreme values of the cutting depth in combination with the change in speed and feed at this moment, an increase in the contact temperature is observed up to a maximum of 1,112.37°C (Table 1). The greatest effect on the temperature of the front face in the studied cutting system is exerted by extreme values of feed at the moment of fluctuation (Fig. 6 a, b, c).

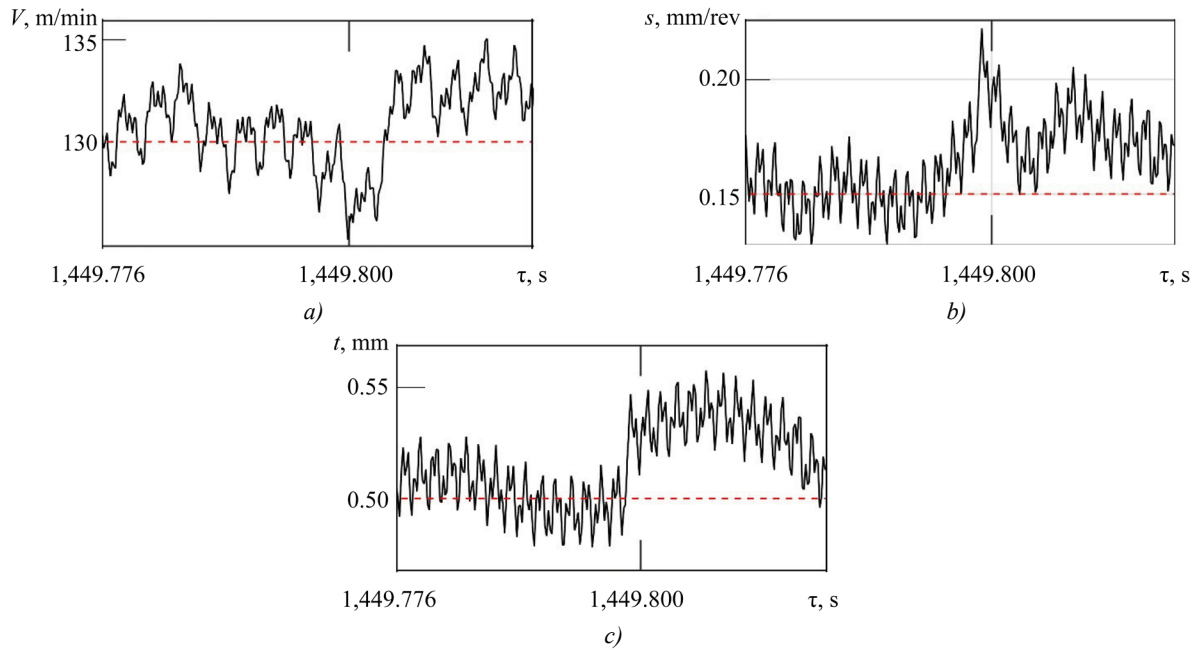


Fig. 6. Cutting mode values at maximum feed:  
 a — cutting speed; b — feed rate; c — cutting depth

The combination of processing modes, when parameter  $s$  reaches its maximum, leads to an increase in the contact temperature  $T_{III}^{\max}$  to 1,141.75°C, while at minimum feed, its decrease to 1,079.83°C is observed (Table 1).

The curves characterizing the temperature distribution along the length of the tribocontact on the front face, according to dependence (1), are shown in Figure 7. For the initial point of  $x$ -axis, the calculated values of the temperature obtained due to heat generation in the zone of *primary plastic deformations* (PPD) are indicated.

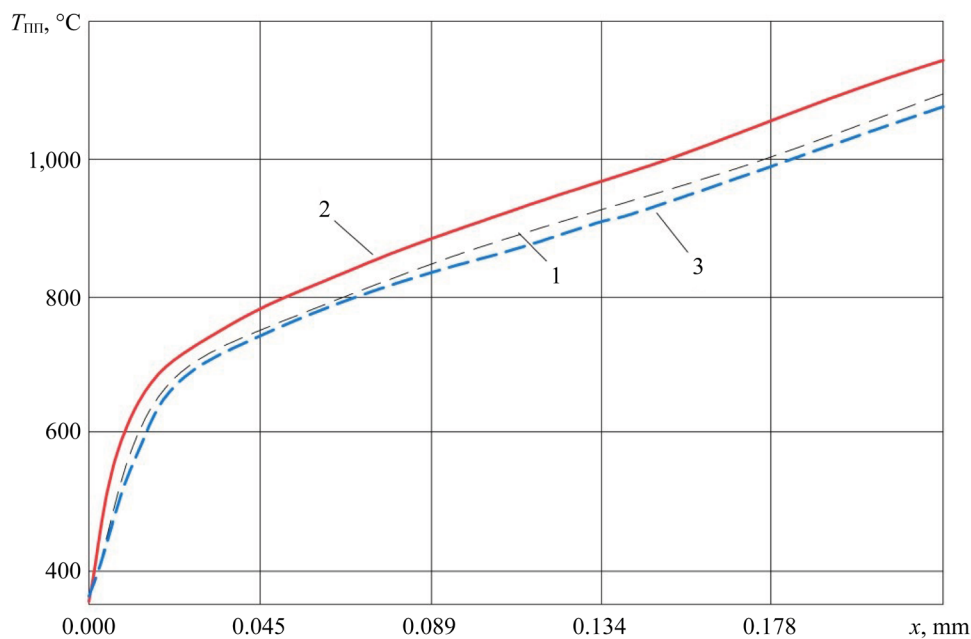


Fig. 7. Temperature distribution in the SPD section on the front face at nominal (1), maximum (2), and minimum (3) feed values  $s$

**Discussion and Conclusion.** During the combined experiment, changes in the trajectories of the processing modes were recorded, which were caused by vibration disturbances in the cutting system under study. The research determined the values of these changes for quasistatic moments, when the speed, feed or depth of the cut layer reached their extreme values as a result of fluctuations. It was established that at the maximum feed deviation amplitude, the greatest temperature variation on the front face of the tool was observed throughout the entire section of the time trajectory. In the considered scenario, a significant feed deviation in combination with a fluctuation in the cutting depth caused a periodic redistribution of cutting forces and a significant change in the dynamics of deformation processes in the zone of primary plastic deformations.

As a result of these phenomena, the greatest deviations in the chip shrinkage coefficient  $Ka$  and its sliding speed  $Vc$  were observed, which significantly affected the contact temperature in the tribosystem “cutter face – chip”. It is interesting to note that the smallest temperature changes occur at maximum cutting speed and depth values, since the combination of actual machining modes at the time of such fluctuations level out possible significant deviations in the tribocontact temperature. Thus, the cutting system under study at the given machining modes is subject to the vibration characteristics of the feed drive, which cause undesirable temperature fluctuations on the front face of the cutter.

This statement necessitates a revision of the traditional understanding of the dependence of the cutting process temperature on the processing modes, specifically considering that the cutting speed is the most significant parameter determining the temperature changes in the contact zone. However, it should be noted that most papers on this topic are based on single-factor experiments, where only one parameter of the cutting system is changed, and its contribution to the temperature variation is assessed, while the effect of vibrations generated by the system itself on the dynamics of heat generation still remains uncertain [18, 19]. Thus, the integral value of temperature is actually analyzed.

The results of this study establish the features of the relationship between operating cutting modes and temperature, considering it not as an integral value, but as a changing trajectory. This trajectory demonstrates a periodic process of constant energy accumulation and its release in the cutting zone, whose dependence on fluctuations in cutting modes caused by kinematic disturbances is extremely important. Fluctuations in the tool movement trajectories relative to the part contribute to an increase in the amplitude of temperature variation, which, in turn, causes local overheating of the tool and an increase in the intensity of wear of the tool material against the background of an increase in the amplitude of the thermo-EMF signal.

Thus, the results of the conducted study emphasize the need to analyze the effect of periodic disturbances on pulse changes in contact temperature in the processing zone. The proposed model of the relationship between tool vibrations and temperature in the cutting zone explores new horizons for selecting optimal turning modes in order to minimize tool wear based on the analysis of calculated temperature variation from the tool vibration activity signal. Such experimental results can serve as fundamental data for developing a new approach to assessing the temperature in the cutting zone, which would take into account a wide range of values of operating modes.

Using the amplitude of temperature fluctuations in the vibration monitoring and compensation systems as an additional parameter for assessing the optimality of cutting modes can significantly improve the stability of the process and reduce the temperature in the cutting zone. This approach is especially relevant for metal-cutting machines that have been in operation for a long time, which are characterized by significant periodic disturbances of the cutting system from the feed and main drives.

## References

1. Fominov EV, Aliev MM, Shuchev KG, Fomenko AV. The Influence of Zirconium and Titanium Nitrides Based Coatings on Tribodeformation Processes of Friction While Cutting by Carbide Inserts. *Journal of Friction and Wear*. 2024;45(1):29–37. <https://doi.org/10.32864/0202-4977-2024-45-1-29-37>
2. Lebedev VA, Aliev MM, Fominov EV, Fomenko AV, Marchenko AA, Mironenko AE. Thermoelectric Characteristics of the Process Steel Turning by Carbide Inserts with Combined Coatings. *Journal of Friction and Wear*. 2023;44(2):114–121. <https://doi.org/10.32864/0202-4977-2023-44-2-114-121>
3. Zhu M, Achache S, Motta MP, Delblouwe A, Pelaingre C, Garcia-Wong AC, et al. Characteristics and Cutting Performance of CVD  $Al_2O_3$  Multilayer Coatings Deposited on Tungsten Carbide Cutting Inserts in Turning of 24CrMoV5-1 Steel. *Coatings*. 2023;13(5):883. <https://doi.org/10.3390/coatings13050883>
4. Rajeswari R. Investigation on the Effect of Turning of AISI 304 Stainless Steel Using MQL Technique with Corn Oil as Cutting Fluid and Comparison with Dry Condition. *Engineering Proceedings*. 2024;61(1):35. <https://doi.org/10.3390/engproc2024061035>
5. Roy S, Kumar R, Panda A, Sahoo AK, Rafighi M, Das D. A Comparative Performance Investigation of Single- and Double-Nozzle Pulse Mode Minimum Quantity Lubrication Systems in Turning Super-Duplex Steel Using a Weighted Pugh Matrix Sustainable Approach. *Sustainability*. 2023;15(20):15160. <https://doi.org/10.3390/su152015160>

6. Abbas AT, Al-Abduljabbar AA, El Rayes MM, Benyahia F, Abdelgalil IH, Elkaseer A. Multi-Objective Optimization of Performance Indicators in Turning of AISI 1045 under Dry Cutting Conditions. *Metals*. 2023;13(1):96. <https://doi.org/10.3390/met13010096>
7. Özbek O. Evaluation of Nano Fluids with Minimum Quantity Lubrication in Turning of Ni-Base Superalloy UDIMET 720. *Lubricants*. 2023;11(4):159. <https://doi.org/10.3390/lubricants11040159>
8. Arun KK, Navaneeth VR, Prabhu S, Ramesh Kumar M, Giriraj M. Experimental Investigation of Turning Process Parameter under Several Cutting Conditions for Duplex Steels for Minimization of Cutting Temperature. *Materials Today: Proceedings*. 2022;62(4):1917–1920. <https://doi.org/10.1016/j.matpr.2022.01.447>
9. Demirpolat H, Binali R, Patange AD, Pardeshi SS, Gnanasekaran S. Comparison of Tool Wear, Surface Roughness, Cutting Forces, Tool Tip Temperature, and Chip Shape during Sustainable Turning of Bearing Steel. *Materials*. 2023;16(12):4408. <https://doi.org/10.3390/ma16124408>
10. Lapshin VP. Turning Tool Wear Estimation Based on the Calculated Parameter Values of the Thermodynamic Subsystem of the Cutting System. *Materials*. 2021;14(21):6492. <https://doi.org/10.3390/ma14216492>
11. Grzesik W. *Advanced Machining Processes of Metallic Materials: Theory, Modelling, and Applications*, 2nd edition. Amsterdam: Elsevier; 2017. 608 p.
12. Juneja BL, Sekhon GS, Seth N. *Fundamentals of Metal Cutting and Machine Tools*, 2nd edition. Delhi: New Age International Publishers; 2017. 626 p.
13. Ryzhkin AA, Chichinadze AV, Shuchev KG, Filipchuk AI, Klimov MM. Temperature Conditions during Friction of Tool Materials Taking into Account the Volumetric Heat Source. *Journal of Friction and Wear*. 1986;7(3):398–407. (In Russ.)
14. Push AV. Features of Statistical Modeling of Output Characteristics of Metal-Cutting Machines. *STIN. STanki Instrument*. 1995;(10):18–22. (In Russ.)
15. Zakovorotny VL, Gvindjiliya VE. The Influence of the Vibration on the Tool Shape-Generating Trajectories When Turning. *Metal Working and Material Science*. 2019;21(3):42–58. <http://doi.org/10.17212/1994-6309-2019-21.3-42-58>
16. Altintas Y, Aslan D. Integration of Virtual and On-Line Machining Process Control and Monitoring. *CIRP Annals*. 2017;66(1):349–352. <https://doi.org/10.1016/j.cirp.2017.04.047>
17. Fominov E, Marchenko A, Suhomlinova V, Pyatnickaya O, Gladkih D. Modeling of the Temperature Distribution on the Lathe Front Surface Taking into Account Geometric Parameters of the Secondary Plastic Zone. *Transport Engineering*. 2023;14(2):4–11. <https://doi.org/10.30987/2782-5957-2023-2>
18. Masafumi Kikuchi. The Use of Cutting Temperature to Evaluate the Machinability of Titanium Alloys. *Acta Biomaterialia*. 2009;5(2):770–775. <https://doi.org/10.1016/j.actbio.2008.08.016>
19. Karaguzel U, Budak E. Investigating Effects of Milling Conditions on Cutting Temperatures through Analytical and Experimental Methods. *Journal of Materials Processing Technology*. 2018;262:532–540. <https://doi.org/10.1016/j.jmatprotec.2018.07.024>

#### **About the Authors:**

**Evgeny V. Fominov**, Cand.Sci. (Eng.), Associate Professor, Acting Head of the Engineering and Computer Graphics Department, Associate Professor of the Metal-Cutting Machines and Tools Department, Don State Technical University (1, Gagarin Sq., Rostov-on-Don, 344003, Russian Federation), [SPIN-code](#), [ORCID](#), [ScopusID](#), [ResearcherID](#), [fominoff83@mail.ru](mailto:fominoff83@mail.ru)

**Valery E. Gvindjilia**, Cand.Sci. (Eng.), Senior Lecturer of Production Automation Department, Don State Technical University (1, Gagarin Sq., Rostov-on-Don, 344003, Russian Federation), [SPIN-code](#), [ORCID](#), [ScopusID](#), [ResearcherID](#), [vvgvindjiliya@donstu.ru](mailto:vvgvindjiliya@donstu.ru)

**Andrey A. Marchenko**, postgraduate student of the Metal-Cutting Machines and Tools Department, Don State Technical University (1, Gagarin Sq., Rostov-on-Don, 344003, Russian Federation), [SPIN-code](#), [ORCID](#), [ScopusID](#), [tobago13@yandex.ru](mailto:tobago13@yandex.ru)

**Constantine G. Shuchev**, Cand.Sci. (Eng.), Professor of the Metal-Cutting Machines and Tools Department, Don State Technical University (1, Gagarin Sq., Rostov-on-Don, 344003, Russian Federation), [SPIN-code](#), [ORCID](#), [ScopusID](#), [cshuchev53@mail.ru](mailto:cshuchev53@mail.ru)

#### **Claimed Contributorship:**

**EV Fominov:** conceptualization, investigation.

**VE Gvindjiliya:** conceptualization, formal analysis.

**AA Marchenko:** investigation, writing — original draft preparation.

**CG Shuchev:** supervision.

**Conflict of Interest Statement: the authors do not have any conflict of interest.**

**All the authors have read and approved the final manuscript.**

**Об авторах:**

**Евгений Валерьевич Фоминов**, кандидат технических наук, доцент, и.о. заведующего кафедрой инженерной и компьютерной графики, доцент кафедры металлорежущих станков и инструментов Донского государственного технического университета, (344003, Российская Федерация, г. Ростов-на-Дону, пл. Гагарина, 1), [SPIN-код](#), [ORCID](#), [ScopusID](#), [ResearcherID](#), [fominoff83@mail.ru](mailto:fominoff83@mail.ru)

**Валерия Енвериевна Гвинджилия**, кандидат технических наук, старший преподаватель кафедры автоматизации производственных процессов Донского государственного технического университета (344003, Российская Федерация, г. Ростов-на-Дону, пл. Гагарина, 1), [SPIN-код](#), [ORCID](#), [ScopusID](#), [ResearcherID](#), [yvgvindjiliya@donstu.ru](mailto:yvgvindjiliya@donstu.ru)

**Андрей Анатольевич Марченко**, аспирант кафедры металлорежущих станков и инструментов Донского государственного технического университета (344003, Российская Федерация, г. Ростов-на-Дону, пл. Гагарина, 1), [SPIN-код](#), [ORCID](#), [ScopusID](#), [tobago13@yandex.ru](mailto:tobago13@yandex.ru)

**Константин Григорьевич Шучев**, кандидат технических наук, профессор, профессор кафедры металлорежущих станков и инструментов Донского государственного технического университета (344003, Российская Федерация, г. Ростов-на-Дону, пл. Гагарина, 1), [SPIN-код](#), [ORCID](#), [ScopusID](#), [eshuchev53@mail.ru](mailto:eshuchev53@mail.ru)

**Заявленный вклад авторов:**

**Е.В. Фоминов:** разработка концепции; проведение исследования.

**В.Е. Гвинджилия:** разработка концепции; формальный анализ.

**А.А. Марченко:** проведение исследования; написание черновика рукописи.

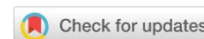
**К.Г. Шучев:** научное руководство.

**Received / Поступила в редакцию** 25.12.2024

**Reviewed / Поступила после рецензирования** 18.01.2025

**Accepted / Принята к публикации** 22.01.2025

# MACHINE BUILDING AND MACHINE SCIENCE МАШИНОСТРОЕНИЕ И МАШИНОВЕДЕНИЕ



UDC 531.788

Original Empirical Research

<https://doi.org/10.23947/2687-1653-2025-25-1-43-51>

## Investigation of the Optimal Vacuum Depth Created by an Ejector Depending on the Value of the Supply Pressure

Sergey I. Savchuk , Ervin D. Umerov  , Aziz U. Abdulgazis 

Crimean Engineering and Pedagogical University named after Fevzi Yakubov, Simferopol, Republic of Crimea

 [Ervin777@yandex.ru](mailto:Ervin777@yandex.ru)



EDN: MPXOWG

### Abstract

**Introduction.** Vacuum ejectors operating on the Venturi principle are used in various industries and are essential pneumatic devices. An important characteristic of a vacuum ejector is the vacuum depth it creates, where the maximum vacuum value is obtained in a certain range of supply pressure. Failure to comply with the supply pressure affects the performance of the ejector itself and automated vacuum systems in general. One of the options for solving this problem is to establish the recommended range of supply pressure in a fairly narrow pressure range, at which a guaranteed value of vacuum depth is reached without using the maximum capabilities of the ejector. At the same time, the technical literature does not provide the values of the dependence of the vacuum depth on the supply pressure over the entire range of ejector operation, which the authors would like to draw attention to in this work. The research objective was to conduct experimental studies on establishing the true values of the maximum vacuum depth depending on the magnitude of the ejector input pressure.

**Materials and Methods.** To conduct experimental research, a special stand was designed, manufactured and used, which allowed for the study of vacuum ejectors operating on the basis of the Venturi principle. This stand provided setting the exact vacuum value depending on the input supply pressure for ejectors with a nozzle diameter from 0.1 to 4.0 mm, which completely covered the entire range of ejectors used in real sectors of the economy. Vacuum ejectors of the VEB, VEBL, VED and VEDL families manufactured by Camozzi were investigated in the range of the inlet supply pressure of the ejector from 2.0 to 6.5 bar. The true values of the vacuum depth were determined experimentally depending on the value of the input supply pressure for each ejector, as well as the maximum values of the vacuum depth reached by each ejector at the corresponding value of the input supply pressure.

**Results.** It was experimentally proved that the recommended values of the input supply pressure given in the catalogs of ejector manufacturers did not always correspond to the true values. It was shown that the character of the obtained graphs also differed. In this regard, it was necessary to adjust the value of the input supply pressure to reach the maximum vacuum depth for each type of ejector.

**Discussion and Conclusion.** The results of the conducted experimental studies allow for a rational choice of vacuum ejectors depending on the required technological tasks. This will ensure the operability of automated vacuum systems and the performance of the ejector itself. The research results can be used by all ejector manufacturers to adjust their basic catalogs and relevant recommendations for the use of these products.

**Keywords:** vacuum depth, vacuum ejector, supply pressure of ejectors

**Acknowledgments.** The authors would like to thank the reviewers and the Editorial board of the Journal for their attentive attitude to the article and the comments indicated, which allowed us to improve the quality of the paper.

**For citation.** Savchuk SI, Umerov ED, Abdulgazis AU. Investigation of the Optimal Vacuum Depth Created by an Ejector Depending on the Value of the Supply Pressure. *Advanced Engineering Research (Rostov-on-Don)*. 2025;25(1):43–51. <https://doi.org/10.23947/2687-1653-2025-25-1-43-51>

## Исследование оптимальной глубины вакуума, создаваемой эжектором в зависимости от величины питающего давления

С.И. Савчук , Э.Д. Умеров ✉, А.У. Абдулгасис 

Крымский инженерно-педагогический университет имени Февзи Якубова, г. Симферополь, Республика Крым

✉ [Ervin777@yandex.ru](mailto:Ervin777@yandex.ru)

### Аннотация

**Введение.** Вакуумные эжекторы, работающие по принципу Вентури, применяются в различных отраслях промышленности и являются незаменимыми пневматическими устройствами. Важной характеристикой вакуумного эжектора является создаваемая глубина вакуума, где максимальное значение вакуума достигается в определенном интервале питающего давления. Несоблюдение питающего давления влияет на производительность самого эжектора и автоматизированных вакуумных систем в целом. Одним из вариантов решения данной проблемы является установление рекомендуемого диапазона питающего давления в достаточно узком интервале давлений, при котором достигается гарантированное значение глубины вакуума, не используя максимальные возможности эжектора. При этом в технической литературе не приводятся значения зависимости глубины вакуума от питающего давления на всем диапазоне работы эжектора, на которые авторы хотели бы обратить внимание в рамках данной работы. Цель работы — проведение экспериментальных исследований по установлению фактических значений максимальной глубины вакуума в зависимости от величины входного давления эжектора.

**Материалы и методы.** Для проведения экспериментальных исследований был спроектирован, изготовлен и использован специальный стенд, позволяющий осуществлять исследования вакуумных эжекторов, работающих на основе принципа Вентури. Данный стенд позволяет установить точное значение вакуума в зависимости от входного питающего давления для эжекторов, имеющих диаметр сопла от 0,1 до 4,0 мм, что полностью перекрывает весь диапазон эжекторов, применяемых в реальных секторах экономики. Были исследованы вакуумные эжекторы семейств VEB, VEBL, VED и VEDL производства компании Camozzi в интервале входного питающего давления эжектор от 2,0 до 6,5 бар. Экспериментально определялись фактические значения глубины вакуума в зависимости от величины входного питающего давления для каждого эжектора, а также максимальные значения глубины вакуума, достигаемые каждым эжектором при соответствующем значении входного питающего давления.

**Результаты исследования.** Экспериментально доказано, что рекомендуемые значения входного питающего давления приведенных в каталогах фирм производителей эжекторов не всегда соответствует действительным значениям. Показано, что отличается и характер полученных графиков. В этой связи необходимо вводить корректировку величины входного питающего давления для достижения максимальной глубины вакуума для каждого типа эжектора.

**Обсуждение и заключение.** Результаты проведенных экспериментальных исследований позволяют осуществлять рациональный выбор вакуумных эжекторов в зависимости от требуемых технологических задач. Это гарантированно обеспечит работоспособность автоматизированных вакуумных систем и производительность самого эжектора. Результаты исследований могут быть использованы всеми фирмами изготовителями эжекторов для корректировки их базовых каталогов и соответствующих рекомендаций по применению этих изделий.

**Ключевые слова:** глубина вакуума, вакуумный эжектор, питающее давление эжекторов

**Благодарности.** Авторы выражают глубокую благодарность рецензентам и редколлегии журнала за внимательное отношение к статье и указанные замечания, которые позволили улучшить качество статьи.

**Для цитирования.** Савчук С.И., Умеров Э.Д., Абдулгасис А.У. Исследование оптимальной глубины вакуума, создаваемой эжектором в зависимости от величины питающего давления. *Advanced Engineering Research (Rostov-on-Don)*. 2025;25(1):43–51. <https://doi.org/10.23947/2687-1653-2025-25-1-43-51>

**Introduction.** Currently, in various industries, the technological movement of products and parts is carried out using industrial robots equipped with vacuum suction cups, whose operation is performed using an ejector [1] based on the Venturi principle. Manufacturers offer a wide range of ejectors [2, 3], which create a vacuum of varying depth depending on the supply pressure [4], which meets the specific needs of production.

The optimum value of the air supply pressure at the inlet of the ejector, at which the maximum vacuum depth is reached, can be defined as the optimum pressure. Deviation of this pressure from the specified value causes a decrease in the vacuum depth, which, in turn, negatively affects the performance of both the ejector and the suction cup, and also increases energy costs. Thus, providing optimal supply pressure for the ejector in order to reach maximum productivity and reduce energy costs becomes an urgent task.

When studying ejectors from manufacturers such as Camozzi, Festo, Schmalz, SMC Pneumatics, and others, it has been noted that only a small number of manufacturers publish in their catalogs the exact vacuum values depending on the supply pressure for different types of ejectors. The information is mainly presented in the form of a general diagram corresponding to the entire range of ejectors of a certain type, without taking into account the diameter of their nozzles.

The practical experience of the authors of the article, as well as long-term cooperation with various production sites using vacuum ejectors, made it possible to identify significant discrepancies between the true and tabulated values of supply pressures and the corresponding values of vacuum depth. Therefore, studies aimed at determining the exact dependences of the maximum vacuum depth created by the ejector on the input supply pressure, with the aim of reaching minimum energy costs, are of considerable interest. A more in-depth study of these parameters is possible using a specially created experimental stand, which allows for a high degree of accuracy in determining the specified parameters, which, in turn, can contribute to an increase in the productivity of the entire system.

Numerous studies are devoted to the use of vacuum ejectors [5] and vacuum technology [6]. The authors draw attention to the theory of vacuum [7] and its physical foundations [8], but do not sufficiently focus on the practical side of its use. In [9], specific cases of practical application of vacuum are considered; in [10], experimental studies with an improved ejector nozzle are presented; and in [11] — flow modeling. However, in modern scientific literature, practically no attention is paid to issues concerning the dependence of the magnitude of the resulting vacuum on the input supply pressure and the parameters of vacuum ejectors. Descriptions of the characteristics of vacuum ejectors can be found mainly in reference literature, such as catalogs of vacuum equipment manufacturers, for example, the Italian company Camozzi or the German company Schmalz.

In [12], it was proposed to change the geometric dimensions of the ejector nozzle, which allowed increasing their productivity. In experimental work [13], the results of a study were presented in which the angle of inclination of the ejector mixing chamber was changed, which also contributed to increasing its productivity. In [14], the author attempted to study the main characteristics of vacuum ejectors and proposed a methodology for experimental research, which received a logical continuation in [15].

Taking into account all of the above, the authors set themselves the objective of conducting experimental studies to determine the true values of the maximum vacuum depth depending on the magnitude of the ejector input pressure.

**Materials and Methods.** To conduct full-scale studies of vacuum ejectors, a special stand [15] was used. It was developed by the authors of the article and presented in Figure 1.

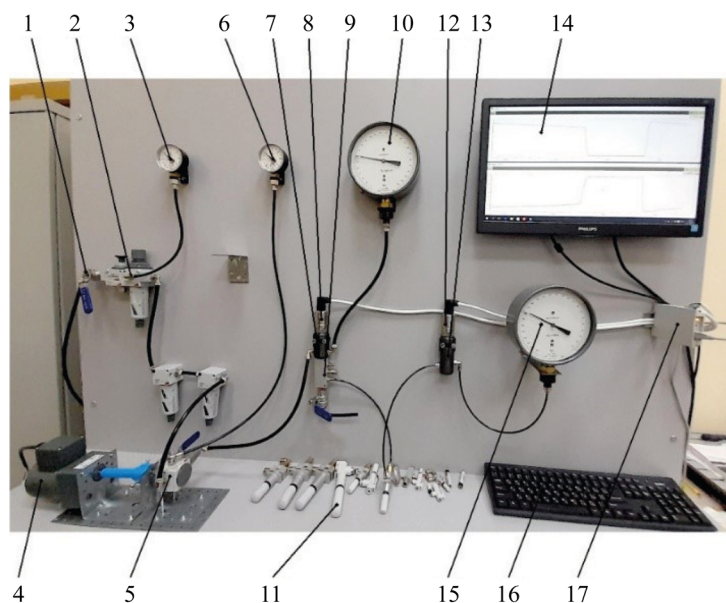


Fig. 1. Stand for conducting experimental research

Components of Stand for Conducting Experimental Studies

	Designator	Type/Model
1	Air inlet valve	Ball valve V2E-316-PP-1/4
2	Inlet unit	Modular air preparation unit MC104-N-5-FL
3	Control pressure gauge	Pressure gauge M063-R12
4	Electronic drive with regulator	Gear motor 80YT25WGV22H/80GK150H with controller WS-L (25W)
5	Main regulator with shut-off valve	Pressure regulator MC104-R05 with ball valve V2E-316-PP-1/4
6	Control pressure gauge	Pressure gauge M063-R12
7	Tee	
8	Pressure sensor	Pressure sensor MIDA-DI-15-RS485-0.15(0.25; 0.5)/0-1.6 MPa-064-M20-DIN C
9	Distribution manifold	Manifold 3053 1/4-3L-1/8
10	Control manometer	Standard deformation manometer with conditional scale, model 11202, accuracy class 0.4 16 kgf/cm <sup>2</sup> ); SM
11	Tested ejector	
12	Absolute pressure sensor	Pressure sensor MIDA-DA-15-RS485-0.15(0.25; 0.5)/0-0.1 MPa-064-M20-DIN C
13	Tee	
14	Computer monitor	
15	Control vacuum gauge	Standard deformation vacuum gauge with conditional scale, model 11201, accuracy class 0.4 (-0.1 MPa); SVG
16	Computer	Only the keyboard is shown conditionally
17	Sensor controller	Communication device MIDA-US-410

The study examined the VEB, VEBL, VED and VEDL vacuum ejectors manufactured by Camozzi [8] in the range of input pressure feeding the ejector from 2.0 to 6.5 bar. The main objective of the study was to establish the true values of the vacuum depth depending on the magnitude of the input supply pressure for each of the ejectors. In addition, it was necessary to experimentally determine the maximum vacuum depth values that each of the ejectors was capable to reach, as well as the input supply pressure corresponding to these vacuum depth values. The parameters obtained will subsequently be needed to conduct the following series of experiments aimed at establishing the time of creating vacuum in a volume of one liter at various specified vacuum depths.

For each ejector from the families under consideration, at least 17 experiments were conducted. In this case, for each individual experiment, its own fixed rotation speed of the flywheel of the main pressure regulator 5 was set. The purpose of these settings was to provide maximum smoothness of the change in parameters, as well as to exclude the omission of any significant events during the experiment.

**Research Results.** Below are the graphs of the dependence of the change in vacuum depth on the value of the supply pressure obtained as a result of the experiment for the ejector series (Fig. 2–5). The comparison of the obtained data with similar parameters of the ejectors provided in the Camozzi catalog is also performed.

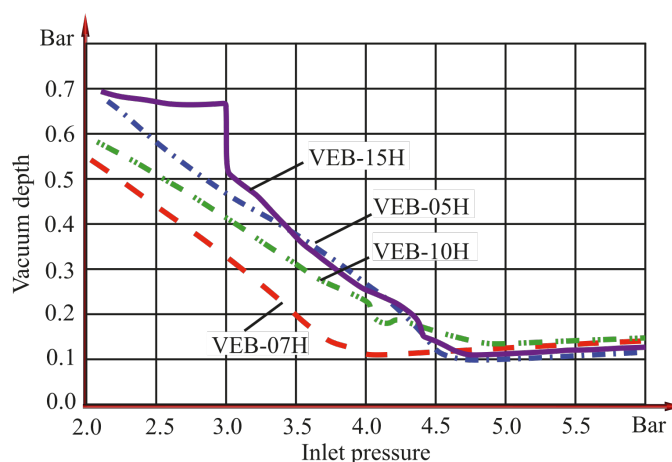


Fig. 2. Vacuum depth change dependence diagrams from the supply pressure value for VEB series ejectors

The experimental data analysis shows that for the VEB-05H ejector, the maximum vacuum depth reaches 90.5% (residual pressure 96 mbar) at supply pressure of 4.73–4.74 bar. According to the information provided in the manufacturer’s catalog for the VEB-05H ejector, the optimal supply pressure is 4.5 bar, while the vacuum depth of 82% should be reached, which corresponds to a residual pressure of 182 mbar. This value is consistent with the diagram in the manufacturer's catalog, which shows the dependence of the vacuum depth on the value of the supply pressure for the VEB family of ejectors. The authors have found that for the VEB-05H ejector at a supply pressure of 4.5 bar (recommended value from the manufacturer), the vacuum depth is also 88.65% (residual pressure 115 mbar).

As for the VEB-07H ejector, the experimental data has shown that its vacuum depth reaches 89.34% (residual pressure 108 mbar) at a supply pressure in the range of 4.07–4.08 bar. Comparing with the data provided by the manufacturer for the VEB-07H ejector, it is found that the optimal supply pressure for this device is also 4.5 bar, at which the vacuum depth should be 85% (residual pressure 152 mbar). This value does not correspond to the values presented in the company's catalog, which shows the dependence of the change in vacuum depth on the value of the supply pressure for VEB family ejectors. It is found that at a supply pressure of 4.5 bar (recommended value for operating the VEB-07H ejector), the vacuum depth reaches 88.65% (residual pressure 115 mbar). Thus, the existing discrepancies between the experimental data and the information provided by the manufacturer require additional analysis and may indicate the need to revise the recommended operating parameters of the ejectors.

It has been experimentally established that for the VEB-10H ejector, the vacuum depth reaches 86.9% (residual pressure 132.6 mbar) at a supply pressure of 4.9 bar. The data provided by the manufacturer of the VEB-10H ejector indicate that the optimal supply pressure is 5 bar, while the vacuum depth should reach 85% (residual pressure 152 mbar). This value corresponds to the dependence diagram presented in the manufacturer's catalog, which demonstrates the change in vacuum depth depending on the value of the supply pressure for VEB family ejectors. In the course of the study, the authors have found that for the VEB-10H ejector at a supply pressure of 5 bar (the value recommended as optimal for the operation of this device), the vacuum depth reaches 86.8% (residual pressure 133.5 mbar).

Of particular interest is the unusual behavior of the dependence graph in the supply pressure range from 4 to 4.2 bar (Fig. 3).

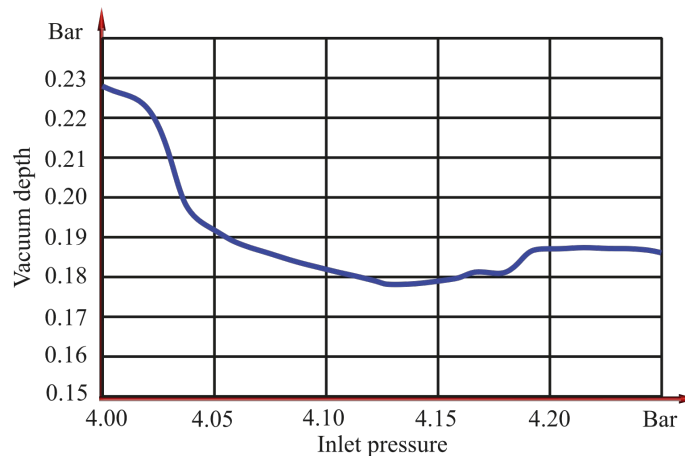


Fig. 3. Unusual behavior of the graph

For the VEB-15H ejector, it has been experimentally established that the vacuum depth reaches 89.24% (residual pressure 109 mbar) at a supply pressure of 4.75 bar. The data provided by the manufacturer of the VEB-15H ejector indicate that the optimal supply pressure is 4.5 bar, provided that the vacuum depth reaches 85% (residual pressure 152 mbar). This value probably corresponds to the diagram presented in the company's catalog, which demonstrates the dependence of the change in the vacuum depth on the value of the supply pressure for the VEB family of ejectors. In the course of the studies, it has been found that for the VEB-15H ejector, with a supply pressure of 4.5 bar recommended by the manufacturer as optimal for its operation, the vacuum depth reached 85.69% (residual pressure 145 mbar).

Particular attention should be paid to the sharp drop in vacuum values in the supply pressure range from 2.95 to 3.0 bar (Fig. 2). The reasons for this behavior of the graph are expected to be studied in the future as part of the development of a mathematical model of the ejector.

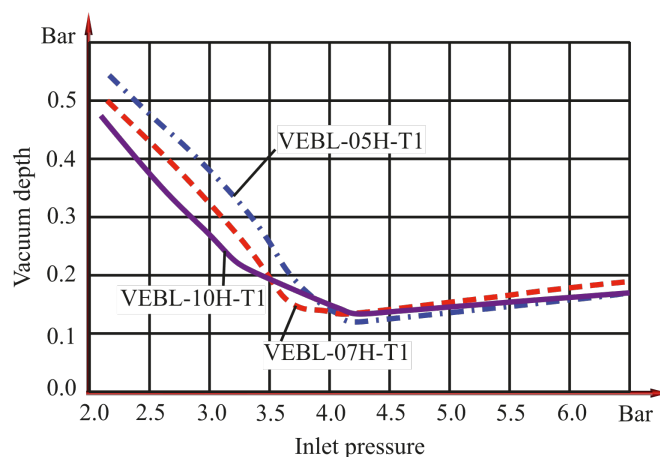


Fig. 4. Vacuum depth change dependence diagrams from the value of the supply pressure for VEBL series ejectors

The experimental data analysis shows that for the VEBL-05N-T1 ejector, the vacuum depth reaches 88.06% (residual pressure 121 mbar) at a supply pressure of 4.2 bar.

The information from the manufacturer on the VEBL-05N-T1 ejector indicates that the optimal supply pressure is 4.5 bar, while the residual pressure in the vacuum line should reach 160 mbar. The data correspond to the graphs presented in the manufacturer's catalog, which demonstrate the dependence of the change in vacuum depth on the supply pressure value for VEBL family ejectors. In the course of the conducted research, it has been established that for the VEBL-05N-T1 ejector with a recommended supply pressure of 4.5 bar, the residual pressure in the vacuum line is 127 mbar, which corresponds to a vacuum depth of 87.47%.

For the VEBL-07N-T1 ejector, it has been experimentally established that the minimum residual pressure in the vacuum line reaches 133 mbar (86.87%) at a supply pressure of 4.1 bar.

The data provided by the manufacturer for the VEBL-07N-T1 ejector, indicate an optimal supply pressure of 4.5 bar. At the same time, the residual pressure in the vacuum line should reach 150 mbar. This value is confirmed by the diagram provided in the manufacturer's catalog, which illustrates the dependence of changes in the vacuum depth on the supply pressure for VEBL family ejectors. The results of the conducted studies show that for the VEBL-07N-T1 ejector, with a supply pressure of 4.5 bar recommended by the manufacturer as optimal for its operation, the residual pressure in the vacuum line is 142 mbar, which corresponds to a vacuum depth of 85.99%.

As for the VEBL-10N-T2 ejector, it has been experimentally established that the minimum residual pressure in the vacuum line reaches 133 mbar, which corresponds to a vacuum depth of 86.87% with a supply pressure of 4.22 bar. The data, provided by the manufacturer for the VEBL-10N-T2 ejector, indicate an optimal supply pressure of 4.5 bar, while the residual pressure in the vacuum line should reach 150 mbar. This value corresponds to the diagram presented in the manufacturer's catalog, which illustrates the dependence of changes in the vacuum depth on the value of the supply pressure for the VEBL family of ejectors. The conducted studies show that for the VEBL-10N-T2 ejector, with the manufacturer's recommended supply pressure of 4.5 bar, the residual pressure in the vacuum line is 138 mbar, which translates into a vacuum depth of 86.38%.

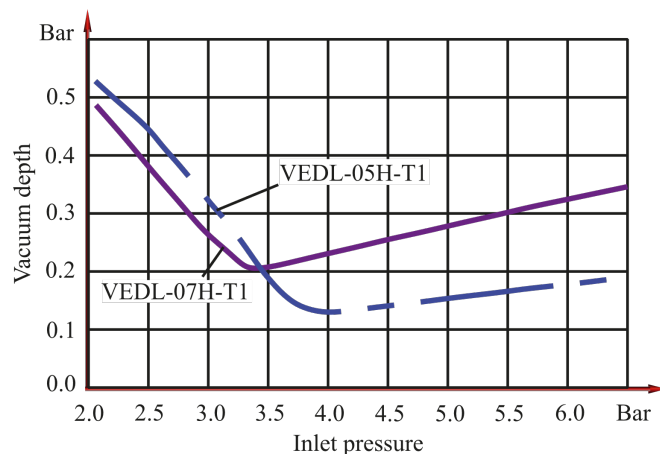


Fig. 5. Vacuum depth change dependence diagrams from the feed pressure value for VEDL series ejectors

The experimental data analysis shows that for the VEDL-05N-T1 ejector, the minimum residual pressure in the vacuum line reaches 130 mbar (vacuum depth 87.17%) at a supply pressure of 4.0 bar. The data, provided by the manufacturer for the VEDL-05N-T1 ejector, indicate an optimal supply pressure of 4.5 bar, while a residual pressure of 170 mbar should be reached in the vacuum line. This value corresponds to the diagram of the dependence of the change in the vacuum depth on the value of the supply pressure for the VEDL family of ejectors given in the manufacturer's catalog. The conducted studies show that for the VEDL-05N-T1 ejector with a feed pressure of 4.5 bar (the value recommended by the manufacturer as optimal for the operation of the VEDL-05N-T1 ejector), the residual pressure in the vacuum line is 142.6 mbar, which corresponds to a vacuum depth of 85.99%.

It has been experimentally established that for the VEDL-07N-T1 ejector, the minimum residual pressure in the vacuum line reaches 207 mbar (79.57%) at a supply pressure of 3.4 bar. The data provided by the manufacturer for the VEDL-07N-T1 ejector indicate an optimal supply pressure of 4.5 bar, while the residual pressure in the vacuum line should reach 150 mbar. This value corresponds to the diagram of the dependence of the change in the vacuum depth on the value of the supply pressure for the VEDL family of ejectors given in the manufacturer's catalog. The conducted studies show that for the VEDL-07N-T1 ejector at a supply pressure of 4.5 bar (the value recommended by the manufacturer as optimal for the operation of the VEDL-07N-T1 ejector), the residual pressure in the vacuum line is 256 mbar, which corresponds to a vacuum depth of 74.73%.

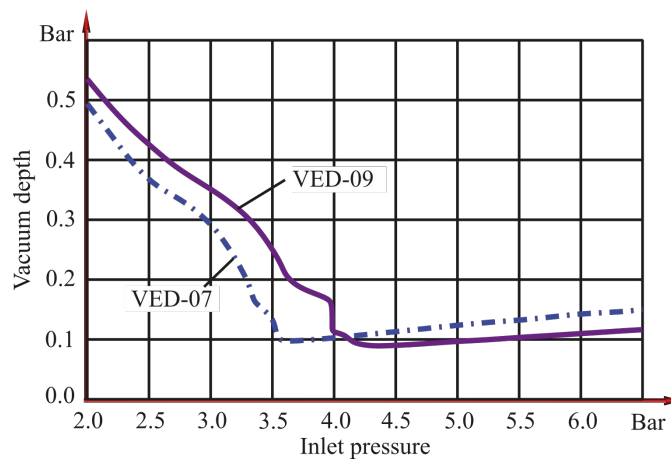


Fig. 6. Vacuum depth change versus supply pressure diagrams for VED series ejectors.

The experimental data analysis shows that for the VED-07 ejector, the minimum residual pressure in the vacuum line reaches 98 mbar (90%) at a supply pressure of 3.63 bar. The data provided by the manufacturer for the VED-07 ejector indicate an optimal supply pressure of 5 bar, in which case a vacuum of 90% should be reached (residual pressure of 101 mbar). This value does not correspond to the diagram of the dependence of the change in the vacuum depth on the value of the supply pressure for the VED family of ejectors given in the manufacturer's catalog. The conducted studies show that for the VED-07 ejector at a supply pressure of 5 bar (the value recommended by the manufacturer as optimal for the operation of the VED-07 ejector), the residual pressure in the vacuum line is 124 mbar, which corresponds to a vacuum depth of 87.76%.

It has been experimentally established that for the VED-09 ejector, the minimum residual pressure in the vacuum line reaches 90 mbar (91.12%) at a supply pressure of 4.34 bar. The data provided by the manufacturer for the VED-09 ejector, indicate an optimal supply pressure of 5 bar, in which case a vacuum of 89% depth should be reached (residual pressure 111.5 mbar). This value does not correspond to the diagram of the dependence of the change in the vacuum depth on the value of the supply pressure for the VED family of ejectors given in the manufacturer's catalog. The conducted studies show that for the VED-09 ejector at a supply pressure of 5 bar (the value recommended by the manufacturer as optimal for operation of the VED-09 ejector), the residual pressure in the vacuum line is 98 mbar, which corresponds to a vacuum depth of 90.33%.

Of interest is the sharp drop in the vacuum depth value and the occurrence of fluctuations in the vacuum depth readings in the range of supply pressure values from 3.95 to 4.4 bar (Fig. 6).

**Discussion and Conclusion.** The moment of occurrence of oscillations, recorded during all experiments, was accompanied by noticeable changes in the exhaust sound. We believe that this type of behavior may be associated with a sharp change in the air flow pattern, which may indicate the presence of a manufacturing flaw in this ejector. To confirm this conclusion, it is necessary to conduct additional experiments with other ejectors from this series. Furthermore, it is worth considering the possibility of studying the surface of the ejector channel in order to assess the accuracy of geometric shapes and the quality of surface treatment.

According to the results of the conducted experimental studies of vacuum ejectors, it can be concluded that the actual values of the vacuum depth vary depending on the magnitude of the input supply pressure, and differ from the values provided by the manufacturer. In addition, the character of the graphs also has its own differences. Specifically, the behavior of the graph in Figure 3 indicates the possible presence of manufacturing flaw in the ejector channel. In this regard, it is important to construct a mathematical model of ejectors, which allows us to study the factors that determine such a specific behavior of the graph at the model level. Understanding these factors will help develop recommendations for improving the technological processes of manufacturing vacuum ejectors.

In this regard, it is necessary to introduce an adjustment to the value of the input supply pressure to reach the maximum vacuum depth for each type of ejector, which will affect the performance of both the ejectors themselves and the automated vacuum systems.

The research results obtained can be useful for all ejector manufacturers for the purpose of adjusting their basic catalogs and corresponding recommendations for the use of these products. In the future, the authors plan to continue a series of experiments aimed at determining the time of creating vacuum in one liter of volume at various specified vacuum depths.

## References

1. Li Macia, Castilla R, Gamez-Montero PJ, Camacho S, Codina E. Numerical Simulation of a Supersonic Ejector for Vacuum Generation with Explicit and Implicit Solver in Openfoam. *Energies*. 2019;12(18):3553. <https://doi.org/10.3390/en12183553>
2. Besagni G, Mereu R, Inzoli F. Ejector Refrigeration: A Comprehensive Review. *Renewable and Sustainable Energy Reviews*. 2016;53:373–407. <https://doi.org/10.1016/j.rser.2015.08.059>
3. Arun Kumar R, Rajesh G. Physics of Vacuum Generation in Zero-Secondary Flow Ejectors. *Physics of Fluids*. 2018;30(6):066102. <https://doi.org/10.1063/1.5030073>
4. Jafarian A, Azizi M, Forghani P. Experimental and Numerical Investigation of Transient Phenomena in Vacuum Ejectors. *Energy*. 2016;102:528–536. <https://doi.org/10.1016/j.energy.2016.02.101>
5. Levchenko D, Meleychuk S, Arseniev V. Regime Characteristics of Vacuum Unit with a Vortex Ejector Stage with Different Geometry of Its Flow Path. *Procedia Engineering*. 2012;39:28–34. <https://doi.org/10.1016/j.proeng.2012.07.004>
6. Kumar V, Sachdeva G. 1-D Model for Finding Geometry of a Single Phase Ejector. *Energy*. 2018;165(A):75–92. <https://doi.org/10.1016/j.energy.2018.09.071>
7. Sobolev AV. Intensification of Mixing by Small-Size Jets in Ejectors with Central Nozzle. *Thermophysics and Aeromechanics*. 2013;20(3):273–276. URL: <https://link.springer.com/article/10.1134/S0869864313030025> (accessed: 10.11.2024).
8. Karthick SK, Srisha MV Rao, Jagadeesh G, Reddy KPJ. Parametric Experimental Studies on Mixing Characteristics within a Low Area Ratio Rectangular Supersonic Gaseous Ejector. *Physics of Fluids*. 2016;28(7):076101. <https://doi.org/10.1063/1.4954669>
9. Hesse S. *Compressed Air as an Energy Carrier*. Moscow: Festo; 2004. 128 p. (In Russ.)
10. Goodman N, Legee BJ, Johnson PE. An Improved de Laval Nozzle Experiment. *International Journal of Mechanical Engineering Education*. 2021;50(2):513–537. <https://doi.org/10.1177/03064190211034165>
11. Moukalled F, Mangani L, Darwish M. *The Finite Volume Method in Computational Fluid Dynamics*. Springer: Cham; 2016. 791 p. <https://doi.org/10.1007/978-3-319-16874-6>
12. Jia Yan, Shengyu Li, Zhan Liu. Numerical Investigation on Optimization of Ejector Primary Nozzle Geometries with Fixed/Varied Nozzle Exit Position. *Applied Thermal Engineering*. 2020;175:115426. <https://doi.org/10.1016/j.applthermaleng.2020.115426>
13. Kun Zhang, Shengqiang Shen S., Yong Yang, Xingwang Tian. Experimental Investigation of Adjustable Ejector Performance. *Journal of Energy Engineering*. 2011;138(3):125–129. [https://doi.org/10.1061/\(ASCE\)EY.1943-7897.0000058](https://doi.org/10.1061/(ASCE)EY.1943-7897.0000058)
14. Savchuk SI. Study of parameters of Vacuum Ejectors Used in the Assembly and Repair of Cars. *Scientific Notes of the Crimean Engineering and Pedagogical University*. 2016;53(3):58–64. URL: <https://uz.kipu-rc.ru:9443/sn/53.pdf> (accessed: 28.11.2024).
15. Savchuk SI, Umerov ED, Abdulgaziz UA. A Stand for Assessing the Depth of Vacuum Supplied to Specialized Suction Cups Used in Technological Processes of Service during Operation and Production of Cars. *Scientific Notes of the Crimean Engineering and Pedagogical University*. 2023;82(4):225–230.

## About the Authors:

**Sergey I. Savchuk**, Cand.Sci. (Eng.), Associate Professor of the Motor Transport Department, Crimean Engineering and Pedagogical University named after Fevzi Yakubov (8, Uchebnyi Lane, Simferopol, 295015, Republic of Crimea), [ORCID](https://orcid.org/0000-0001-9151-1000), [ofelos@outlook.com](mailto:ofelos@outlook.com)

**Ervin D. Umerov**, Cand.Sci. (Eng.), Associate Professor of the Motor Transport Department, Crimean Engineering and Pedagogical University named after Fevzi Yakubov (8, Uchebnyi Lane, Simferopol, 295015, Republic of Crimea), [SPIN-code](#), [ORCID](#), [ScopusID](#), [ResearcherID](#), [Ervin777@yandex.ru](mailto:Ervin777@yandex.ru)

**Aziz U. Abdulgazis**, Cand.Sci. (Eng.), Associate Professor of the Motor Transport Department, Crimean Engineering and Pedagogical University named after Fevzi Yakubov (8, Uchebnyi Lane, Simferopol, 295015, Republic of Crimea), [SPIN-code](#), [ORCID](#), [abdulgazis.aziz@mail.ru](mailto:abdulgazis.aziz@mail.ru)

**Claimed Contributorship:**

**SI Savchuk:** conducting the research.

**ED Umerov:** manuscript writing — reviewing and editing.

**AU Abdulgazis:** visualization.

**Conflict of Interest Statement:** the authors do not have any conflict of interest.

*All the authors have read and approved the final manuscript.*

**Об авторах:**

**Сергей Игоревич Савчук**, кандидат технических наук, доцент кафедры автомобильного транспорта Крымского инженерно-педагогического университета имени Февзи Якубова (295015, Республика Крым, г. Симферополь, пер. Учебный, 8), [ORCID](#), [ofelos@outlook.com](mailto:ofelos@outlook.com)

**Эрвин Джеватович Умеров**, кандидат технических наук, доцент кафедры автомобильного транспорта Крымского инженерно-педагогического университета имени Февзи Якубова (295015, Республика Крым, г. Симферополь, пер. Учебный, 8), [SPIN-код](#), [ORCID](#), [ScopusID](#), [ResearcherID](#), [Ervin777@yandex.ru](mailto:Ervin777@yandex.ru)

**Азиз Умерович Абдулгазис**, кандидат технических наук, доцент кафедры автомобильного транспорта Крымского инженерно-педагогического университета имени Февзи Якубова (295015, Республика Крым, г. Симферополь, пер. Учебный, 8), [SPIN-код](#), [ORCID](#), [abdulgazis.aziz@mail.ru](mailto:abdulgazis.aziz@mail.ru)

**Заявленный вклад авторов:**

**С.И. Савчук:** проведение исследования.

**Э.Д. Умеров:** написание рукописи — рецензирование и редактирование.

**А.У. Абдулгазис:** визуализация.

**Конфликт интересов:** авторы заявляют об отсутствии конфликта интересов.

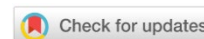
*Все авторы прочитали и одобрили окончательный вариант рукописи.*

Received / Поступила в редакцию 15.12.2024

Reviewed / Поступила после рецензирования 10.01.2025

Accepted / Принята к публикации 17.01.2025

# MACHINE BUILDING AND MACHINE SCIENCE МАШИНОСТРОЕНИЕ И МАШИНОВЕДЕНИЕ



UDC 62.621

Original Empirical Research

<https://doi.org/10.23947/2687-1653-2025-25-1-52-64>

## Using Surrogate Models in the Construction of a Pareto-Optimal Positioning Electropneumatic Actuator with Discrete Pneumatic Valves



EDN: OETHVA

Maxim O. Sheykin ✉, Sergey N. Cherkasskikh , Denis V. Shilin ,  
Vladimir V. Fedenkov 

National Research University MPEI, Moscow, Russian Federation

✉ [sheykinmo@mpei.ru](mailto:sheykinmo@mpei.ru)

### Abstract

**Introduction.** Pneumatic actuators are widely used in industry due to their reliability, simplicity of design, and ability to operate under complex conditions. However, when solving positioning problems, the use of traditional proportional valves is often redundant, which causes an unjustified increase in cost and complexity of the design. The application of simpler discrete distributors faces the problem related to the need to reach a compromise between their switching frequency and positioning accuracy.

Existing studies mainly focus on optimizing individual performance indicators of pneumatic actuators and do not offer effective methods for finding a compromise between conflicting criteria. Using classical methods for constructing a Pareto set for multicriteria optimization requires significant computational resources, which complicates their practical application.

The research objective is to develop a methodology for multicriteria optimization of the parameters of a positioning electropneumatic actuator with discrete distributors based on the construction of a Pareto set using surrogate models, which provides finding the optimal balance between switching frequency and positioning accuracy.

**Materials and Methods.** The research was conducted on a model of a positioning pneumatic actuator with discrete distributors, implemented in MATLAB Simulink. The Latin hypercube method was used to analyze the parameters, which provided uniform filling of the parameter space. To reduce computational costs, surrogate models, built using neural networks, were used. Sliding control was selected as a control algorithm, which effectively compensated for external disturbances and uncertainties of the system.

**Results.** The optimization of control parameters has shown the possibility of reaching high positioning accuracy with a minimum frequency of distributor switching. The use of the Latin hypercube method provided a uniform distribution of the calculation points, which made it possible to construct an accurate surrogate model. It has been experimentally proven that the proposed approach reduces computational costs by 48%, while maintaining high accuracy of modeling and analysis.

**Discussion and Conclusion.** The research results confirm that sliding control is an effective solution for discrete pneumatic drives in the context of multicriteria optimization. The developed approach makes it possible to significantly reduce the frequency of switching distributors without substantial losses in the quality of transients, which helps to extend the service life of equipment and increase the reliability of automated systems. The use of surrogate models and neural network technology opens up new prospects for faster design of complex systems.

**Keywords:** pneumatic actuator, discrete pneumatic valves, sliding control, multicriteria optimization, surrogate models

**For Citation.** Sheykin MO, Cherkasskikh SN, Shilin DV, Fedenkov VV. Using Surrogate Models in the Construction of a Pareto-Optimal Positioning Electropneumatic Actuator with Discrete Pneumatic Valves. *Advanced Engineering Research (Rostov-on-Don)*. 2025;25(1):52–64. <https://doi.org/10.23947/2687-1653-2025-25-1-52-64>

## Использование суррогатных моделей при построении множества Парето позиционного электропневматического привода с дискретными пневмораспределителями

М.О. Шейкин ✉, С.Н. Черкасских , Д.В. Шилин , В.В. Феденков 

Национальный исследовательский университет «МЭИ», г. Москва, Российская Федерация

✉ [sheykinmo@mpei.ru](mailto:sheykinmo@mpei.ru)

### Аннотация

**Введение.** Пневматические приводы находят широкое применение в промышленности благодаря своей надежности, простоте конструкции и способности функционировать в сложных условиях. Однако при решении задач позиционирования использование традиционных пропорциональных распределителей зачастую оказывается избыточным, что ведет к неоправданному увеличению стоимости и усложнению конструкции. Применение более простых дискретных распределителей сталкивается с проблемой, связанной с необходимостью достижения компромисса между частотой их переключения и точностью позиционирования. Существующие исследования, в основном, фокусируются на оптимизации отдельных показателей качества работы пневмоприводов и не предлагают эффективных методов поиска компромисса между конфликтующими критериями. Использование классических методов построения множества Парето для многокритериальной оптимизации требует значительных вычислительных ресурсов, что затрудняет их практическое применение. Целью исследования является разработка методологии многокритериальной оптимизации параметров позиционного электропневматического привода с дискретными распределителями на основе построения множества Парето с использованием суррогатных моделей, позволяющей найти оптимальный баланс между частотой переключений и точностью позиционирования.

**Материалы и методы.** Исследование проводилось на модели позиционного пневмопривода с дискретными распределителями, реализованной в MATLAB Simulink. Для анализа параметров использовался метод латинского гиперкуба, который обеспечивает равномерное заполнение пространства параметров. Для снижения вычислительных затрат были применены суррогатные модели, построенные с использованием нейронных сетей. В качестве алгоритма управления было выбрано скользящее управление, которое эффективно компенсирует внешние возмущения и неопределенности системы.

**Результаты исследования.** Оптимизация параметров управления показала возможность достижения высокой точности позиционирования при минимальной частоте переключений распределителей. Использование метода латинского гиперкуба обеспечило равномерное распределение расчетных точек, что позволило построить точную суррогатную модель. Экспериментально было доказано, что предложенный подход снижает вычислительные затраты на 48 %, сохраняя высокую точность моделирования и анализа.

**Обсуждение и заключение.** Результаты исследования подтверждают, что скользящее управление является эффективным решением для дискретных пневмоприводов в контексте многокритериальной оптимизации. Разработанный подход позволяет значительно уменьшить частоту переключений распределителей без ощутимых потерь в качестве переходных процессов, что способствует продлению сроков службы оборудования и повышению надежности автоматизированных систем. Использование суррогатных моделей и нейросетевых технологий открывает новые перспективы для более быстрого проектирования сложных систем.

**Ключевые слова:** пневмопривод, дискретные распределители, скользящее управление, многокритериальная оптимизация, суррогатные модели

**Для цитирования.** Шейкин М.О., Черкасских С.Н., Шилин Д.В., Феденков В.В. Использование суррогатных моделей при построении множества Парето позиционного электропневматического привода с дискретными пневмораспределителями. *Advanced Engineering Research (Rostov-on-Don)*. 2025;25(1):52–64. <https://doi.org/10.23947/2687-1653-2025-25-1-52-64>

**Introduction.** Pneumatic drives are widely used in various industries due to the simplicity of their design, the ability to provide high speeds of movement of controlled objects, environmental friendliness, fire safety, and the ability to work in aggressive environments.

In systems oriented to tracking, proportional valves are in routine used to control the pneumatic actuator, which provide continuous regulation. However, when the basic task of the pneumatic actuator is to arrange the output element in a specified position, rather than following a given trajectory, the use of such distributors may be redundant. In this case, it is advisable to consider the application of simpler discrete valves [1].

Existing research papers suggest various approaches to positioning control, including algorithms using pulse-width modulation, as well as sliding and predictive control principles [2]. Improvement in positioning accuracy is reached either by modifying the control algorithm near the breaking point [3], or by implementing specialized mechanical or hydraulic braking devices [4]. However, despite the improvement in accuracy, the use of braking devices significantly complicates the design, which in turn can negate the advantages of using discrete pneumatic valves [5].

The analysis of the current state of research has revealed significant gaps in the understanding of the problem. First of all, there is no holistic approach to assessing the efficiency of various structures of positional electropneumatic drives with discrete valves. In addition, the issue of reaching a compromise between the frequency of switching distributors and the quality of positioning has not been sufficiently studied. Existing methods of multicriteria optimization of parameters of such systems do not provide the required efficiency. Authors of publications often focus on individual aspects of quality, such as accuracy or speed. Little attention is paid to the relationship between increasing the accuracy of positioning and increasing the frequency of switching distributors, which directly affects equipment wear and service life.

The pneumatic actuator considered in this paper does not have special braking devices, and the positioning of the output link at a given point is performed exclusively by switching discrete pneumatic distributors at the right moments in time, according to the applied control algorithms. This provides for the simplicity of the design and low cost of the solution, but leads to frequent switching of pneumatic distributors. The strictness of the requirements for the quality of the transient process, in turn, inevitably leads to an increase in the number of switches.

Thus, there is a need to find a trade-off decision that takes into account two contradictory criteria: positioning accuracy and intensity of the distributors. The construction of the Pareto front will allow us to determine a set of unimprovable solutions, where it is impossible to improve one quality indicator without degrading the other, which will provide the developer with the opportunity to make a justified selection of system parameters. However, traditional methods for constructing the Pareto set require multiple calculations of complex dynamic models [6], which makes the process extremely labor-intensive and time-consuming.

The use of surrogate models in constructing the Pareto set [7] opens up new horizons for solving this problem, although it requires the development of specialized methods adapted to a specific class of pneumatic devices.

This research is aimed at developing a methodology for multicriteria optimization of the parameters of a positional electropneumatic drive with discrete valves, based on the use of surrogate models, which provide for an effective search for trade-off decisions between the switching frequency and the quality of positioning. To accomplish this purpose, it is necessary to develop a methodology of creating a surrogate model for assessing the quality indicators of a positional electropneumatic drive. It is also required to create an algorithm for multicriteria optimization of drive parameters using a surrogate model and conduct a study of the efficiency of the proposed approach on a specific drive design.

**Materials and Methods.** This paper examines a positional pneumatic drive with discrete pneumatic distributors without special braking devices. It is shown in Figure 1. It contains a single-rod, double-acting pneumatic cylinder controlled by four 2/2 pneumatic distributors. Using four 2/2 pneumatic distributors instead of two 3/2 pneumatic distributors allows for better dynamic characteristics of the pneumatic drive with an acceptable increase in the cost of the design.

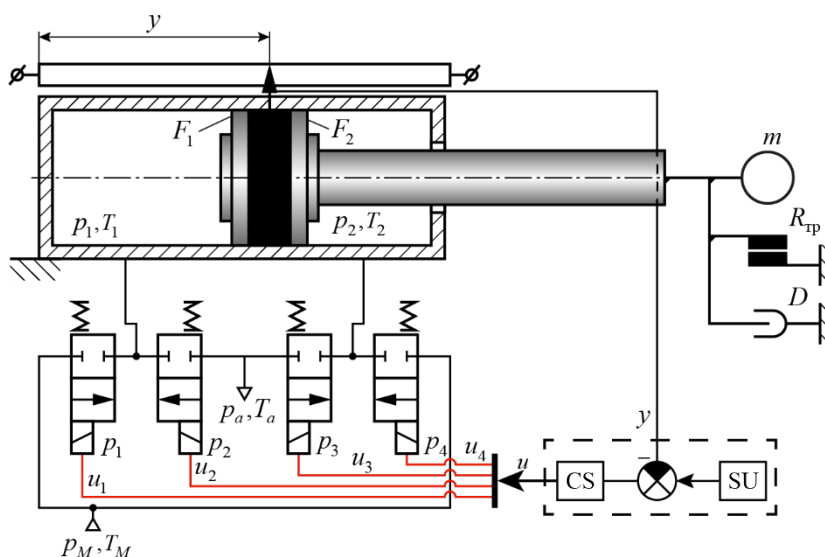


Fig. 1. Pneumatic actuator circuit with discrete distributors

To control discrete pneumatic distributors, a control system (CS) is used, shown in Figure 2. It implements the principle of sliding control in accordance with the input signal determined by the setup unit (SU). The sliding mode provides robust control, allowing the system to effectively cope with the uncertainties and disturbances characteristic of pneumatic systems.

The basic idea of the method is to make the system move along a predetermined trajectory, called a “sliding surface” [8]. When the system gets on this trajectory, it starts to “slide” along it to the desired target, ignoring numerous external actions.

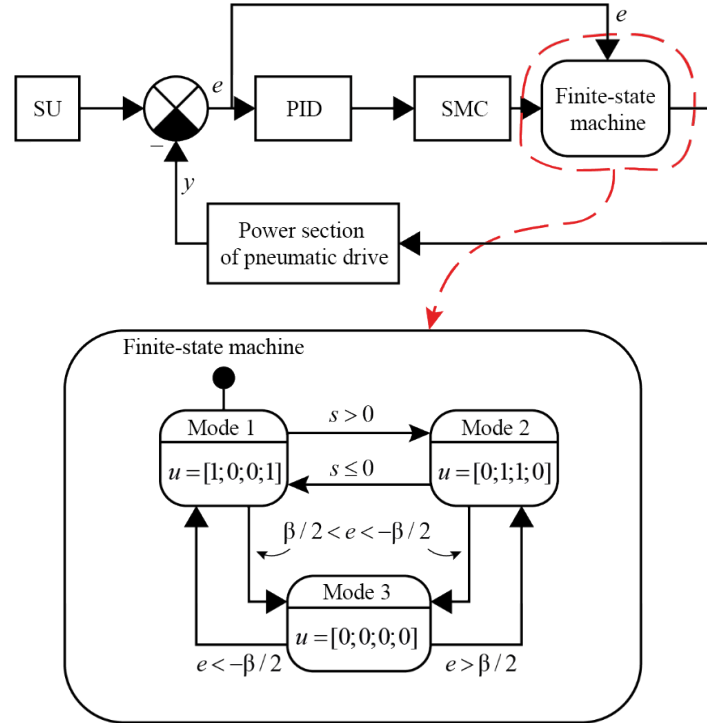


Fig. 2. Control system structure

In this paper, we use the sliding straight line described by the equation:

$$s = C_1 e + C_2 \dot{e},$$

where  $s$  — switch function;  $e$  — control error;  $\dot{e}$  — rate of error change;  $C_1$  and  $C_2$  — positive coefficients determining the slope and characteristics of the sliding straight line.

Control consists of two parts: one part keeps the system on the desired trajectory, and the other quickly brings it back if something tries to mislead the system [9]. This second part can cause rapid unwanted oscillations.

The control signal from the sliding mode controller is fed to the input of the finite-state machine, which generates the corresponding combinations of control actions for the pneumatic distributors. The system implements three main operating modes: piston extension (P1 and P4 are active), piston retraction (P2 and P3 are active), and braking (P1 and P2 are active). The braking mode, in which the charge pressure is supplied to both cavities of the pneumatic cylinder, is switched on when the control error reaches values from the range  $[-\beta/2; +\beta/2]$ , where  $\beta$  — width of the braking corridor.

The mathematical model of the pneumatic power part includes the equation of the dynamic balance of forces on the piston of the pneumatic cylinder, the equations of filling and emptying the cavities of the pneumatic cylinder, and the equations of mass flows for the discharge and exhaust cavities [10].

$$p_1 \cdot F_1 - p_2 \cdot F_2 = m \frac{d^2 y}{dt^2} + D \cdot y \frac{dy}{dt} + R_{\text{тп}} \cdot \text{sign} \left( \frac{dy}{dt} \right) + R_{\text{yn}},$$

where  $p_1, p_2$  — pressure in the piston and rod cavities of the pneumatic cylinder;  $F_1, F_2$  — piston and rod areas of the piston;  $m$  — reduced mass;  $R_{\text{тп}}$  — Coulomb friction force;  $D$  — coefficient of viscous friction;  $R_{\text{yn}}$  — reaction force of stops in the pneumatic cylinder;  $y$  — piston displacement.

The reaction of the stops limiting the piston movement can be calculated using the following formulas:

for the case when the piston approaches the lower stop (at  $y < -0.5H$ ):

$$R_{\text{yn}} = C_{\text{yn}} \cdot (y + 0.5H) + \beta_{\text{yn}} \dot{y}.$$

For the case when the piston is within the working stroke (at  $-0.5H \leq y \leq 0.5H$ ):

$$R_{\text{yn}} = 0.$$

For the case when the piston approaches the upper stop (at  $y > 0.5H$ ):

$$R_{y_{in}} = C_{y_{in}} \cdot (y - 0.5H) + \beta_{y_{in}} \dot{y},$$

where  $H$  — stroke of the pneumatic cylinder piston;  $C_{y_{in}}, \beta_{y_{in}}$  — coefficients of rigidity and dissipation of the contact interaction of the pneumatic cylinder piston with the stop, respectively.

The equation for filling and emptying the left cavity has the form [11]:

$$kR(T_M G_1 - T_1 G_2) = k p_1 F_1 \dot{y} + F_1 (y_{10} + y) \dot{p}_1, \quad (1)$$

where  $k$  — adiabatic index;  $R$  — specific gas constant;  $T_M, T_1$  — air temperature in the line and in the left cavity of the pneumatic cylinder;  $G_1, G_2$  — mass air flow rates through the pneumatic distributors P1 and P2, respectively. The value takes into account the selection of the origin of  $y$  coordinates, as well as the dead volume of the left part of the pneumatic cylinder, including the volume of the supply line and is determined by the expression:

$$y_{10} = \frac{V_{10}}{F_1} + 0.5H.$$

Mass flow rates  $G_1$  and  $G_2$  for an adiabatic process are calculated using the Saint-Venant – Wantzel equation [12]:

$$G_1 = \mu f_1 p_M \sqrt{\frac{2k}{(k-1)T_M}} \varphi(p_M, p_1); \quad (2)$$

$$G_2 = \mu f_2 p_1 \sqrt{\frac{2k}{(k-1)T_1}} \varphi(p_1, p_a), \quad (3)$$

where  $p_M, p_a$  — line and atmospheric pressure;  $\mu$  — flow rate coefficient,  $f_1, f_2$  — areas of the throttle slots of pneumatic distributors P1 and P2, respectively.

Flow function  $\varphi(p_a, p_b)$  for a diatomic ideal gas is defined as follows:

at the subcritical flow regime (when  $p_a / p_b > 0.528$ ):

$$\varphi(p_a, p_b) = \sqrt{\left(\frac{p_b}{p_a}\right)^{\frac{2}{k}} - \left(\frac{p_b}{p_a}\right)^{\frac{k+1}{k}}}.$$

under critical and supercritical flow conditions (when  $p_a / p_b \leq 0.528$ ):

$$\varphi(p_a, p_b) = 0.259,$$

where  $k$  — adiabatic index (for a diatomic gas usually  $k = 1.4$ ).

Temperature  $T_1$  during the adiabatic emptying process is equal to:

$$T_1 = T_a \left(\frac{p_1}{p_a}\right)^{\frac{k-1}{k}}. \quad (4)$$

Substituting (1), (2) and (3) into (4), we obtain:

$$F_1 (y_{10} + y) \dot{p}_1 = g(f_1, f_2, p_1) - k p_1 F_1 \dot{y},$$

where

$$g(f_a, f_b, p) = \mu f_a p_M \sqrt{\frac{2k^3 RT_M}{(k-1)}} \cdot \varphi(p_M, p) - k \mu f_b p^{\frac{3k-1}{2k}} p_a^{\frac{1-k}{2k}} \sqrt{\frac{2k}{k-1}} RT_a \varphi(p, p_a).$$

The processes of filling and emptying the right cavity are described by the following equation:

$$kR(T_M G_4 - T_2 G_3) = -k p_2 F_2 \dot{y} + F_2 (y_{20} - y) \dot{p}_2, \quad (5)$$

where  $T_2$  — air temperature in the right cavity of the pneumatic drive;  $G_3, G_4$  — mass air flow rates through pneumatic distributors P3 and P4 respectively. Value  $y_2$  is determined by the formula:

$$y_{20} = \frac{V_{20}}{F_2} + 0.5H.$$

In the expression,  $V_{20}$  — dead volume of the right cavity of the hydraulic cylinder, including the volume of the exhaust line. Temperature  $T_2$  during the adiabatic emptying process is equal to:

$$T_2 = T_a \left(\frac{p_2}{p_a}\right)^{\frac{k-1}{k}}. \quad (6)$$

Mass flows  $G_3$  and  $G_4$  are equal to:

$$G_1 = \mu f_1 p_m \sqrt{\frac{2k}{(k-1)T_m}} \varphi(p_m, p_1); \tag{7}$$

$$G_2 = \mu f_2 p_1 \sqrt{\frac{2k}{(k-1)T_1}} \varphi(p_1, p_a), \tag{8}$$

where  $f_3, f_4$  — areas of the throttle gaps of pneumatic distributors P3 and P4, respectively.

Substituting (6), (7) and (8) into (5), we obtain:

$$F_2(y_{20} - y) \dot{p}_2 = g(f_4, f_3, p_2) + kp_2 F_2 \dot{y}.$$

The presented mathematical model of the pneumatic drive was subsequently implemented in the MATLAB Simulink software package (Fig. 3). Numerical modeling of the system was performed considering the parameters, whose values are presented in Table 1.

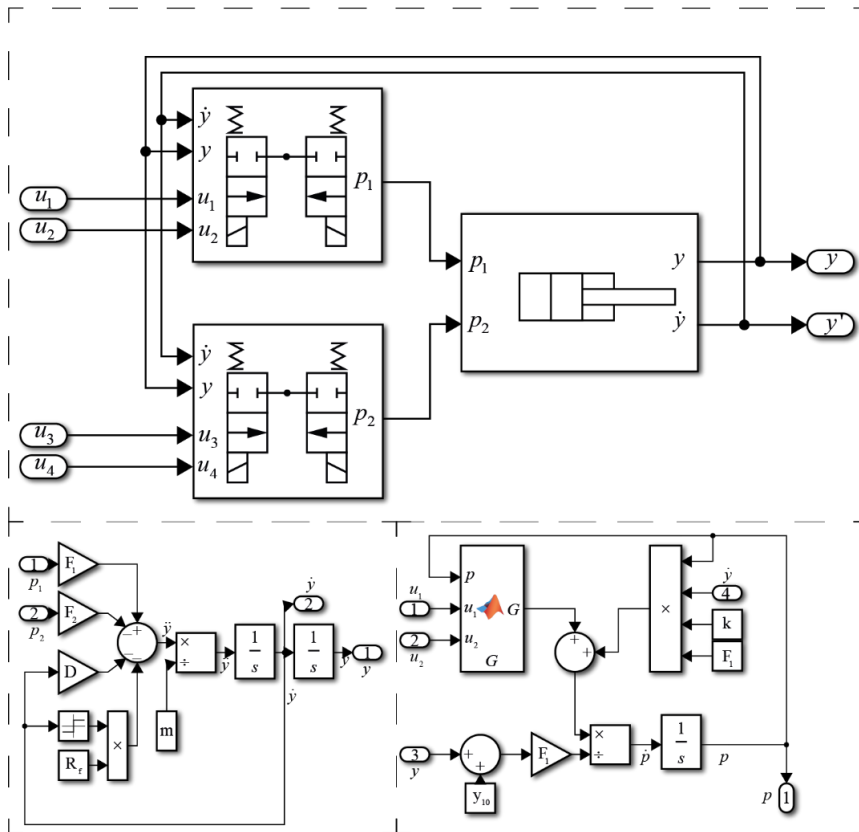


Fig. 3. Model of a pneumatic drive with discrete pneumatic valves in MATLAB Simulink

Table 1

Values of Model Parameters for Numerical Simulation

Parameter	Value
Reduced mass at the end of the rod, kg	6
Main line pressure, bar	4
Exhaust pressure, bar	1
Pneumatic cylinder piston diameter, mm	32
Pneumatic cylinder rod diameter, mm	12
Working environment temperature, K	293.15
Breakaway friction force, N	20
Sliding friction force, N	15
Coefficient of viscous friction, mm/s	350

The proposed method for constructing the Pareto set for the pneumatic drive structure under consideration is presented in the form of an algorithm in Figure 4 and includes several stages.

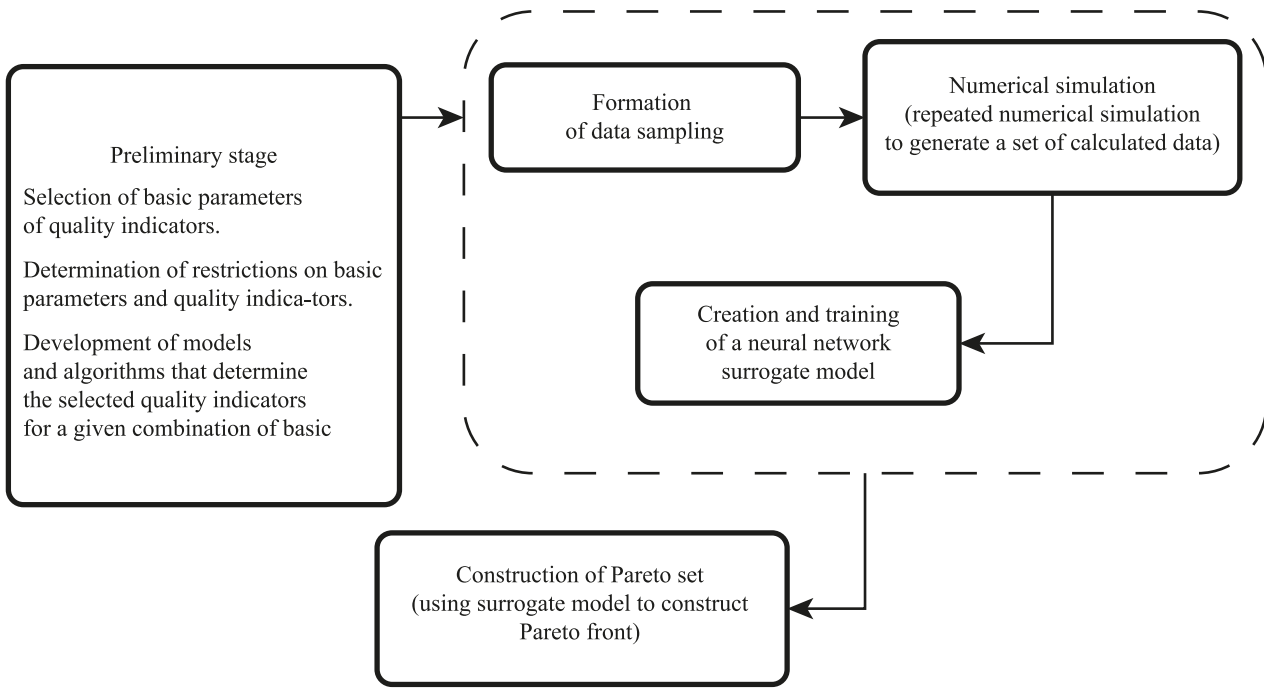


Fig. 4. Algorithm for constructing Pareto set

Selection of basic parameters of quality indicators.

Determination of restrictions on basic parameters and quality indicators.

Development of models and algorithms that allow determining the selected quality indicators for a given combination of basic parameters.

Numerical modeling (repeated numerical modeling to create a set of calculated data).

Creation and training of a neural network surrogate model.

Construction of the Pareto set (use of a surrogate model to construct the Pareto front).

At the preliminary stage, quality indicators are selected that evaluate the perfection of the system under study. For a comprehensive assessment of the quality of the transient process, a generalized integral quadratic estimate can be used [1]:

$$J_{21} = \int_0^{\infty} [e^2(t) + \tau \dot{e}(t)] dt,$$

where  $e$  — transient component of the error, normalized from 0 to 1;  $\tau$  — weight coefficient.

Improving the quality of the transient process is related to an increase in the number of switchings of the pneumatic distributors  $n$ . In this regard, it is of interest to study the limiting capabilities of the pneumatic drive structure for two conflicting quality indicators  $J_{21}$  and  $n$ . At the preliminary stage, quality indicators are selected that evaluate the efficiency of the system under study. Thus, a space of quality indicators in which the surface corresponding to the Pareto front will be identified, is formed.

From the design parameters of the system, a group of basic parameters is identified. It determines the main control characteristics: slope coefficients of the sliding line  $C_1$  and  $C_2$ , response time of the distributors, and width of the braking corridor. The ranges of variation of these parameters determine the search space for optimal solutions. They are presented in Table 2.

Table 2

Intervals of Values of Variable Parameters

Coefficient $C_1$	1.0–4.0
Coefficient $C_2$	0.1–1.0
Distributor response time, ms	5–45
Size of the braking corridor, mm	2–4

To calculate the vector of quality indicators based on the vector of basic parameters, corresponding models are formed. For the case under consideration, a nonlinear dynamic model was used, which includes both a power pneumatic part and a control system based on sliding modes.

At the next stage, the parameter space is filled with computation points, in which the vector of quality indicators will be calculated. In this case, the number of points should be minimal to reduce computational costs, but sufficient to provide for the desired accuracy of the surrogate model. An important requirement is also the uniform distribution of points in the parameter space.

To construct a surrogate model, various methods of filling the parameter space were investigated: random sampling, the Latin hypercube method (LHC), the Sobol method, and the grid method. Figure 5 shows a comparison of filling a two-dimensional space by the uniform direct search method and the LHC method. Despite the apparent visual uniformity, direct search provides worse filling quality compared to the LHC method.

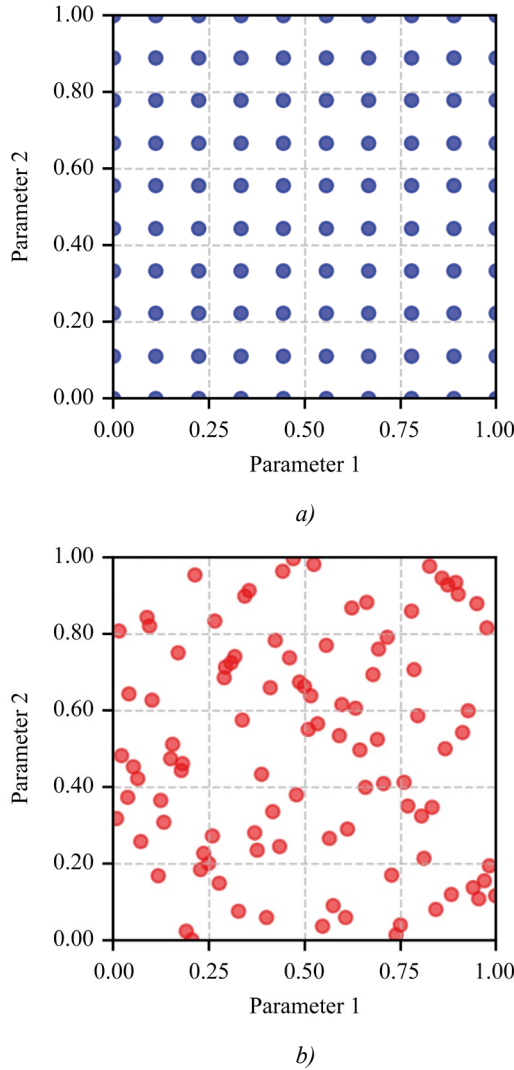


Fig. 5. Filling the parameter space with computation points:  
 a — uniform filling; b — filling by the LHC method

To quantitatively assess the uniformity of the parameter space coverage, a metric method [2] was developed based on the comparison of the specific average distance between nearby points. The method includes normalization of the parameters in a single hypercube, generation of points by the studied filling method, and calculation of the Monte Carlo coefficient. This coefficient is the ratio of the actual average distance between nearby points to the expected average distance:

$$I = \frac{0.5}{\sqrt{\frac{n}{A}}},$$

where  $n$  — number of real points;  $A$  — area of the region (in the case under consideration,  $A = 1$ ).

For the selected combinations of parameters, parallel calculations of the model and calculations of quality indicators were performed, which made it possible to form a data set for constructing a surrogate model. The research used a direct propagation neural network of the following architecture [3, 13]: an input layer (3 inputs with data normalization), two fully connected layers (16 and 8 neurons) with ReLU activation functions, an output layer for regression. The network was trained using the ADAM algorithm, which provided adaptive adjustment of the learning rate and efficient work with noisy data.

At the final stage, the Pareto front was constructed by the NSGA-II evolutionary algorithm [4, 14], which used the quality indicator estimates obtained through the surrogate model. This algorithm provided for the efficient identification of a set of non-dominated solutions in the quality criteria space [15].

**Research Results.** The developed method was tested on a positional pneumatic drive with discrete distributors. At the first stage, a study on the dynamic characteristics of the control system was conducted. Figure 6 shows transient processes demonstrating the key features of the drive operation. The analysis of the graphs shows symmetry in the number of switchings of the control signal during the forward and reverse stroke, which indicates the stability of the control algorithm. At the same time, asymmetry is observed in the positioning accuracy: for the forward stroke of the system, the control error reaches 1.5 mm, which is explained by the design features of the single-rod pneumatic cylinder.

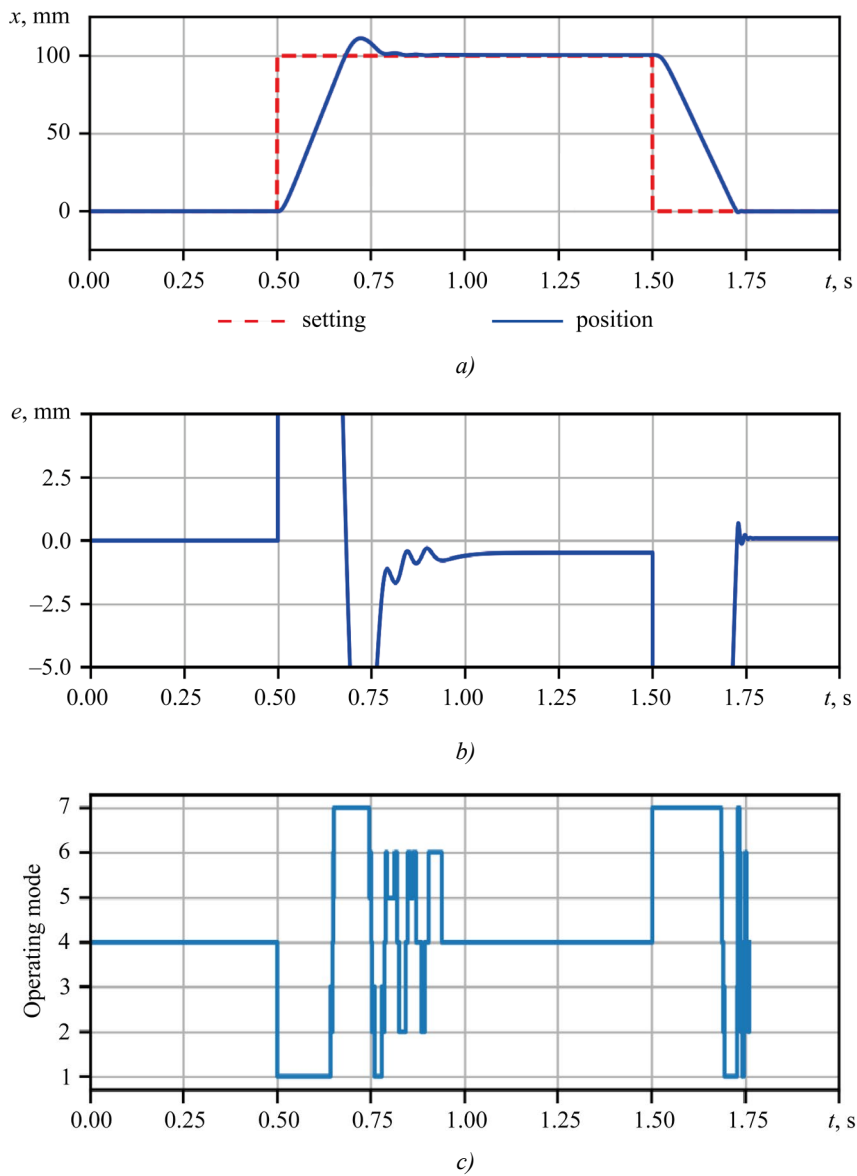


Fig. 6. Transient processes of pneumatic drive with discrete pneumatic distributors:  $a$  — transient process;  $b$  — control error;  $c$  — switching modes

An assessment of the effect of the system parameters on transient processes has established that reducing the width of the braking corridor increases the positioning accuracy, accompanied by an increase in the number of switchings of the pneumatic distributors. Similarly, an acceleration of the response speed of the pneumatic distributors increases the positioning accuracy, but leads to an increase in the oscillation of the transient process and a growth of the number of switchings. At the same time, the magnitude of the displacement did not have a significant effect on the transient process, which indicated the linearity of the system in a wide range of working displacements and confirmed the efficiency of the control algorithm.

When constructing a surrogate model, the parameter area was filled with computation points, with preference given to the Latin hypercube method, which provides for a uniform distribution of points compared to direct enumeration, random sampling, the Sobol method, and the network method. The calculation of the Monte Carlo coefficient (Table 3) demonstrated that the Latin hypercube method was characterized by the smallest dispersion of distances between nearby points, which made it possible to form a sample of 2,500 combinations of basic parameters. The application of surrogate models compromised the labor intensity of constructing the Pareto set, which resulted in a 48% reduction in calculation time. The surrogate model was built on the basis of neural network technology, while the analysis of various approaches to the formation of a training data sample confirmed the feasibility of using the Latin hypercube method.

Table 3

Comparison of Uniformity of Parameter Space Coverage by Different Sampling Methods

Sampling method	Monte Carlo coefficient
Random sampling	1.024
Latin hypercube method	0.997
Sobol's method	0.980

For each combination of basic parameters, a mathematical model was calculated with the definition of quality indicators, which made it possible to consider the set of calculated points of each iteration of the algorithm as a generation. Within the framework of the non-dominant sorting procedure, unimprovable solutions were identified that formed the Pareto front of zero rank, and the remaining points formed the Pareto front of the first rank. Subsequent generation of the next generation was performed by operations similar to crossover, mutation and selection, while a fixed generation size was maintained by cutting off the least high-quality options. The optimization algorithm terminated when the maximum number of generations or the required convergence level was reached. The result of the algorithm implemented using the evolutionary algorithm NSGA-II was the Pareto front. It is shown in Figure 7, reflecting unimprovable solutions with a balance between the number of switchings of pneumatic distributors and the quality of the transient process. At the same time, a small steepness of the front provides for considerable reduction of the number of switchings without significant deterioration of the transient characteristics.

Using a neural network with 4 hidden intermediate layers and a training sample consisting of 2,500 points allowed us to provide for an average accuracy of the surrogate model equal to 91%, with a maximum deviation of 12%. An additional increase in the number of points by 50% has led to an increase in the accuracy of the surrogate model by 15%.

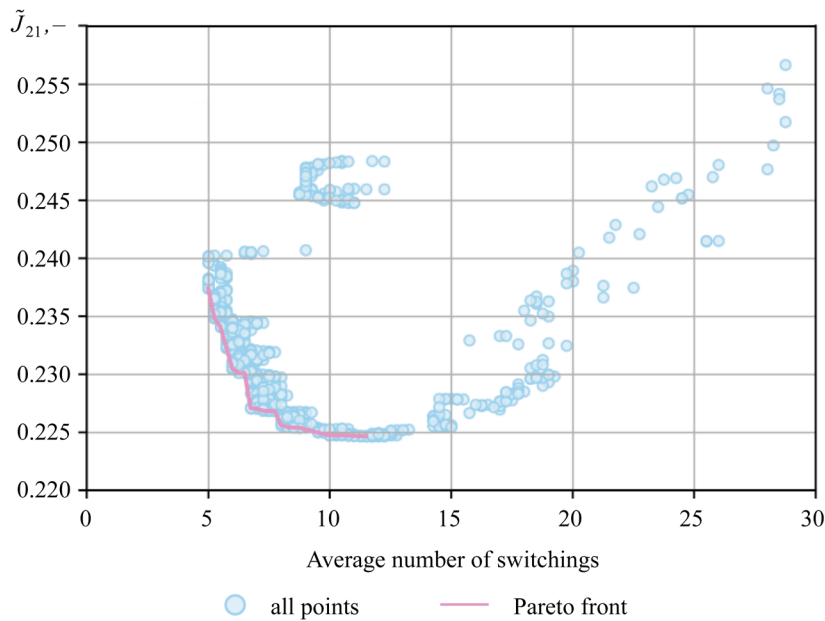


Fig. 7. Pareto set for a pneumatic actuator with discrete distributors

**Discussion and Conclusion.** The obtained results indicate high stability of the control algorithm, providing symmetrical switching of signals during forward and reverse strokes, which confirms correctness of the approach applied to pneumatic drive control. The revealed asymmetry of positioning accuracy, expressed in an error of up to 1.5 mm for forward stroke, indicates the need for further optimization of the design features of the pneumatic cylinder.

The analysis of the effect of system parameters on dynamic characteristics has shown that the compromise between positioning accuracy and the number of switchings of pneumatic distributors requires an optimal selection of the width of the braking corridor and the speed of the distributors. The use of the Latin hypercube method to form a training sample has provided for uniform filling of the parametric space, which is confirmed by calculations of the Monte Carlo coefficient.

The use of replacement surrogate models built on the basis of neural network technologies made it possible to compromise the labor intensity of constructing the Pareto set and reduce the calculation time by 48%, which indicates the prospects of this approach in optimization problems. The efficiency of the evolutionary algorithm NSGA-II used to construct the Pareto front is validated through obtaining trade-off decisions that provide for a balance between the number of switchings of pneumatic distributors and the quality of the transient process.

Reaching an average accuracy of the replacement model at 91% and reducing the maximum deviation to 12% when using a neural network with 4 hidden layers demonstrates the high efficiency of neural network technologies. At the same time, an increase in accuracy by 15% with an expansion of the training sample by 50% indicates the potential for further improvement of the accuracy of the models.

Thus, the results of the conducted research confirm the potential of the proposed method for increasing the efficiency of positional pneumatic drives with discrete distributors, and determine promising directions for further optimization research in this area.

### References

1. Yousry M, Elmayyah W, Mabrouk M. Position Control of a Pneumatic Cylinder Actuator Using Modified PWM Algorithm. *Journal of Engineering Science and Military Technologies*. 2020;4(1):121–126. <http://doi.org/10.21608/ejmtc.2020.31861.1145>
2. Nguyen T, Leavitt J, Jabbari F, Bobrow JE. Accurate Sliding-Mode Control of Pneumatic Systems Using Low-Cost Solenoid Valves. *IEEE/ASME Transactions on Mechatronics*. 2007;12(2):216–219. <https://doi.org/10.1109/TMECH.2007.892821>
3. Bone GM, Xue M, Flett J. Position Control of Hybrid Pneumatic–Electric Actuators Using Discrete-Valued Model-Predictive Control. *Mechatronics*. 2014;25:1–10. <https://doi.org/10.1016/j.mechatronics.2014.10.009>
4. The Anh Dao, Sidorenko VS, Dymochkin DD. Study on Positioning Accuracy of Automated Pneumatic Drive with an Outer Brake. *Vestnik of Don State Technical University*. 2015;15(4):46–53. <https://doi.org/10.12737/16077>
5. Grishchenko VI, Sidorenko VS. Modeling of the Positioning Process of Actuators of Technology Equipment with Discrete Pneumohydraulic Device and Pneumatic Communication Lines. *Vestnik of Don State Technical University*. 2009;(S2):81–90.
6. Podinovskiy VV, Nogin VD. *Pareto-Optimal Solutions to Multicriteria Problems*. Moscow: Fizmatlit; 2007. 256 p. (In Russ.)
7. Diaz-Manriquez A, Toscano G, Barron-Zambrano JH, Tello-Leal E. A Review of Surrogate Assisted Multiobjective Evolutionary Algorithms. *Computational Intelligence and Neuroscience*. 2016;2016:9420460. <http://doi.org/10.1155/2016/9420460>
8. Yongping Pan, Chenguang Yang, Lin Pan, Haoyong Yu. Integral Sliding Mode Control: Performance, Modification, and Improvement. *IEEE Transactions on Industrial Informatics*. 2018;14(7):3087–3096. <https://doi.org/10.1109/TII.2017.2761389>
9. Sheykin MO, Cherkasskikh SN. Experimental Study of a Pneumatic Actuator with a Fuzzy Logic Controller. In: *Proc. XII All-Russian Scientific and Technical Conference “Hydraulic Machines, Hydraulic Drives and Hydropneumatic Automation. Current Status and Development Prospects”*. St. Petersburg: Politekh-Press; 2022. P. 257–267.
10. Sheykin MO, Cherkasskikh SN, Shilin DV. Application of Sliding Mode Control in Pneumatic Actuators. *Gidravlika*. 2024;(23):24–32. (In Russ.)
11. Incremona GP, Rubagotti M, Ferrara A. Sliding Mode Control of Constrained Nonlinear Systems. *IEEE Transactions on Automatic Control*. 2017;62(6):2965–2972. <https://doi.org/10.1109/TAC.2016.2605043>
12. Ley C. *Applied Directional Statistics: Modern Methods and Case Studies*. London: Chapman & Hall/CRC Press; 2018. 318 p. <https://doi.org/10.1201/9781315228570>
13. Raisch A, Sawodny O. Analysis and Optimal Sizing of Pneumatic Drive Systems for Handling Tasks. *Mechatronics*. 2019;59:168–177. <https://doi.org/10.1016/j.mechatronics.2019.04.003>

14. Yagoubi M, Bederina H. Surrogate-Assisted NSGA-II Algorithm for Expensive Multiobjective Optimization. In: *Proceedings of the Companion Conference on Genetic and Evolutionary Computation*. New York, NY: Association for Computing Machinery; 2023. P. 431–434. <https://doi.org/10.1145/3583133.3590746>

15. Deb K, Pratap A, Agarwal S, Meyarivan T. A Fast and Elitist Multi-Objective Genetic Algorithm: NSGA-II. *IEEE Transactions on Evolutionary Computation*. 2002;6(2):182–197. <https://doi.org/10.1109/4235.996017>

**About the Authors:**

**Maxim O. Sheykin**, Junior Researcher of the Hydromechanics and Hydraulic Machines Department, National Research University MPEI (17, Krasnokazarmennaya Str., Moscow, 111250, Russian Federation), [SPIN-code](#), [ORCID](#), [SheykinMO@mpei.ru](mailto:SheykinMO@mpei.ru)

**Sergey N. Cherkasskikh**, Cand.Sci. (Eng.), Associate Professor of the Hydromechanics and Hydraulic Machines Department, National Research University MPEI (17, Krasnokazarmennaya Str., Moscow, 111250, Russian Federation), [SPIN-code](#), [ORCID](#), [ScopusID](#), [CherasskikhSN@mpei.ru](mailto:CherasskikhSN@mpei.ru)

**Denis V. Shilin**, Cand.Sci. (Eng.), Associate Professor of the Hydromechanics and Hydraulic Machines Department, National Research University MPEI (17, Krasnokazarmennaya Str., Moscow, 111250, Russian Federation), [SPIN-code](#), [ORCID](#), [ScopusID](#), [ResearcherID](#), [ShilinDV@mpei.ru](mailto:ShilinDV@mpei.ru)

**Vladimir V. Fedenkov**, Dr.Sci. (Eng.), Professor of the Hydromechanics and Hydraulic Machines Department, National Research University MPEI (17, Krasnokazarmennaya Str., Moscow, 111250, Russian Federation), [SPIN-code](#), [ORCID](#), [FedenkovVV@mpei.ru](mailto:FedenkovVV@mpei.ru)

**Claimed contributorship:**

**MO Sheykin:** methodology, software, formal analysis, investigation, visualization, validation, writing — original draft preparation.

**SN Cherkasskikh:** conceptualizations, methodology, formal analysis, validation, writing — review & editing, supervision.

**DV Shilin:** supervision.

**VV Fedenkov:** supervision.

**Conflict of Interest Statement:** the authors claimed no conflict of interest.

*All the authors have read and approved the final version of manuscript.*

**Об авторах:**

**Максим Олегович Шейкин**, младший научный сотрудник кафедры гидромеханики и гидравлических машин им. В.С. Квятковского Национального исследовательского университета «МЭИ» (111250, Российская Федерация, г. Москва, ул. Красноказарменная, д. 17), [SPIN-код](#), [ORCID](#), [SheykinMO@mpei.ru](mailto:SheykinMO@mpei.ru)

**Сергей Николаевич Черкасских**, кандидат технических наук, доцент кафедры гидромеханики и гидравлических машин им. В.С. Квятковского Национального исследовательского университета «МЭИ» (111250, Российская Федерация, г. Москва, ул. Красноказарменная, д. 17), [SPIN-код](#), [ORCID](#), [ScopusID](#), [CherasskikhSN@mpei.ru](mailto:CherasskikhSN@mpei.ru)

**Денис Викторович Шилин**, кандидат технических наук, доцент кафедры гидромеханики и гидравлических машин им. В.С. Квятковского Национального исследовательского университета «МЭИ» (111250, Российская Федерация, г. Москва, ул. Красноказарменная, д. 17), [SPIN-код](#), [ORCID](#), [ScopusID](#), [ResearcherID](#), [ShilinDV@mpei.ru](mailto:ShilinDV@mpei.ru)

**Владимир Васильевич Феденков**, доктор технических наук, профессор кафедры гидромеханики и гидравлических машин им. В.С. Квятковского Национального исследовательского университета «МЭИ» (111250, Российская Федерация, г. Москва, ул. Красноказарменная, д. 17), [SPIN-код](#), [ORCID](#), [FedenkovVV@mpei.ru](mailto:FedenkovVV@mpei.ru)

**Заявленный вклад авторов:**

**М.О. Шейкин:** разработка методологии, разработка программного обеспечения, формальный анализ, проведение исследования, визуализация, валидация результатов, написание черновика рукописи.

**С.Н. Черкасских:** разработка концепции, разработка методологии, формальный анализ, валидация результатов, написание рукописи — рецензирование и редактирование, научное руководство.

**Д.В. Шилин:** научное руководство.

**В.В. Феденков:** научное руководство.

*Конфликт интересов: авторы заявляют об отсутствии конфликта интересов.*

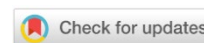
*Все авторы прочитали и одобрили окончательный вариант рукописи.*

**Received / Поступила в редакцию 25.01.2025**

**Reviewed / Поступила после рецензирования 17.02.2025**

**Accepted / Принята к публикации 24.02.2025**

# INFORMATION TECHNOLOGY, COMPUTER SCIENCE AND MANAGEMENT ИНФОРМАТИКА, ВЫЧИСЛИТЕЛЬНАЯ ТЕХНИКА И УПРАВЛЕНИЕ



UDC 517.977.56, 532.522.2

Original Theoretical Research

<https://doi.org/10.23947/2687-1653-2025-25-1-65-76>

## Analysis and Optimization of Hydrocannon Nozzle Shape Based on Direct Extreme Approach

Victor K. Tolstykh , Yuliia V. Dmitruk  

Donetsk State University, Donetsk, Donetsk People's Republic

✉ [mail@tolstykh.com](mailto:mail@tolstykh.com), [loktyushina.julia@yandex.ru](mailto:loktyushina.julia@yandex.ru)

EDN: RVWIZA

### Abstract

**Introduction.** Controllability analysis is a required stage for the correct formulation and solution of any optimal control problem. This problem becomes specifically relevant in the context of optimizing systems with distributed parameters, which are described by partial difference equations. Such problems include the considered problem of optimization of the shape of the nozzle of a hydrocannon. The optimal nozzle should provide the maximum value of the functional expressed through the average force of the impulse of the jet of a hydrocannon. The relevance of this research is due to the lack of a unified approach to the analysis of controllability of systems with distributed parameters, which complicates the correct formulation and solution of optimization problems. In particular, previous attempts to solve the problem of hydrocannon nozzle optimization using classical variational calculus were unsuccessful due to ignoring aspects of controllability. The objective of this research was to apply a new approach proposed by V.K. Tolstykh to controllability analysis to solve the problem of optimal design of the shape of a hydrocannon nozzle.

**Materials and Methods.** The research method used was controllability analysis based on the Tikhonov conditional correctness of the inverse problem. This approach allowed us to identify the conditions for the existence of the gradient of the objective functional and construct a regularization of the solution to the inverse problem using adaptive gradient methods. It was of current interest for multiextremal problems, including the problem of the optimum nozzle shape. It was solved by a direct extreme approach in the form of direct maximization of the objective functional based on its gradient. In the process of research, a nonlinear, quasi-one-dimensional mathematical model of isentropic water flow in a hydrocannon nozzle was used. The flow was considered inviscid, compressible, and subsonic.

**Results.** As part of the research, controllability conditions were obtained that allowed us to radically simplify the problem of optimizing the shape of the hydrocannon nozzle. It was found that in order to correctly determine the gradient of the objective functional, it was required to narrow the solution area of the conjugate problem to a small rectangular area. The use of adaptive gradient methods with satisfactory step factors provided for the regularization of the solution. For the first time, two optimum shapes of the hydrocannon nozzle were found. The first shape provided a local maximum of the objective functional, the second — a global maximum of the functional with a restriction on the expansion of the nozzle.

**Discussion and Conclusion.** The results obtained show that it is impossible to perform a directed search for an optimal solution using the Frechet derivative without taking into account controllability conditions. The first proposed approach, in combination with the desired adaptive gradient optimization methods, allowed us not only to correctly formulate the optimization problem, but also to find optimal nozzle shapes that provided the maximum average pulse force of the ultrajet. In some cases, for the stability of the solution, it was necessary to introduce expansion limitation of the nozzle beyond the barrel of the hydrocannon. This made it possible to meet the requirements of the controllability theorem and guaranteed the correctness of the results obtained. The theoretical relevance of the research is in the development of controllability analysis methods for systems with distributed parameters, which creates new opportunities for solving similar problems in other areas. The research results can be used to optimize devices operating on the basis of pulsed jets, as well as for further study of more complex models of fluid flow.

**Keywords:** nozzle shape, hydrocannon nozzle, jet impulse force, nozzle expansion limitation, maximization of objective functional, gradient

**Acknowledgements.** The authors appreciate the scientific teams of the Departments of Computer Technology and General Physics, Donetsk State University, and Donetsk Institute of State Fire Service, the RF Ministry for Civil Defense, Emergencies and Elimination of Consequences of Natural Disasters, for fruitful discussions of the research materials.

**Funding Information.** The research is done at the Federal State Budgetary Educational Institution of Higher Education “DONSU” with the financial support from the Azov-Black Sea Mathematical Center (Agreement No. 075–02–2025–1608, dated 02.27.2025), as well as within the framework of the state-financed research “Development of Intelligent Systems for Analyzing and Forecasting the Condition of Natural and Technical Facilities (FRRE-2023–0012)” (State Registration No. 124012400344–1).

**For Citation.** Tolstykh VK, Dmitruk YuV. Controllability Analysis and Optimization of Hydrocannon Nozzle Shape Based on Direct Extreme Approach. *Advanced Engineering Research (Rostov-on-Don)*. 2025;25(1):65–76.

<https://doi.org/10.23947/2687-1653-2025-25-1-65-76>

*Оригинальное теоретическое исследование*

## Анализ управляемости и оптимизация формы сопла гидропушки на основе прямого экстремального подхода

В.К. Толстых , Ю.В. Дмитрук  

Донецкий государственный университет, Донецк, Донецкая Народная Республика

 [mail@tolstykh.com](mailto:mail@tolstykh.com), [loktyushina.julia@yandex.ru](mailto:loktyushina.julia@yandex.ru)

### Аннотация

**Введение.** Анализ управляемости является необходимым этапом для корректной постановки и решения любой задачи оптимального управления. Эта проблема становится особенно актуальной в рамках оптимизации систем с распределенными параметрами, которые описываются уравнениями в частных производных. К таким задачам относится рассматриваемая задача оптимизации формы сопла гидропушки. Оптимальное сопло должно обеспечивать максимальное значение функционала, выражаемого через среднюю силу импульса струи гидропушки. Актуальность данного исследования обусловлена отсутствием единого подхода к анализу управляемости систем с распределенными параметрами, что затрудняет корректную постановку и решение задач оптимизации. В частности, предыдущие попытки решения задачи оптимизации сопла гидропушки с использованием классического вариационного исчисления не увенчались успехом из-за игнорирования аспектов управляемости. Целью данной работы являлось применение нового подхода, предложенного Толстых В.К., к анализу управляемости для решения задачи оптимального дизайна формы сопла гидропушки.

**Материалы и методы.** В качестве метода исследования использовался анализ управляемости, основанный на условной корректности по Тихонову обратной задачи. Такой подход позволил выявить условия существования градиента целевого функционала и построить регуляризацию решения обратной задачи адаптивными градиентными методами. Это актуально для многоэкстремальных задач, в том числе для задачи оптимальной формы сопла. Она решалась прямым экстремальным подходом в виде непосредственной максимизации целевого функционала на основе его градиента. В процессе исследования использовалась нелинейная, квазиодномерная математическая модель изоэнтропического течения воды в сопле гидропушки. Течение при этом считалось невязким, сжимаемым и дозвуковым.

**Результаты исследования.** В рамках исследования были получены условия управляемости, которые позволили радикально упростить задачу оптимизации формы сопла гидропушки. Установлено, что для корректного определения градиента целевого функционала необходимо сузить область решения сопряженной задачи до малой прямоугольной области. Использование адаптивных градиентных методов с удовлетворительными шаговыми множителями обеспечило регуляризацию решения. Впервые были найдены две оптимальные формы сопла гидропушки. Первая форма обеспечивает локальный максимум целевого функционала, вторая — глобальный максимум функционала при ограничении на расширение сопла.

**Обсуждение и заключение.** Полученные результаты показывают, что направленный поиск оптимального решения невозможно осуществить по производной Фреше без учета условий управляемости. Впервые предложенный подход, в сочетании с необходимыми адаптивными градиентными методами оптимизации, позволил не только корректно поставить задачу оптимизации, но и найти оптимальные формы сопла, обеспечивающие максимальную среднюю силу импульса ультраструи. В некоторых случаях для обеспечения устойчивости решения потребовалось введение ограничения на расширение сопла за пределы ствола гидропушки. Это позволило выполнить требования теоремы об управляемости и гарантировало корректность полученных результатов. Теоретическая

значимость приведенного исследования заключается в развитии методов анализа управляемости для систем с распределенными параметрами, что создает новые возможности для решения схожих задач в других областях. Результаты работы могут быть применены для оптимизации устройств, работающих на основе импульсных струй, а также для дальнейшего исследования более сложных моделей течения жидкости.

**Ключевые слова:** форма сопла, сопло гидропушки, сила импульса струи, ограничение на расширение сопла, максимизация целевого функционала, градиент

**Благодарности.** Авторы выражают признательность за плодотворные обсуждения материалов работы научным коллективам кафедр компьютерных технологий и общей физики Донецкого государственного университета и Донецкого института государственной противопожарной службы Министерства Российской Федерации по делам гражданской обороны, чрезвычайным ситуациям и ликвидации последствий стихийных бедствий.

**Финансирование.** Исследования проводились в ФГБОУ ВО «ДОНГУ» при финансовой поддержке Азово-Черноморского математического центра (Соглашение от 27.02.2025 № 075–02–2025–1608), а также в рамках государственной темы «Разработка интеллектуальных систем анализа и прогнозирования состояния природно-технических объектов (FRRE-2023–0012)» (номер госрегистрации 124012400344–1).

**Для цитирования.** Толстых В.К., Дмитрук Ю.В. Анализ управляемости для системы с распределенными параметрами в задаче оптимального дизайна формы сопла гидропушки. *Advanced Engineering Research (Rostov-on-Don)*. 2025;25(1):65–76. <https://doi.org/10.23947/2687-1653-2025-25-1-65-76>

**Introduction.** Despite the significant amount of research on the control theory, there is still no unified approach to the analysis of controllability for systems with distributed parameters. Existing studies are usually limited to considering controllability as the possibility of transferring a system from an initial state to a given final state [1]. However, this approach turns out to be insufficient for optimization problems of spatially distributed systems described by partial differential equations. Controllability by the final state does not guarantee controllability by the conditions specified in the objective functional, which makes the analysis of such systems complex and non-obvious. In this paper, the authors use the concept of controllability proposed by V.K. Tolstykh [2] and apply it to find the optimal shape of the hydrocannon nozzle.

Hydraulic cannons designed to generate pulsed jets of high-pressure liquid are widely used, e.g., in the mining industry to destroy rocks [3]. The efficiency of such devices largely depends on the shape of the nozzle [4], which makes the task of its optimization urgent. Despite significant interest in this problem, existing papers, such as the works of Zuikova Z.G. [5], Zubov V.I. [6], and Atanova G.A. [7], are primarily theoretical. These authors formulated the required conditions for optimality, but the numerical results were not supported by evidence of their optimality. Moreover, as it is shown in this research, the previously obtained “optimal” nozzle shapes are not such. Thus, despite multi-year research, the problem of designing an optimal nozzle shape remains unsolved.

The solution to this complex problem is possible only through using a direct extreme approach with original adaptive gradient methods described in the work of V.K. Tolstykh [8]. The objective of this work was to apply the new approach proposed in [2] to the analysis of the controllability of a system with distributed parameters for the problem of optimal design of the hydrocannon nozzle shape. Thus, the article is aimed at developing the controllability theory for systems with distributed parameters and demonstrating its practical applicability using the example of optimizing the shape of a hydrocannon nozzle.

**Materials and Methods.** The essence of the direct extreme approach is the direct maximization of some objective functional using gradient methods:

$$J(u) = \int_{\omega} I(v, u) d\omega \rightarrow \max, \omega \subset \bar{\Omega}, \quad (1)$$

provided that  $\mathbb{D}(v, u)v = 0$  on  $\bar{\Omega}$ .

Here, the control (in our case — function of the nozzle shape along the length  $x$ )  $u(x) \in U(S)$ ,  $S = (x_a, x_b)$  — domain of control definition,  $U$  — admissible set of controls,  $v(x, t) \in V(\bar{\Omega})$  — state of the nonstationary process of ultra-jet formation on the closed space-time set  $\{x, t\} = \bar{\Omega}$ . Operator  $\mathbb{D}$  includes a specific type of differential equations of water flow in a hydrocannon and acts on  $v$ . Objective function  $I(v, u)$  is defined on the set  $\omega$ , and its value clearly depends on the parameters  $v$  and  $u$ .

The direct approach does not use any intermediate conditions (e.g., required optimality conditions), but solves the problem immediately:

$$u_* = \arg \max J(u), \quad (2)$$

where  $u_*$  — optimal control.

The original problem with the equations of the distributed system  $(v, u)v = 0$  is characterized by a direct mapping:

$$U(S) \rightarrow V(\bar{\Omega}), S \subset \bar{\Omega}.$$

At the same time, optimization problem (1) is inverse. Such problems are usually ill-posed in the classical sense [9]. The solution to direct and inverse problems differs significantly. The latter require regularization of the solution to narrow the set of possible solutions  $U$  to the compact of correctness  $\mathcal{U} \subseteq U$ , which leads to conditional correctness according to Tikhonov. In the direct extreme approach, regularization is performed by gradient methods.

According to the definition of controllability [2], the distributed system in problem (1) will be controllable by  $u(x) \in U(S)$  with respect to objective functional  $J$ , when the inverse problem of mapping the elements of space  $V(\omega)$  of model states into element  $u_*$  is correct according to Tikhonov, provided that  $\max J$ :

$$V(\omega) \xrightarrow{\max J} u_* \in U(S), \quad \omega \subset \bar{\Omega}.$$

Next, when solving problem (2), we will perform a controllability analysis and obtain controllability conditions that can allow us to correctly formulate and solve the problem of optimizing the shape of the hydrocannon nozzle using gradient methods [10].

Paper [8] describes in detail the formulation of the problem under consideration for subsonic, axisymmetric flows of compressible fluid in smoothly changing channels. Let us recall it in the form required for further research. The isentropic motion of water in the nozzle is described by a quasi-one-dimensional, quasi-linear hyperbolic system of equations [11]:

$$\mathbb{D}v = \frac{\partial v}{\partial t} + A \frac{\partial v}{\partial x} + F = 0 \text{ на } \Omega. \quad (3)$$

The state of the system is characterized by vector function  $v = \{\rho, w\} \in V(\bar{\Omega})$ , where  $\rho$  — density of water,  $w$  — speed of water. Operator  $\mathbb{D} = \frac{\partial}{\partial t} + A \frac{\partial}{\partial x} + F$ , its matrix  $A(v) = \begin{pmatrix} w & \rho \\ c^2 & w \end{pmatrix}$  and vector  $F(v, u) = \begin{pmatrix} \varphi \\ 0 \end{pmatrix}$ ,  $\varphi = \rho w u \Theta(x - x_a)$ ,

$\Theta$  — Dirac theta function,  $x_a$  — beginning of the nozzle at the end of the barrel of hydrocannon,  $c^2 = \frac{Bn\rho^{n-1}}{\rho_0^n}$  — square of the speed of sound in water,  $B$  and  $n$  — constants in the equation of state of water in theta form.

The control is described by the formula:

$$u(x) = \frac{1}{\sigma(x)} \frac{d\sigma(x)}{dx} \in U(S), \quad S = (x_a, x_b). \quad (4)$$

Here,  $\sigma$  — nozzle cross-sectional area,  $\sigma(x) = \sigma_a e^{\int_{x_a}^x u(\zeta) d\zeta}$ ,  $x \in [x_a, x_b]$ ,  $\sigma_a = \sigma(x_a)$ . In the barrel of the hydrocannon, when  $x \leq x_a$ , there is no control  $u(x)$ , and free term  $\varphi = 0$ .

Boundary and initial conditions of problem (3):

$$\frac{dw}{dt} + \frac{uB}{m_p} \left( \left( \frac{\rho}{\rho_0} \right)^n - 1 \right) = 0 \text{ on } \Gamma_p,$$

$$\rho = \rho_0 \text{ on } \Gamma_{b0} \cup \Gamma_{b1},$$

$$v(x, t_0) = (\rho_0, w_0) \text{ on } \Gamma_0.$$

Here,  $m_p$  — piston mass,  $\rho_0$  — density of water at atmospheric pressure,  $w_0$  — speed of water and piston before it starts flowing into the nozzle. The boundaries of process  $\Gamma$  for domain  $\Omega$ , are shown in Figure 1. The type of  $\Omega$  is important for the controllability analysis.

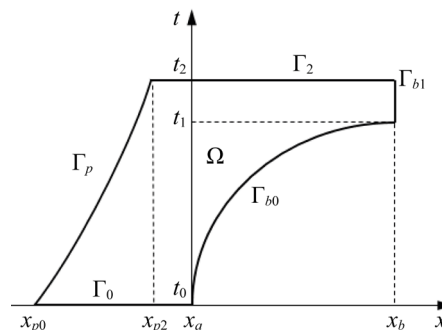


Fig. 1. Area of water flow in the hydrocannon

We specify  $\Omega$ . The origin of coordinates is aligned with the nozzle entrance  $x_a$ , and  $t_0$  — time of the beginning of water flow into the nozzle. On the one hand, the water is limited by the piston moving in the barrel of the hydrocannon along the trajectory  $\Gamma_p$ , and on the other hand — by the free surface of the inflow  $\Gamma_{b0}$  from  $t_0$  to  $t_1$  and the outflow  $\Gamma_{b1}$  from  $t_1$  to  $t_2$ . The line of the initial state of system (3) is  $\Gamma_0$ , coordinates  $x_{p0}$  and  $x_{p2}$  — initial and final positions of the piston. The specified  $\Gamma$ -lines for  $\Omega$  form the closure of  $\bar{\Omega}$ . The domain of definition of the control  $S = P_x(\Omega|_{x>x_a})$ , i.e., for  $x > x_a$ ,  $S$  is the projection of a part of domain  $\Omega$  onto  $x$  axis.

The optimization problem (optimal design of the nozzle shape) is formulated as follows: it is necessary to find the control  $u(x)$  that delivers the maximum to the functional:

$$J(u) = \int_{t_1}^{t_2} I(w, u)|_{\omega} dt, \quad I(w, u)|_{\omega} = \frac{\rho_0 \sigma(x_b) w^2(x_b, t)}{t^2 - t^1}. \quad (5)$$

The objective functional is set at  $\omega = \Gamma_{b1}$ , i.e., at the nozzle exit of the hydrocannon, and determines the average force of the jet on a possible obstacle [12].

The gradient algorithm for maximizing functional (5) has the form:

$$u^{k+1}(x) = u^k(x) + b^k \nabla J(u^k; x), \quad x \in S, \quad k = 0, 1, \dots, \quad (6)$$

where  $k$  — iteration number;  $b^k$  — step multiplier that controls the rise to  $\max J$  in the direction of gradient  $\nabla J^k$ .

The gradient is the functional Frechet derivative  $J'_u$ , which can be found from the first variation of the objective functional  $\delta J = \langle J'_u, \delta u \rangle_{U^*(S)}$ . Here, the angle brackets denote the scalar product, in this case, in the conjugate control space  $U^*(S)$ . The superscript \* denotes conjugacy.

It should be noted that sometimes the gradient of a functional on a Hilbert space is confused with the Frechet derivative of this functional [13]. Derivative  $J'_u(u; x)$  may be insensitive to the control  $u(x)$  on the entire set  $S$  or on parts of  $S$  of nonzero measure. Therefore, in the general case,  $J'_u(u; x)$  in (6) will not indicate a reliable direction of correction  $u^k$  for the directed search for the optimal solution  $u_*(x)$ . The gradient from the Frechet derivative can be obtained only when the controllability conditions are realized.

Approaches to solving problems of hydrocannon nozzle optimization with the aim of maximizing the average jet impulse force [5], the functional depending on the flow parameters [6], and maximizing the outflow velocity [7] were mentioned earlier. In these papers, after varying  $\delta J$ , a formal expression for derivative  $J'_u$  was obtained. It depends on the solution  $f = (f_1, f_2) \in V^*(\bar{\Omega})$  of the linear conjugate hyperbolic problem:

$$-\frac{\partial f}{\partial t} - A^T \frac{\partial f}{\partial x} + F_v'^T f = 0 \text{ on } \Omega. \quad (7)$$

The superscript  $T$  means transposition,  $F'_v$  — deriva  $F$  tive of the free term  $F$  with respect to  $v$ . Boundary and initial (terminal on  $\Gamma_2$ ) conditions:

$$\begin{aligned} \frac{d}{dt} \left( \frac{m_p f_2}{F_a \rho} \right) + f_1 \rho &= 0 \text{ on } \Gamma_p, \\ f_1 &= 0 \text{ on } \Gamma_{b0}, \\ \rho_0 f_1 + w_b f_2 + I'_w &= 0, \quad I'_w|_{\omega} = \frac{2\rho_0 \sigma_b w_b}{t_2 - t_1} \text{ on } \Gamma_{b1}, \\ f_1 &= 0, f_2 = 0 \text{ on } \Gamma_2. \end{aligned}$$

Frechet derivative  $J'_u$  is sometimes called the residual or gradient. It is more convenient to represent it in operator form:

$$J'_u(u; x) = \mathbb{U}^*_{\emptyset} f(x, t) \equiv \mathbb{U}^* f(x, t) + \kappa J \in U^*(S). \quad (8)$$

Here, the conjugate inhomogeneous operator  $\mathbb{U}^*_{\emptyset} = \mathbb{U}^* + \kappa J$ ,  $\mathbb{U}^*$  — conjugate homogeneous operator, the dot denotes the location of argument  $f$  of the operators,  $\kappa$  — weight coefficient for equalizing the computational noise of the numerical solution of the original and conjugate problems [8]. Expression (8) contains the value of the functional in the form of the number  $J$ . This is the value of derivative  $J'_u$ .

The heterogeneity of operator  $\mathbb{U}^*_{\emptyset}$  is a consequence of the dependence of the objective function  $I(w, u)$  on the control  $u$ . Such a dependence is a rare feature of optimization problems and can significantly complicate the calculation of the gradient.

The value of homogeneous operator  $\mathbb{U}^*$  in derivative (8) has the form:

$$\mathbb{U}^* f = \int_{\Gamma_{b0}}^{t_2} F_u'^T f dt = \int_{\Gamma_{b0}}^{t_2} \rho w f_1 dt,$$

where integration is performed from the lower nonlinear boundary  $\Gamma_{b0}$  (Fig. 1) when water flows into the nozzle.

The meaning and objective of the conjugate problem is to map derivative  $J'_w$  (sensitivity of  $J$  to  $w$ ) from domain  $\omega$  to domain  $S$ , where the gradient and control are defined. Such a mapping with the help of  $f$  is done using the intermediate set  $\Omega \subset \bar{\Omega}$ , which, according to controllability, specifies the correct domain  $V^*(\Omega)$  of the definition of the homogeneous operator  $\mathbb{U}^*$ , so that in expression (8) from  $J'_u$ , we obtain gradient  $\nabla J$ .

That is, the conjugate problem implements the mapping:

$$f : V^*(\omega) \rightarrow V^*(\Omega).$$

Next, using operator  $\mathbb{U}^* : V^*(\Omega) \rightarrow U^*(S)$ , we can obtain the gradient from Frechet derivative  $J'_u$ :

$$J'_u \mathbb{U}^*_{\mathcal{O}} \rightarrow \mathbb{U}^*_{\mathcal{O}} f|_{\Omega} = \nabla J \in U^*(S).$$

Domain  $\Omega$  is determined from the controllability analysis.

**Research Results.** The requirements for controllability conditions within the framework of the direct extreme approach are formulated in the following theorem (for the proof, see [2]).

**Theorem.** The mathematical model  $(v, u)v = 0$  in problem (3) is controllable by  $u(x)$  on  $S$  with respect to functional  $J$  if:

- 1) there exists domain  $V^*(\Omega)$ ,  $\Omega \subset \bar{\Omega}$  of a correct conjugate state, which is the domain of definition of operator  $\mathbb{U}^*$  with its values in the gradient domain  $U^*(S)$ ;
- 2) operator  $\mathbb{U}^*$  — non-degenerate;
- 3) algorithm (6) for  $u^0 \in \mathcal{U}$  uses satisfactory regularization parameters  $b^k$ .

We start with the first and most difficult requirement of the theorem. First, it is necessary to verify the classical correctness of the original and conjugate problems. Original (3) and conjugate (7) systems are of the hyperbolic type. The eigenvalues of the matrices  $A$  and  $A^T$  are the same. Therefore, in both systems, the characteristics  $\xi_{1,2}$  will be the same — as the trajectories of the propagation of disturbances in the plane  $(x, t)$  along the characteristic directions  $\frac{d\xi_{1,2}}{dt} = w \pm c$ . The conjugate waves

generated by derivative  $I'_w|_{\omega} \in V^*(\omega)$  at the nozzle exit  $\Gamma_{b1} = \omega$ , will move with the same characteristics as the original ones, but in the opposite direction. The initial condition for the conjugate problem is specified on the terminal line  $\Gamma_2$ .

All characteristics in domain  $\Omega$  emerge from the boundary sections  $\partial\Omega$  with known solutions given by the boundary conditions. In the case of shock-free wave flows (it is precisely such flows that are considered in this research), the characteristics of the same family do not intersect, and at the intersection of two characteristics of a different family  $\xi_1$  and  $\xi_2$  at any point  $\bar{\Omega}$ , a solution to the hyperbolic system of two equations [14] can be found in the form of two-dimensional vector functions  $v$  and  $f$ .

To find the domain of operator  $\mathbb{U}^*$ , it is necessary to conduct an analysis and identify the existence of the following sequence of mappings, starting from the control  $u \in U(S)$  and ending with gradient  $\nabla J \in U^*(S)$ :

$$U(S) \ni u \xrightarrow{\text{uniquely}} I'_w|_{\omega} \xrightarrow{\text{uniquely}} f|_{\Omega} \in V^*(\Omega) \xrightarrow{\mathbb{U}^*} U^*(S).$$

The problem under discussion can be described more simply. First, objective functional  $J(u)$ , specified on  $\omega$ , must be sensitive to the control defined on  $S$  (sensitivity is characterized by derivative  $I'_w|_{\omega}$ ). Second, from the set of conjugate solutions on the entire  $\bar{\Omega}$ , it is necessary to select such a subset  $\Omega$ , where the conjugate solutions  $f|_{\Omega}$  will uniquely depend on the values of the objective functional in the form  $I'_w|_{\omega}$ . There may not be such a dependence on the entire domain  $\bar{\Omega}$ . Thirdly, the set  $\Omega$  must provide operator  $\mathbb{U}^*$  with the ability to map the conjugate states  $f|_{\Omega}$  into  $U^*(S)$ . This mapping is represented by the last branch, where operator  $\mathbb{U}^*$  from the obtained domain of definition  $V^*(\Omega)$  can produce a mapping into the domain of values  $U^*(S)$ , where there is gradient  $\Delta J = \mathbb{U}^*_{\mathcal{O}} f|_{\Omega}$ .

From the correctness of the original direct problem, it follows that any functions  $u(x) \in U(S)$  will uniquely affect the value of the derivative of the objective function  $I'_w$  on  $\omega = \Gamma_{b1}$  through the characteristics  $\xi_1$ , if at least one of them has passed through the entire nozzle. The loss of such effect is possible in the presence of dissipation in the system, but this is not the case with isentropic flows. That is, there is a left branch of mappings in (9):

$$U(S) \ni u \xrightarrow{\text{uniquely}} I'_w|_{\omega}.$$

Let us proceed to identifying the set  $\Omega$ , required for domain  $V^*(\Omega)$  of the definition of operator  $\mathbb{U}^*$ . Term  $I'_w|_{\omega}$  in the boundary condition of conjugate problem (7) causes perturbations of the conjugate solution  $f$ . They propagate in the form of waves along the characteristics of the first family  $\xi_1$  in the reverse time direction from the nozzle exit toward the piston (Fig. 2).

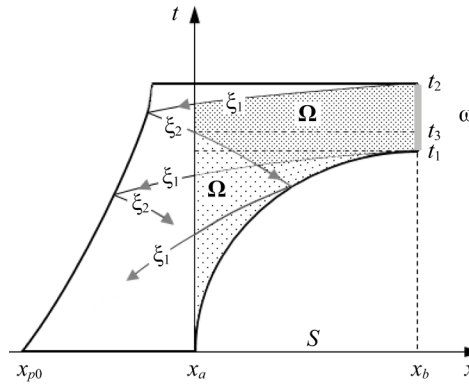


Fig. 2. Space-time diagram of domain  $\Omega$  with redundant domain  $\omega$

These disturbances propagate along the entire nozzle and transfer information about the objective functional from the points  $\omega$  to the points on  $S = (x_a, x_b)$ . On the piston, the waves described by the characteristics of the first family  $\xi_1$ , are reflected and, changing the direction of their propagation, continue to transfer information received from  $\xi_1$  about disturbances  $I'_w|_{\omega}$ , adding new information about the piston motion. This process of wave reflections from the piston and from the inner part of the nozzle continues until the moment  $t_0$ .

Starting from the moment  $t_3$  and below, two conjugate waves  $\xi_1$  and  $\xi_2$ , generated by different values of  $I'_w$  and with unnecessary information (noise), at a minimum, will arrive at the same point of some sections of the set  $S$  from the piston. And below the characteristic  $\xi_1$ , which came out of the nozzle below  $t_1$ , unnecessary information from the nozzle will be added. This information is not needed, since it does not contain information about the optimization goal from  $I'_w|_{\omega}$ .

Figure 2 shows an example of a possible set  $\Omega$  (the entire area shaded with different densities under the upper characteristic  $\xi_1$  from  $x_a$  to  $x_b$ ). In this case,  $\Omega$  corresponds to the Frechet derivative  $J'_u$ . In domain  $\Omega$ , under characteristic  $\xi_2$  (reflection  $\xi_1$ , which came out at  $t_2$ ) and under  $\xi_1$  (which came out at  $t_1$ ), a light area of ambiguous influence of the values of function  $I'_w|_{\omega}$  on the conjugate state  $f$  is formed. Obviously, that it is pointless to solve the conjugate problem and calculate the gradient in such a domain  $\Omega$ .

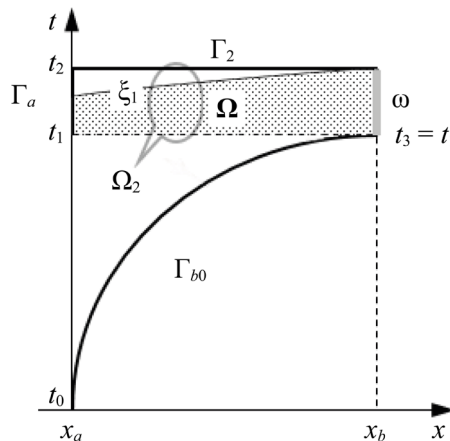
It is reasonable to limit ourselves to considering (Fig. 2) the conjugate state of  $f$  on the part of  $\Omega$ , enclosed in the rectangle:

$$\Omega_1 = (x_a, x_b) \times (t_1, t_2).$$

In this case, rectangle  $\Omega_1$  should be considered too large if the piston is relatively close to the beginning of the nozzle, affecting the conjugate state.

In this rectangle  $\Omega_1$ , the set  $\Omega$  (shaded with different density in Figure 2 from  $t_1$  to  $t_2$ ) will correspond to the redundant set  $\omega$ . That is, in the objective functional  $J$ , the interval  $(t_1, t_2)$  will be redundant. At the same time, in the considered domain  $\Omega$ , there may be unacceptable interference on the left (low density of shading in  $\Omega_1$ ) for calculating gradient  $\nabla J$ .

Redundancy  $\omega$  is eliminated by further reducing  $\Omega_1$  to  $t_3 = t_1$ , i.e., when  $t_3$  corresponds to the start of the outflow (Fig. 3 a).



a)

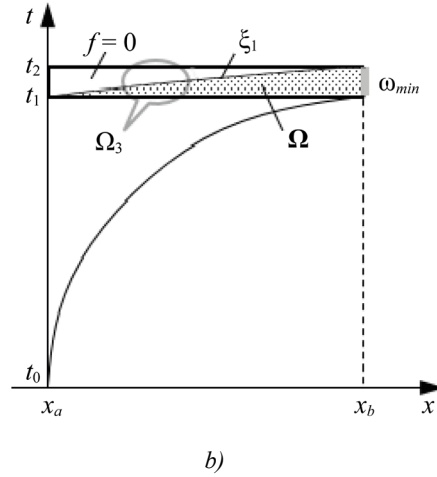


Fig. 3. Space-time diagrams of correct domains  $\Omega$  for determining the gradient:  
 a —  $\Omega$  in domain  $\Omega_2$ ; b —  $\Omega$  in domain  $\Omega_3$

In this case, the entire domain of a sufficient solution to the conjugate problem is narrowed to an even smaller rectangle:

$$\Omega_2 = (x_a, x_b) \times (t_1, t_2).$$

Here, the piston will not “interfere” with the display  $I'_w|_{\omega} \xrightarrow{\text{uniquely}} f|_{\Omega}$ .

If the technical conditions for designing a hydrocannon allow for an even greater reduction in the flow time  $t_2 - t_1$ , then the solution rectangle of the conjugate problem can be reduced even further, to rectangle  $\Omega_3$  with a corresponding triangular domain  $\Omega$  (Fig. 3 b):

$$\Omega_3 = (x_a, x_b) \times (t_1, t_2).$$

Here there is a minimally sufficient set  $\omega_{min}$  to form the domain of definition  $V^*(\Omega)$  of operator  $\mathbb{U}^*$ .

It is in the obtained domains  $\Omega$ , located inside  $\Omega_2$  and  $\Omega_3$  (Fig. 3), that there is a domain of definition  $V^*(\Omega)$  of operator  $\mathbb{U}^*$  with a unique mapping of the derivatives  $I'_w|_{\omega}$  by means of  $f$  into the domain of values of gradient  $U^*(S)$ .

Conjugate problem (7) and its solution in the rectangles  $\Omega_{2,3}$  become significantly simpler:

$$\begin{aligned} -\frac{df}{dt} - A^T \frac{df}{dx} + F_v'^T f &= 0 \text{ on } \Omega_{2,3}, \\ f &= 0 \text{ on } \Gamma_a \cup \Gamma_2, \\ \rho_0 f_1 + w_b f_2 + I'_w &= 0 \text{ on } \Gamma_{b1}. \end{aligned} \tag{10}$$

Here,  $\Gamma_a = x_a \times (t_1, t_2)$ . Now there is no impact of the piston from line  $\Gamma_p$ , and there is no flow into the nozzle at the boundary  $\Gamma_{b0}$ .

Formula (8) for calculating the gradient of the objective functional also takes a simplified form (there is no nonlinear integration boundary  $\Gamma_{b0}$ ):

$$\nabla J(u; x) = \mathbb{U}_{\emptyset}^* f = \int_{t_1}^{t_2} \rho w f_1 dt + \kappa J, \quad x \in (x_a, x_b). \tag{11}$$

The resulting set  $\Omega \subset \Omega_{2,3}$  will correctly define domain  $V^*(\Omega)$  of the definition of operator  $\mathbb{U}^*(\Omega)$  with the range of values in  $U^*(S)$ . The corresponding expression for the time required to form such  $\Omega$  depends on the characteristics of the first family  $\xi_1$  and has the form:

$$t_2 \geq t_1 + \int_{x_a}^{x_b} \frac{dx}{w+c}, \quad t_1 \geq t_3. \tag{12}$$

That is, firstly, the upper characteristic  $\xi_1$  must pass through the entire nozzle from  $x_b$  to  $x_a$ . Secondly, the start of the outflow  $t_1$  should not be less than the moment  $t_3$  of the start of the entry of waves reflected from the piston into the nozzle.

This expression is the controllability condition in the problem under consideration. In this case, the remaining branches of the mappings are fulfilled (9):

$$I'_w|_{\omega} \xrightarrow{\text{uniquely}} f|_{\Omega} \xrightarrow{\mathbb{U}^*} U^*(S).$$

Now we discuss requirement 2) in the theorem on the nondegeneracy of operator  $\mathbb{U}^*$ . Let us start with operator  $\mathbb{U}_{\emptyset}^*$ , which defines gradient (8). If the objective function  $I$  did not depend explicitly on the control  $u$ , then  $\mathbb{U}_{\emptyset}^* \equiv \mathbb{U}^*$  and the set of conjugate states in the kernel  $f_{ker} = \{f: \mathbb{U}^*f=0 \text{ on } S\}$  would be zero for an unbounded optimal control  $u_*$ . In our case, for  $\mathbb{U}_{\emptyset}^*$ , the values of the elements of the kernel  $f_{ker}$  will not be zero, i.e., the optimal control will correspond to non-zero conjugate states. The subscript  $\emptyset$  means the absence of a zero kernel. Obviously, if  $\mathbb{U}^*$  was nondegenerate, then operator  $\mathbb{U}_{\emptyset}^*$  will also be nondegenerate. The nonhomogeneity of operator  $\mathbb{U}_{\emptyset}^*$  in our problem leads only to a shift in the zero kernel of the homogeneous operator  $\mathbb{U}^*$ .

We estimate the possible degeneracy of the homogeneous operator  $\mathbb{U}^*$ . It is obvious that for any values of  $\rho$  and  $w$ , the result of integration in  $\mathbb{U}^*f = \int_{t_1}^{t_2} \rho w f_1 dt$  can become zero on  $S$  only when  $f_1 = 0$  on  $\Omega$ . This means that operator  $\mathbb{U}^*$  is nondegenerate, and therefore,  $\mathbb{U}_{\emptyset}^*$  is also nondegenerate.

The last requirement of the theorem remains. Regularization in the direct extreme approach is provided by:

- selection of the initial approximation  $u^0 \in \mathcal{U}$ ;
- subsequent steps of algorithms of type (6) with a satisfactory regularization parameter, i.e., with parameter  $b^k$ , that does not take the control  $u^{k+1}$  beyond the compact set  $\mathcal{U}$ .

Paper [8] describes the required regularizing gradient methods for algorithm (6) in the problem under consideration.

Thus, all the requirements of the theorem for providing controllability are met. The distributed system (3) is controllable by  $u(x)$  on  $S$  according to functional  $J(5)$  under condition (12).

**Results of Using Controllability Conditions for a Hydrocannon.** The parameters of the experimental setup were borrowed from the research of A.N. Semko [15]:

- origin  $x_a = 0$ ;
- nozzle length  $x_b = 0.253$  m;
- initial position of the piston with the left boundary of water  $x_{p0} = -0.28$  m;
- piston mass  $m_p = 2.25$  kg;
- initial velocity of the piston and water  $\omega_0 = 76.2$  m/s;
- water density at atmospheric pressure  $\rho_0 = 10^3$  kg/m<sup>3</sup>;
- hydrocannon barrel radius  $R_a = 33 \cdot 10^{-3}$  m;
- start of water flow into the nozzle  $t_0 = 0$ .

The original problem was solved in a complex closed domain  $\bar{\Omega}$ , and conjugate problem — on a small rectangle  $\bar{\Omega}_2 = [x_a, x_b] \times [t_1, t_2]$ . Two spatial grids were constructed, each containing 50 steps. The first grid was movable and was used to calculate the water flow from the piston to the nozzle exit section, while the second grid was stationary and was designed to describe the nozzle shape. The number of layers over time was variable and reached  $10^3$ . The exact value depended on the nozzle shape and was determined by the final time  $t_2$ . The original and conjugate problems were solved by the method of characteristics on identical movable grids in  $\bar{\Omega}$  and in  $\bar{\Omega}_2$ , respectively.

The start of the jet flow from the nozzle was observed at  $t_1 \approx 2.7 \cdot 10^{-3}$  s. The average value of the impulse force of the obtained jet was estimated by objective functional  $J(u)$  in the interval  $t_2 - t_1 = 3 \cdot 10^{-4}$  s. This interval was approximately  $2 \int_{x_a}^{x_b} \frac{dx}{w+c}$ . In this case, the begin time of the flow  $t_1 > t_3$ , i.e., the piston did not affect the flow. Thus, the specified time  $t_2$  satisfied the controllability condition (12).

In [8], the required adaptive computational extremal algorithms were implemented taking into account the controllability conditions described here. And the optimal nozzle shapes obtained for the first time were presented.

In Figure 4, nozzle 1 corresponds to the internal local maximum of functional  $J(u)$ , and nozzle 2 — to the edge maximum under the constraint on nozzle expansion:  $u(x) \leq 0, \forall x \in S$ . The first nozzle practically has the shape of a cone, while the second one provides that the objective functional reaches a global maximum, whose value  $J$  is approximately three times greater than the value obtained for the first nozzle.

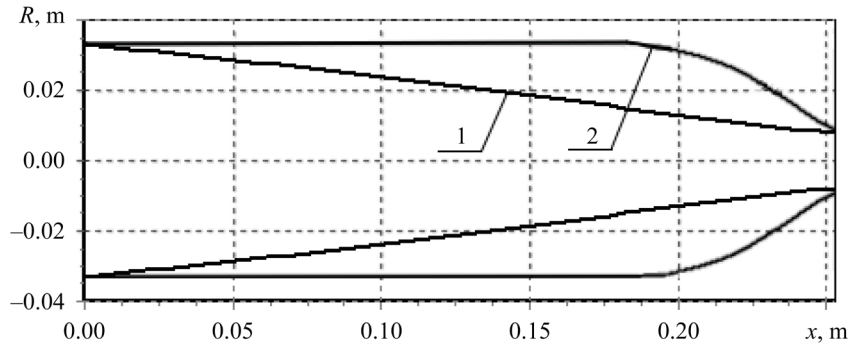


Fig. 4. Optimal shapes of hydrocannon nozzles

The initial approximation  $u^0(x)$  was set in the form of a pipe — as a continuation of the cannon barrel. At the first iterations of nozzle narrowing, functional  $J(u)$  grew with its convexity (growth of the norm  $\nabla J$ ). Then, the convexity changed to concavity (decrease of the norm  $\nabla J$ ), at the end of which there were very small regions of maximum (minimum norm  $\nabla J$  with concavity of the functional) with a subsequent convex minimum. Nozzle 1 was obtained in the local maximum. The transition through these local extrema was further accompanied by unlimited convex growth of  $J(u)$ . Only adding a constraint on the control made it possible to stop the uncontrolled expansion of the nozzle on the boundary with reasonable shape 2.

Recall that attempts were previously made to obtain a satisfactory solution using the classical calculus of variations. To do this, the authors [5] and [7] used relaxation methods to find root  $u_*$  from the required optimality condition  $J'_u(u; x) = 0$  (the Frechet derivative  $J'_u$  on the incorrect  $\Omega$  from Figure 2). However, this approach did not give the desired results. Moreover, it requires an additional restriction on the nozzle exit area to prevent its collapse. Such collapse also confirms the incorrectness of using  $J'_u(u; x)$  for the directed search for  $u_*(x)$  without isolating the controllability domain  $\Omega$  inside  $\Omega_{2,3}$ . In other words, instead of the Frechet derivative, it is required to obtain a gradient with the justification.

**Discussion and Conclusion.** The research results show that the application of the controllability analysis proposed in [2] made it possible to identify the key controllability conditions (12) required for the correct formulation and solution of the problem of optimizing the shape of the hydrocannon nozzle.

According to the controllability conditions, the optimization problem must be set and solved in a small rectangular domain  $\Omega_2$  or even  $\Omega_3$ , and not in a large and complex domain  $\Omega$ . This is due to the fact that the nozzle shape optimization problem with a statement in  $\Omega$  does not reduce the Frechet derivative  $J'_u$  to gradient  $\nabla J$ , which makes it impossible to search for the optimal solution. It was this circumstance that caused failures of the previous studies, where the optimality of solutions was not proven.

Our recommendations are as follows: first, perform a controllability analysis until the correct controllability domain  $\Omega$  is identified, and then, for the resulting  $\Omega$ , identify the solution region of the conjugate problem (in our case, it is  $\Omega_2$  or  $\Omega_3$ ) and find the variation  $\delta J = \langle J'_u, \delta u \rangle_{U^*(S)}$ . Next, you can continue the controllability analysis and obtain gradient  $\nabla J$  from derivative  $J'_u$ . It is with the help of  $\Omega$  inside  $\Omega_{2,3}$ , that you can find the value of gradient  $\nabla J(u; x)$ , which is distributed along the entire nozzle and uniquely corresponds to the objective functional of the problem  $J(u)$ . And then, you can purposefully search for the optimal nozzle shape.

The major advantage of the proposed approach is the use of a direct extreme method, which allows for direct maximizing the objective functional using gradient algorithms. This provides not only for the clarity of the controllability analysis, but also the possibility of obtaining numerically confirmed optimal solutions.

The theoretical value of the research is in the development of controllability analysis methods for distributed parameter systems, which opens up new prospects for solving similar problems in other areas. Further research can be aimed at expanding the method for more complex fluid flow models, as well as optimizing other devices operating on the basis of pulsed jets.

**References**

1. Egorov AI, Znamenskaya LN. *Introduction to Distributed Parameter Control Theory*. St. Petersburg: Lan; 2022. 292 p. (In Russ.) URL: <https://e.lanbook.com/book/167413> (accessed: 10.11.2024).

2. Tolstykh VK. Controllability of Distributed Parameter Systems. *Computational Mathematics and Mathematical Physics*. 2024;64(6):1211–1223. <https://doi.org/10.1134/S0965542524700453>
3. Merzlyakov VG, Derevyashkin IV, Boykova IE, Tolmachev AI. Coal and Rock Fracturing by High-Velocity Water Jets. *MIAB. Mining Informational and Analytical Bulletin*. 2023;(4):140–156. URL: [https://giab-online.ru/files/Data/2023/4/04\\_2023\\_140-156.pdf](https://giab-online.ru/files/Data/2023/4/04_2023_140-156.pdf) (accessed: 10.11.2024).
4. Ocheretyanyi SA, Prokofiev VV. Effect of Cavitator and Nozzle Parameters on the Efficiency Job of the Impulse Jet Generator. *Fluid Dynamics*. 2023;(5):10–24. <https://doi.org/10.31857/S1024708422600981>
5. Zuikova ZG. *Variational Problem of the Inflow of a Compressible Fluid into a Narrowing Channel*. Cand.Sci. (Phys.-Math.), diss. Donetsk: DonSU; 1984. 84 p. (In Russ.)
6. Zubov VI, Zuikova ZG. A Class of Solutions to the Problem of Optimizing the Nozzle of a Water Cannon. *Journal of Computational Mathematics and Mathematical Physics*. 1994;34(10):1541–1550.
7. Atanov GA. The Optimal Control Problem of Profiling the Hydro-Cannon Nozzle to Obtain the Maximum Outlet Speed. *Proceedings of the Institution of Mechanical Engineers, Part C*. 1997;211(7):541–547.
8. Tolstykh VK. Algorithms for Optimizing Systems with Multiple Extremum Functionals. *Computational Mathematics and Mathematical Physics*. 2024;64(3):392–400. <https://doi.org/10.1134/S0965542524030163>
9. Kabanikhin SI. Inverse Problems of Natural Science. *Computational Mathematics and Mathematical Physics*. 2020;60:911–914. <https://doi.org/10.1134/S0965542520060044>
10. Artemyeva LA, Dryazhenkov AA, Potapov MM. Stable Solution of the Quadratic Minimization Problem with a Nonuniformly Perturbed Operator by the Regularized Gradient Method. *Computational Mathematics and Mathematical Physics*. 2022;62(1):12–22. <https://doi.org/10.31857/S0044466922010033>
11. Semko AN, Loktyushina JV. About Compressibility of a Liquid at Current Calculation in the Hydrocannon. *Bulletin of Donetsk National University*. 2011;(2):95–101. URL: [https://donnu.ru/public/journals/files/Vestnik\\_DonNU\\_2011\\_N2\\_compr.pdf#page=96](https://donnu.ru/public/journals/files/Vestnik_DonNU_2011_N2_compr.pdf#page=96) (accessed: 10.11.2024).
12. Gusev AA. *Fundamentals of Hydraulics*, 3rd rev. and enl. ed. Moscow: Urait; 2019. 218 p. (In Russ.)
13. Korpusov MO, Panin AA. *Lectures on Linear and Nonlinear Functional Analysis. Vol. III. Nonlinear Analysis*. Moscow: Lomonosov Moscow State University; 2016. 235 p. (In Russ.)
14. Emelyanov VN. *Numerical Methods: Introduction to the Theory of Difference Schemes*. Moscow: Urait; 2023. 188 p. (In Russ.)
15. Semko AN. *High Velocity Pulsed Liquid Jets and Their Application*. Donetsk: DonNU; 2014. 370 p. (In Russ.)

#### **About the Authors:**

**Victor K. Tolstykh**, Dr.Sci. (Phys.-Math.), Professor of the Computer Technology Department, Donetsk State University (24, Universitetskaya Str., Donetsk, 283001, Donetsk People's Republic), [SPIN-code](#), [ORCID](#), [Scopus](#), [ResearcherID](#), [mail@tolstykh.com](mailto:mail@tolstykh.com)

**Yuliia V. Dmitruk**, Senior Lecturer of the Department of General Physics and Didactics of Physics, Donetsk State University (24, Universitetskaya Str., Donetsk, 283001, Donetsk People's Republic), [SPIN-code](#), [ORCID](#), [loktyushina.julia@yandex.ru](mailto:loktyushina.julia@yandex.ru)

#### **Claimed Contributorship:**

**VK Tolstykh**: conceptualization, supervision.

**YV Dmitruk**: visualization, writing — original draft preparation.

**Conflict of Interest Statement: the authors do not have any conflict of interest.**

**All the authors have read and approved the final manuscript.**

#### **Об авторах:**

**Виктор Константинович Толстых**, доктор физико-математических наук, доктор технических наук, профессор кафедры компьютерных технологий Донецкого государственного университета (283001, Донецкая Народная Республика, г. Донецк, ул. Университетская, д. 24), [SPIN-код](#), [ORCID](#), [Scopus](#), [ResearcherID](#), [mail@tolstykh.com](mailto:mail@tolstykh.com)

**Юлия Владимировна Дмитрук**, старший преподаватель кафедры общей физики и дидактики физики Донецкого государственного университета (283001, Донецкая Народная Республика, г. Донецк, ул. Университетская, д. 24), [SPIN-код](#), [ORCID](#), [loktyushina.julia@yandex.ru](mailto:loktyushina.julia@yandex.ru)

***Заявленный вклад авторов:***

**В.К. Толстых:** разработка концепции, научное руководство.

**Ю.В. Дмитрук:** визуализация, написание черновика рукописи.

***Конфликт интересов:*** авторы заявляют об отсутствии конфликта интересов.

***Все авторы прочитали и одобрили окончательный вариант рукописи.***

**Received / Поступила в редакцию** 20.12.2024

**Reviewed / Поступила после рецензирования** 17.01.2025

**Accepted / Принята к публикации** 20.01.2025